

HYDROLOGIC CHARACTERIZATION OF GROUND-WATER
RESOURCES IN SOUTH-CENTRAL HUDSPETH COUNTY, TEXAS

William F. Mullican III and Rainer K. Senger

Prepared for

Texas Low-Level Radioactive Waste Disposal Authority
under Interagency Contract Number IAC (90-91) 0268

Bureau of Economic Geology
W. L. Fisher, Director
The University of Texas at Austin
Austin, Texas 78713

June 1990

CONTENTS

Abstract.....	1
Introduction	2
Hydrogeologic Setting.....	2
Previous Regional Hydrologic Investigations	5
Methods	9
Aquifer Test Results	15
Well 22 Aquifer Tests	15
Wells 72 and 73 Aquifer Tests.....	18
Well 91 Aquifer Test	20
Well 94 Aquifer Test	23
Well 98 Aquifer Tests	24
Well 99 Aquifer Test	27
Well 107 Slug Test	28
Well 126 Slug Test	29
Summary of Hydraulic Properties	31
Hydraulic-Head Distribution.....	32
Modeling of Regional Ground-Water Flow.....	34
Conceptual Model of Ground-Water Flow	34
Boundary conditions.....	35
Delineation of permeability zones	35
Diablo Plateau aquifer	36
Hueco Bolson silt and sand aquifer.....	37
Rio Grande alluvium aquifer	38
Additional permeability zones	38

Discussion of Simulation Results.....	39
Relationship between Ground-Water Flow and Water Chemistry	43
Implication of Paleohydrologic Conditions.....	45
Evaluation of Ground-Water Resources, Hudspeth County	46
Water Usage.....	46
Water Supply	48
Conclusions.....	50
Acknowledgments.....	51
References.....	53

Figures

1. Location of water wells and spring within regional hydrologic study area	57
2. Hydrologic cross section illustrating relationship between potentiometric surface and stratigraphy from the Diablo Plateau to the Rio Grande.....	58
3. Fluctuations in water levels of wells in study area.....	59
4. Schematic diagrams illustrating well 22 during aquifer test and well 22* after recompletion.....	60
5. Hydrologic plots of data from aquifer test conducted in well 22 from October 5–6, 1988	62
6. Hydrologic plots of data from aquifer test conducted in well 22* from October 10–13, 1989	63
7. Schematic diagram of wells 72 and 73 during aquifer tests conducted in November and December 1989	64
8. Hydrologic plots of data from aquifer test conducted in well 73 from November 26 to December 18, 1989.....	65
9. Hydrologic plots of data from aquifer test conducted in well 91 on April 28, 1989.....	66
10. Hydrologic plots of data from aquifer test conducted in well 94 October 1–3, 1989.....	67
11. Schematic diagram of well 98 during aquifer tests conducted in May and September 1989.....	68
12. Hydrologic plots of data from aquifer test conducted in well 98 May 30–31, 1989	69

13. Hydrologic plots of data from aquifer test conducted in well 98* September 14–15, 1989	70
14. Hydrologic plots of data from aquifer test conducted in well 99.....	71
15. Hydrologic plots of data from slug (aquifer) test conducted in well 107 on September 30, 1989	72
16. Schematic drawing of well 126 during slug test.....	73
17. Hydrologic plots of data from slug (aquifer) test conducted in well 126 on September 13, 1989	74
18. Potentiometric surface map of regional hydrologic study.....	75
19. Distribution of total dissolved solids and tritium concentrations of water samples collected at wells in the area.....	76
20. Delineation of permeability zones in the model area that are incorporated in the planar ground-water flow model	77
21. Distribution of simulated hydraulic heads for simulation S-34.....	78
22. Streamlines and fluxes calculated for each element on the basis of simulation S-34	79
23. Photographs of dirt tank located west of study area taken immediately before and after rainfall event in July 1988	80

Tables

1. Summary of pumping test results in bolson deposits	81
2. Geologic and hydrologic units in study area.....	83
3a. Transmissivity results of aquifer test analyses for wells tested during study.....	84
3b. Permeability results of aquifer test analyses for wells tested during study	85
3c. Transmissivity and permeability results of aquifer (slug) test analyses for wells tested during study	86
4. Transmissivities assigned to permeability zones in the model.....	87
5. Water wells within 10 mi of principal study area.....	88

ABSTRACT

Regional and local hydrologic investigations have been conducted in Trans-Pecos Texas at the principal study area for a low-level radioactive waste repository. The area is approximately 40 mi (65 km) southeast of El Paso in the Hueco Bolson, a fault-bounded desert basin that developed in the late Tertiary. Ground water in the principal study area is found in Hueco Bolson silts and sands at depths of 361 ft (110 m) and 478 ft (146 m), and at depths of 592 ft (180 m) in Cretaceous limestones. The unsaturated zone consists of approximately 50 ft (15 m) of alluvial silt, sand, and gravel underlain by 300 to 500 ft (91 to 152 m) of lacustrine and fluvial clay, silt, and fine sand. The scope of this investigation included (1) evaluating ground-water resources in the area, (2) determining ground-water flow paths and velocities, and (3) testing hydrologic hypotheses using ground-water flow models.

Development of ground-water resources in the vicinity of the principal study area is limited by two key factors: (1) costs of drilling and completing wells and of producing water at depths typically greater than 400 ft (122 m) and (2) the very low productivity of aquifers. Transmissivities of aquifers in bolson and Cretaceous strata, as revealed by 11 aquifer tests, range from approximately 0.19 to 290.0 ft²/d (0.018 to 26.9 m²/d); corresponding permeabilities range from 0.0015 to 2.82 ft/d (0.0005 to 0.861 m/d). A composite potentiometric surface based on water levels measured in all available wells and on the hydrologic interconnection of the Diablo Plateau aquifer, Hueco Bolson silt and sand aquifer, and Rio Grande alluvium aquifer indicates that ground water is recharged on the Diablo Plateau and flows to the south and southwest toward the Rio Grande beneath the bolson pediment. The inferred distribution of permeability zones focuses flow from the eastern Diablo Plateau toward Cretaceous outcrops along the Campo Grande fault, creating an observed potentiometric high. The relatively low hydraulic heads near the principal study area are caused by preferential drainage along relatively permeable bolson deposits to the west and southwest toward the Rio Grande. Water chemistry data, particularly on tritium, carbon-

14, and total dissolved solids, generally support the interpreted flow pattern; some discrepancies can be related to paleohydrologic effects associated with the incision of the Rio Grande during Quaternary time.

INTRODUCTION

Geologic and hydrologic investigations in Trans-Pecos Texas were initiated in 1985 at the request of the Texas Low-Level Radioactive Waste Disposal Authority to characterize areas that were candidates for hosting a low-level radioactive waste repository. Results of the preliminary investigations (Kreitler and others, 1987) led the Authority to select an area of the southeastern Hueco Bolson near Fort Hancock, Texas, for more detailed studies. The principal study area is located approximately 40 mi (65 km) southeast of El Paso and 14 mi (22 km) north of the Rio Grande in southern Hudspeth County (fig. 1). The program and results of investigations of physical hydrogeology of the saturated zone, including hydrogeologic setting, hydrologic properties, ground-water modeling, and ground-water resources, are presented in this report. Evaluation of ground-water resources involved locating existing wells, operational or abandoned, at which water levels, discharge rates, and/or water samples could be measured or collected (fig. 1). Characterization of ground-water systems included delineating the water-bearing units, measuring representative transmissivities, and modeling and interpreting local and regional flow patterns. Fisher and Mullican (1990) discussed the chemical hydrogeology of the study area. Scanlon and others (1990 a, b) detailed the physical and chemical hydrology of the unsaturated zone in the Hueco Bolson.

HYDROGEOLOGIC SETTING

The principal study area lies primarily within the Hueco Bolson, a large desert basin in the eastern part of the Basin and Range structural province. Fine-grained lacustrine and fluvial

sediments were deposited in the Hueco Bolson over a basement of mostly Cretaceous shallow-marine strata. Hill (1900) was the first to apply the term "bolson," Spanish for "purse," to the intermontane basins of the Trans-Pecos region of Texas and New Mexico. The term bolson is used to describe closed basins with centripetal drainage (Sayre and Livingston, 1945). The Hueco Bolson was filled with detrital materials washed in from adjacent mountains such as the Franklin, Hueco, Organ, Sacramento, Finlay, Quitman, Malone, and other mountain chains in Mexico. Individual strata within bolsons range in thickness up to 100 ft (30 m) and are typically composed of poorly sorted sediment (Davis and Leggat, 1965). Cretaceous and older rocks are exposed on the Diablo Plateau north of the principal study area, and equivalent strata, strongly deformed by Laramide tectonism, are exposed in isolated outcrops south of the principal study area. Basin and Range extension, which began regionally about 24 mya (Henry and Price, 1985), produced areas of normal faulting, including the northwest-oriented Campo Grande fault trend located about 3.7 mi (6.0 km) southwest of well 126, along the southern boundary of the principal study area. Figure 2 depicts the general geometry of the different hydrostratigraphic units from the Diablo Plateau to the Rio Grande. Cretaceous strata crop out locally near the northwest-oriented Campo Grande fault trend. Along this fault trend Cretaceous strata are displaced against bolson deposits southwest of the fault. The southwestern edge of the Diablo Plateau shows a flexure of Cretaceous strata that dip beneath bolson deposits in the central part of the study area.

The upper part of the Hueco Bolson section consists of an unsaturated zone in silty and sandy alluvial gravels from land surface to a depth of about 50 ft (15 m) and lacustrine clay, silt, and sand from depths of about 50 to 450 ft (15 to 137 m). Beneath the unsaturated zone is the Hueco Bolson silt and sand aquifer. This aquifer is located in northern Mexico, Trans-Pecos Texas, and southeastern New Mexico, extending along the Rio Grande from the Quitman Mountains near Sierra Blanca to the Franklin Mountains in El Paso and north into New Mexico. It is locally a highly transmissive unit. Bolson deposits consisting of unconsolidated sand, silt, and gravel provide the primary water resources for the city of El Paso. The Hueco Bolson silt and sand aquifer is sand-poor within the study area.

The Rio Grande alluvial aquifer covers the Hueco Bolson in a narrow band adjacent to the Rio Grande and typically consists of poorly sorted sand, gravel, silt, and clay. The availability and quality of water in the Rio Grande alluvial aquifer in the El Paso area are less than those of the Hueco Bolson silt and sand aquifer. Peckham (1963) reported the alluvial deposits as typically being around 200 ft (61 m) thick, thinning to the northwest. Davis and Leggat (1965) stated that the Rio Grande alluvium probably never exceeds 150 ft (45.7 m) in thickness.

Kreitler and others (1987) referred to hydrostratigraphic units on the Diablo Plateau as aquifers A and B because no formal hydrostratigraphic unit has been defined outside of the Dell City irrigation district. In the Dell City area, the producing aquifer is named the Victorio Peak and Bone Springs limestone aquifer (Texas Department of Water Resources, 1984). The naming of aquifers A and B served to distinguish areas where water was found in Cretaceous limestones and sandstones (aquifer A) from areas where ground water probably was being produced from Permian strata (aquifer B). Several lines of evidence (potentiometric surface, isotopic composition, hydrochemical facies) indicated that ground waters produced from Cretaceous and Permian strata on the Diablo Plateau are, to varying degrees, in hydrologic communication with Cretaceous strata bearing ground water under the Hueco Bolson. Mullican and others (1989) proposed naming as the Diablo Plateau aquifer the hydrostratigraphic unit previously mapped as aquifers A and B on the Diablo Plateau (Kreitler and others, 1987) and including the Cretaceous strata that yields ground water beneath the Hueco Bolson.

Regional ground-water flow on the Diablo Plateau is predominantly from the southwest to the northeast. The hydrologic divide separating ground-water flow in the Hueco Bolson from that in the Diablo Plateau occurs within the study area and is located along the southwest edge of the Diablo Plateau. A cross-sectional view of this hydrologic divide is illustrated in figure 2. Flow velocities in the Diablo Plateau aquifer reported by Kreitler and others (1987) are typically greater than those in the Diablo Plateau aquifer where it is overlain by the Hueco Bolson (this report). Controlling factors for these greater flow velocities include very shallow depth to bedrock (often exposed at the surface) and extensive fracture systems that trend predominantly southeast-

northwest over large areas of the Diablo Plateau (for example, the Babb Flexure; see Kreitler and others, 1987). Modern tritium was found to be occurring in ground water throughout the entire Diablo Plateau study area. Chloride profiles indicate that recharge to the water table occurs during flash floods in fracture-controlled arroyos where bedrock is either very shallow (less than 30 to 40 ft [9.1 to 12.2 m]) or commonly exposed at the surface.

Climate at the study area is subtropical arid (classification of Thornthwaite, 1931, as modified by Larkin and Bomar, 1983) with a mean rainfall of 9.8 in/yr (24.9 cm/yr); minimum and maximum average annual temperatures are 45° (7.2°C) and 81° (27.2°C), respectively. Subtropical arid climates are characterized by (1) marked fluctuations of temperature over broad diurnal and annual ranges and (2) low mean precipitation with widely separated annual extremes (Orton, 1964). Approximately 60 percent of the annual precipitation occurs during afternoon thunderstorms from June to September. Summer storms in this desert region are intense, brief, and localized. Evaporation pan data at the Ysleta station near El Paso averaged 99 inches (2.51 m) per year for the period of 1953 through 1960; thus, the rate of evaporation was approximately 10 times greater than the rate of precipitation.

PREVIOUS REGIONAL HYDROLOGIC INVESTIGATIONS

No data have been published on the hydrologic properties of any of the three aquifers encountered in the regional study area. Limited data exist for the Hueco Bolson silt and sand aquifer and Rio Grande alluvium aquifer in and around the city of El Paso and for Cretaceous strata to the north of the study area on the Diablo Plateau. The following is a sequential review and compilation of a part of this data.

Slichter (1905) compiled early data on measured water levels, basic water chemistry, specific yield, and specific capacity for water wells in southern New Mexico and Trans-Pecos Texas. The ranges in specific yield and specific capacity reported from 18 aquifer tests are 191 to 1,325

gallons per minute (gpm), or 36,773 to 255,100 ft³/d (1,041 to 7,221 m³/d), and 1,122 to 16,930 ft²/d (104 to 1,573 m²/d), respectively.

Sayre and Livingston (1945) described in detail the geology and hydrology of the El Paso area. They cited an average coefficient of permeability of about 200 gallons per day (gpd). They also estimated, on the basis of Slichter's (1905) water-level records, that the maximum drawdown from original measured water levels (prior to well pumpage) was 45 ft (13.7 m) in the old Mesa well field for the period 1901 through 1936. They calculated that in the area the volume of the 45-ft-deep (13.7-m) cone of depression was equivalent to 22,000 acre-ft of water. For the period of record, however, 90,000 acre-ft of water had been produced, and therefore only about 25 percent of the water produced was from storage and the rest was from recharge.

Sundstrom and Hood (1952) conducted artificial recharge experiments from 1947 to 1951 at the Montana and Mesa well fields, main contributors to El Paso water supplies. The goal of these studies was to determine the feasibility of injecting surplus surface water from the Rio Grande available during winter months into well fields used by the city of El Paso. At the time of this study, ground-water production from the city well field was estimated to exceed natural recharge by 668,500 ft³/d (18,924 m³/d), or 25 percent of the pumpage. Transmissivity estimated at four wells in the Montana well field, an area under artesian conditions, ranged from 10,955 to 18,704 ft²/d (1,018 to 1,739 m²/d), and storativity estimates ranged from 0.00063 to 0.00271. The conclusions of that study were that water could be injected into the Montana well field at a rate of 6,000,000 gpd, or 802,200 ft³/d (22,708 m³/d), throughout the winter months and that injection into the Mesa well field, under water-table conditions, could be conducted at a rate many times greater than that determined for the Montana field (Sundstrom and Hood, 1952).

Smith (1956) divided the ground-water resources in the El Paso area into four hydrologic systems: the Hueco Bolson, the City artesian system, the Upper Valley, and the Lower Valley. The average pumpage rate in 1954 from the Hueco Bolson and City artesian system was 38,800,000 gpd, or 5,187,560 ft³/d (146,847 m³/d), and from the Upper and Lower Valleys was 36,000,000 gpd, or 4,813,200 ft³/d (136,250 m³/d), and 107,000,000 gpd, or 14,305,900 ft³/d (404,965

m³/d), respectively. The maximum water-level decline was reported to be near Biggs Air Force Base and near El Paso's Mesa field. The maximum amount of decline was 10 ft (3 m), and the cone of influence extended 9 mi (14.5 km) to the north and 6 mi (9.6 km) to the east of the main area of withdrawal.

Leggat (1962) expanded on the Smith report (1956) and stated that ground-water usage increased from 43,000,000 gpd, or 5,749,100 ft³/d (162,743 m³/d), in 1955 to 62,300,000 gpd, or 8,329,510 ft³/d (235,788 m³/d), in 1959. Water levels in one of the well fields in the Mesa area had declined 33.9 ft (10.3 m) from 1937 to 1962. Transmissivity ranged from 2,939 to 20,040 ft²/d (273 to 1,863 m²/d) in bolson deposits and from 4,556 to 20,770 ft²/d (422 m²/d to 1,925 m²/d) in deposits of the Upper Valley (Leggat, 1962). Transmissivity and storage for 22 aquifer tests are also reported by Leggat (1962). Myers (1969) listed data from the Leggat (1962) report and assigned well ID numbers still in use by the Texas Water Commission (table 1).

Peckham (1963) reported that in the El Paso area of the Rio Grande drainage basin, bolson and Rio Grande alluvial deposits are hydrologically connected and are therefore considered to compose one aquifer. He defined limits of the Rio Grande basin in Hudspeth County, however, that are much narrower than the Hueco Bolson silt and sand aquifer mapped in this report. Peckham reported well yields in El Paso County from 1,000 to 3,000 gpm, or 192,528 to 577,584 ft³/d (5,450 to 16,350 m³/d), whereas wells in Hudspeth County typically yield less than 500 gpm, or 96,264 ft³/d (2,725 m³/d). Reported specific capacities ranged from 577 to 11,735 ft²/d (53.6 to 1,090.7 m²/d) and averaged about 3,848 ft²/d (357.6 m²/d).

Davis and Leggat (1965) reported a range of transmissivities from 26,720 ft²/d (2,484 m²/d) for the Mesa subarea of the Hueco Bolson to 2,939 ft²/d (273 m²/d) in the City artesian subarea of El Paso. They calculated that the bolson deposits near El Paso contain at least 9,000,000 acre-ft of theoretically recoverable water in storage.

Myers (1969) reported the results of several aquifer tests conducted in El Paso County and one aquifer test (48-15-201) in Hudspeth County. A summary of this data is presented in table 1.

The Dell City area, located along the Texas–New Mexico border in northeast Hudspeth County, clearly has the most productive ground-water system in Hudspeth County. Ground water in this area is produced from Permian carbonates, named the Victorio Peak and Bone Springs limestone aquifer (for the complete hydrostratigraphic column for study area see table 2). Well yield is almost entirely dependent on the density of intersected fractures and solution cavities. The depth to Victorio Peak and Bone Springs strata in the Dell City area ranges from 5 to 150 ft (1.5 to 45.7 m) (Davis and Leggat, 1965).

The Soil Conservation Service (SCS) used aerial photographs to successfully locate 10 of 11 wells to be used as artificial recharge wells in a flood control project in the Dell City area (Logan, 1984). In this project, the SCS was able to project fracture systems visible on the surface into the subsurface so that a maximum number of fractures could be intersected by each recharge well. The requirement for a successful recharge well was that the well have a minimum specific capacity of approximately 385,000 ft²/d (35,800 m²/d).

Young (1976) discussed water resources and ground-water quality from the Rio Grande alluvial aquifer in the Fort Hancock area of Hudspeth County. Typical well yields ranged from 150 gpm, or 28,879 ft³/d (817 m³/d), in the Fort Hancock area to 530 gpm, or 102,040 ft³/d (2,888 m³/d), for a well southwest of Fabens (Young, 1976). After 15 yr of production, maximum drawdown of water levels in the area was 31 ft (9.4 m).

Transmissivities in the El Paso area range from 1,335 ft²/d (124.2 m²/d) to 37,384 ft²/d (3,477.6 m²/d) (Alvarez and Buckner, 1980). Sayre and Livingston (1945) and Peckham (1963) reported that Hueco Bolson deposits range in thickness from a few feet to more than 4,900 ft (1,493 m).

Knorr and Cliett (1985) discussed in detail an artificial recharge project constructed as part of the Hueco Bolson well field (formerly the Mesa well field) which, at the time of their writing, supplied 65 percent of the water resources to the city of El Paso. They reported that there has been a decrease in the percentage of mined water, which is replaced annually by natural recharge, to approximately 5 percent. They mapped transmissivity for this well field as ranging from 13,360 to

24,048 ft²/d (1,242 to 2,236 m²/d) and permeability as ranging from 26.7 to 60.1 ft/d (8.1 to 18.3 m/d). The goal of the recharge project, in part based on the modeling work of Meyer (1976), was to recharge by a direct-injection type system 10,000,000 gpd, or 1,337,000 ft³/d (38,000 m³/d).

Kreitler and others (1987) found transmissivities on the Diablo Plateau to range from 0.32 ft²/d (0.03 m²/d) to 69.0 ft²/d (6.4 m²/d). The mean transmissivity calculated from 22 separate interpretations for the seven wells tested was 21.0 ft²/d (1.9 m²/d); the standard deviation was 22.0 ft²/d (2.1 m²/d). In all seven tests, fractures were determined to be either directly or indirectly controlling production of the wells. In three of the wells, the discharge rate over extended periods (48 hr and longer) was insufficient to stress the aquifer, and no drawdown was recorded.

METHODS

The direction of regional ground-water flow was inferred from a potentiometric surface. Because of limited data and the nonuniform distribution of hydraulic-head measurements, a composite potentiometric surface was constructed for the entire area by pooling water-level measurements from different aquifer units. In the southern part of the regional study area, water-level data are mostly from the Rio Grande alluvium aquifer. In the western and central parts, water levels from the Hueco Bolson silt and sand aquifer were used, and in the northeastern part, only water levels from the Diablo Plateau aquifer, on both the Diablo Plateau and underlying the Hueco Bolson near the principal study area, were available. The degree of hydrologic communication between the Rio Grande alluvium, Hueco Bolson silt and sand, and the underlying and adjacent Cretaceous and older strata is poorly known, and the hydraulic-head gradient between the different units may not accurately represent the actual flow patterns. Figure 2 depicts the hydrogeologic cross-section delineated in figure 1.

For monitoring water-level fluctuations, water levels in wells 22, 72, 73, 94, 98, 99, and 126 were recorded at 30-min intervals using a pressure transducer connected to a computerized datalogger for a minimum period of 7 days to document representative fluctuation patterns (fig. 3).

Aquifer tests were performed at wells 73 (using well 72 as an observation well), 98, and 99 in the Hueco Bolson silt and sand aquifer and at wells 22 (two separate tests with different completion intervals), 91, and 94 in the Diablo Plateau aquifer. Production rates varied from 96.3 ft³/d (2.7 m³/d) in well 22 to 6,353 ft³/d (179.6 m³/d) in well 91. Water levels were recorded in the pumped well using a pressure transducer and computerized datalogger. Aquifer test results were analyzed utilizing standard techniques including type-curve matching using the Theis (1935) curve,

$$T = \frac{Q W(u)}{\Delta s}, \quad (1)$$

where T is transmissivity [ft/d],
 Q is pumpage rate [ft³/d],
 Δs is drawdown [ft], and
 $W(u)$ is the well function, given by the exponential integral

$$W(u) = \int_u^{\infty} \frac{e^{-u} du}{u};$$

Walton's (1962) leaky type curves

$$T = \frac{Q W(u, r/B)}{\Delta s}, \quad (2)$$

where $W(u, r/B)$ is the leaky well function (Hantush, 1956);

Jacob's semilogarithmic approximation method for drawdown data (Cooper and Jacob, 1946)

$$T = \frac{2.3Q}{4\pi \Delta s'}, \quad (3)$$

where $\Delta s'$ is the drawdown for one log cycle of elapsed time; and

Theis' semilogarithmic approximation method for recovery data (Kruseman and De Ridder, 1983),

$$T = \frac{2.3 Q}{4\pi \Delta s''}, \quad (4)$$

where $\Delta s''$ is the residual drawdown for one log cycle of t/t'' (with t = time since pumping started; t'' = time since pumping stopped).

To analyze aquifer test data from well 73, Neuman's (1975) method for analyzing data from unconfined aquifers with delayed yield was also used:

$$T = \frac{Q W(u_A, u_B, R)}{4\pi \Delta s} \quad (5)$$

where $W(u_A, u_B, R)$ is the unconfined well function.

All drawdown and recovery data were analyzed using the computer program AQTESOLV (Duffield and Rumbaugh, 1989). This program generates "best fit" matches after a specified number of iterations for each of the analytical techniques listed above but also can be used to numerically fit aquifer test data to specific type curves.

In wells 107 and 126, initial aquifer tests were unsuccessful because no significant drawdown (drawdown not attributed to wellbore storage) was observed after extended periods of production (greater than 24 hr). The open wellbore down to the saturated section was less than 4 inches in diameter, which restricted the selection of production equipment to a 2-inch-diameter, reciprocating, air-driven piston pump. At water depths present in these wells (measured water level is 347.1 ft [105.8 m] below land surface in well 107 and 478.9 ft [146.0 m] in well 126), the piston pump is capable of maximum discharge rates of 1 gpm, or 192 ft³/d (5.4 m³/d), or slightly less. To estimate the transmissivity, permeability, and storage coefficient in these wells, slug tests were performed (Ferris and Knowles, 1954). Ferris and Knowles (1954) modified the Theis (1935) equation for an instantaneous vertical line-source, or sink (see equation 1) to

$$s = \frac{V e^{-r^2 S/4Tt}}{4\pi Tt} \quad (6)$$

where s = residual head following injection of slug of water,
 r = distance from injection well to observation well,
 t = time since slug was injected,
 V = volume of slug,

T = coefficient of transmissibility, and
S = coefficient of storage.

During a slug test, water-level changes are measured in the injection well only. This results in a very small value for r , which, when coupled with an increasing value for t , produces an exponential value approaching unity (Ferris and Knowles, 1954). Therefore, if V is measured in cubic feet, t in minutes, and s in feet, the equation

$$T = \frac{18.4 V (1/t_m)}{s} \quad (7)$$

will provide T in gpd/ft.

Cooper and others (1967) developed type curves for analysis of slug tests. Values for transmissivity, permeability, and storage coefficients for both slug tests (wells 107 and 126) were calculated using the method described by Ferris and Knowles (1954) and were matched with the type curves of Cooper and others (1967). The program AQTESOLV also contains methods for analyzing slug tests on the basis of the methods of Cooper and others (1967) and Bouwer and Rice (1976), and both were used for comparative purposes. The Bouwer and Rice method of slug test analysis was developed for wells producing from unconfined aquifers. The water-level response in well 126 poorly matched the shape of the type curve, however. Kipp's method (1985), which takes into account the inertial effects in the well during a slug test, was also considered. No additional resolution was gained using this method.

The duration of aquifer tests at the different wells generally was brief (less than 30 min to as much as 185 hr), and drawdown and recovery curves were commonly influenced to varying degrees by wellbore storage and skin effects. In order to evaluate this influence, recovery data from the different aquifer tests were also analyzed using type curves of Agarwal and others (1970) with specific values of dimensionless wellbore storage (C_D) and skin effect (S), which are not taken into account in the aquifer test analyses mentioned above.

Hydraulic conductivity was calculated using the following equation by matching type curves (Agarwal and others, 1970) to data plots of water-level rise during recovery, which is expressed as

the logarithm of pressure change versus the logarithm of time during the drawdown or recovery period:

$$K = \frac{0.06848 Q B \mu \left(\frac{P_D}{\Delta P} \right)}{h}, \quad (8)$$

where K is hydraulic conductivity (ft/d),

Q is pumping rate(ft³/d),

h is test zone interval (ft),

B is a dimensionless formation volume factor (assumed to be 1.0),

μ is the viscosity (cp),

P_D and ΔP are dimensionless pressure and observed pressure change (pounds per square inch [psi]) of the match point, respectively, and

0.06848 is a unit conversion factor.

Results of aquifer test analyses using the different methods are summarized in table 3. Note that hydraulic conductivity values calculated from Agarwal's method are consistently higher by about one order of magnitude than those obtained using the standard methods. The latter techniques yielded reasonably consistent values of hydraulic conductivity. Typically, only the latest part of the brief data record matched the type curves, resulting in uncertainty about the match point location. Selection of the type curve by Agarwal and others (1970) for a specific dimensionless wellbore storage (C_D) was based on estimates of C_D from well and formation specifications. Dimensionless wellbore storage (Van Everdingen and Hurst, 1949) is given by

$$C_D = \frac{C E_w}{2 \pi n h r^2}, \quad (9)$$

where E_w is bulk modulus of elasticity of water (psi),

n is porosity,

r is well radius (ft), and

C is the unit storage factor given by

$$C = \frac{Q B \Delta t}{\Delta P}, \quad (10)$$

where Δt and ΔP are time and pressure during the early part of the curve dominated by wellbore storage (Ramey, 1970).

Although accurate estimates of C_D are limited mostly by uncertainty about formation porosity (assumed to be 0.25 for wells producing from the Hueco Bolson silt and sand aquifer, and 0.05 for wells producing from the Diablo Plateau aquifer), they were used to select the appropriate type curve for data fitting. The approach on which the type curves are based assumes a fully confined system (i.e., the type curve that is unaffected by skin effects corresponds to the Theis curve). As a result, effects of leakage are not accounted for by this method.

A numerical flow model was constructed to better understand the regional ground-water flow regime. For this purpose, a planar, finite-difference model was constructed incorporating the major hydrogeologic features of the study area. Hydraulic properties determined from aquifer tests were used as initial estimates for simulations. Hydraulic properties were adjusted to yield simulated hydraulic heads that matched the composite potentiometric surface.

The model was implemented with the computer programs FRESURFK and FRESTRK, which are modifications of the original version of FREESURF, developed by Neuman and Witherspoon (1970). The program FRESURFK solves for hydraulic head in the steady-state flow equation

$$\frac{\partial}{\partial x} \left(T_x \frac{\partial h}{\partial x} \right) + \frac{\partial}{\partial y} \left(T_y \frac{\partial h}{\partial y} \right) = 0, \quad (11)$$

and the program FRESTRK solves for stream function in the corresponding steady-state flow equation

$$\frac{\partial}{\partial x} \left(\frac{1}{T_y} \frac{\partial \psi}{\partial x} \right) + \frac{\partial}{\partial y} \left(\frac{1}{T_x} \frac{\partial \psi}{\partial y} \right) = 0, \quad (12)$$

where T_x and T_y are transmissivities in the principal flow directions, respectively.

Fogg and Senger (1985) and Frind and Matanga (1985) reviewed the theory behind equation (12) and its associated boundary conditions. The programs, which use a finite-element method and a direct-solution technique (Gaussian elimination), have been tested according to standard quality-assurance procedures. Contouring of computed hydraulic heads gives a potentiometric surface, and contouring of stream functions gives the streamlines of a flow net.

AQUIFER TEST RESULTS

Well 22 Aquifer Tests

Several aquifer tests were conducted at well 22, located on the northern boundary of the principal study area (fig. 1), and completed in the saturated zone in Lower Cretaceous limestones of the Diablo Plateau aquifer. The construction of this well for this test is shown in figure 4a. On the basis of regional data, the water level expected in well 22 was approximately 500 ft (152 m); the well was cored to 875 ft (267 m) and reamed out to a depth of 615 ft (187 m) to complete an anticipated 115-ft-thick (35-m) saturated section for testing. Measured water level at the start of the test however, was 592 ft (180 m) below land surface, leaving only a 23-ft-thick (7-m) saturated section for testing above the steel plug. Water-level fluctuations in well 22 are semidiurnal and have a maximum range of about 1 ft (0.3 m).

Well 22 was reentered during September 1989 and deepened (reamed out) to a depth of 719 ft (219.1 m) to test a thicker saturated section (fig. 4b). The equivalent of several wellbore volumes was pumped using a 3-horsepower submersible pump to remove drilling mud from the borehole and to use in aquifer tests. The measured water level at the start of the aquifer test was 592 ft (180.4 m) below land surface (3,644 ft [1,111 m] above sea level).

The first aquifer test was begun at 10:29:30 hr on October 5 by pumping the well at an initial rate of 0.5 gpm, or 96.3 ft³/d (2.7 m³/d), using a piston pump. At 226 min into the drawdown

phase, a surge of mud temporarily clogged the pump, decreasing flow rate and allowing partial recovery of the water level. Figure 5a illustrates water-level response during this aquifer test.

Drawdown data from this aquifer test was analyzed using the Jacob semilogarithmic approximation method (fig 5b), which assumes a constant discharge and other assumptions. Recovery data were analyzed using the Theis recovery semilogarithmic approximation method (fig. 5c) and curve matching using Agarwal, Theis, and Walton type curves (figs. 5d, e, and f). Estimated dimensionless wellbore storage coefficient for well 22 is $C_D = 10^{6.3}$, and the data were fitted with the type curve for $C_D = 10^5$ and $S = 5$ (fig. 5d). The positive skin effect ($S = 5$) suggests damaged wellbore conditions. Only recovery data after 100 min fit the type curve; the early part shows a slope of less than 45° , which suggests a decrease in wellbore storage during the recovery. Only drawdown data after 40 min into the test were matched to the Theis curve (fig. 5e). Recovery data were then matched to Walton's type curve ($r/B = 0.6$) (fig. 5f).

Calculated transmissivities and permeabilities for this well range from 0.45 to 12.5 ft²/d (0.042 to 1.16 m²/d) and from 0.020 to 0.546 ft/d (0.0060 to 0.166 m/d), respectively (table 3). Calculated values from the different methods of analysis are very similar, with the exception of those obtained from Agarwal type curves, which are greater by more than one order of magnitude (table 3). The discrepancy may be due to the fact that the standard methods do not incorporate effects of wellbore storage. On the other hand, the early recovery data do not show the 45° slope characteristic for constant wellbore storage, which may introduce an error in the analysis using Agarwal's type curves. Furthermore, recovery data were fitted to a leaky type curve (fig. 5f), indicating leaky aquifer conditions that the Agarwal method does not take into account.

The drawdown phase of the second aquifer test was conducted on October 10 (13:07:15 to 16:35:47 hr) and the recovery monitored from October 10 to 9:50:27 hr on October 13, 1989. The measured water level at the beginning of the test was 592 ft (180.4 m) below land surface. Production rates throughout the drawdown phase of the test were maintained as closely as possible to 1.6 gpm, or 308 ft³/d (28.6 m³/d). At the end of the test, 97.6 percent of the test drawdown had been recovered.

Water-level response throughout the aquifer test is illustrated in figure 6a. Type-curve matching using Agarwal, Theis, and Walton type curves, drawdown data using the Jacob semilogarithmic approximation method, and recovery data using the Theis recovery semilogarithmic approximation method are illustrated in figures 6b through 6f.

Hydrologic parameters selected for Agarwal's type curve include an estimated dimensionless wellbore storage coefficient of $C_D = 10^{5.5}$, and the data were fitted with the type curve for $C_D = 10^5$ and $S = -5$. The negative skin (stimulation) effect ($S = -5$) might be explained by fracture flow. Note that in this test, the early recovery data fit the 45° slope of the type curve (fig. 6b), which suggests constant wellbore storage.

The influence of wellbore storage on the drawdown response was sufficient to prevent the use of drawdown data for analysis of transmissivity using either a Theis type curve or the Jacob semilogarithmic approximation method (figs. 6c, e). Using a Walton type curve ($r/B = 0.2$) with the recovery data did result in a good match (fig. 6d). The recovery data were also used with the Theis recovery method to calculate transmissivity (fig. 6f). Calculated transmissivities (table 3) range from 0.19 to 1.44 ft²/d (0.018 to 0.134 m²/d). Permeability estimates range from 0.0015 to 0.0114 ft/d (0.0005 to 0.0035 m/d). Calculated transmissivities based on type-curve matching using the Walton and Theis recovery methods are within the same order of magnitude.

The combined effects of an excessive rate of recovery during the early part (beyond what would be expected from Agarwal type curves) and the neglect of leakage result in match points having relatively low ΔP values and relatively high calculated values of permeability and transmissivity. The exception is the recovery match for the aquifer test in well 22* where the early part follows the type curve and the type curve shows a negative skin factor ($S = -5$), resulting in a relatively large ΔP value for the match point. Thus, the computed transmissivity is relatively low, within the same order of magnitude as the other methods.

Calculated transmissivities and permeabilities are generally lower in the second test at well 22 than in the first test, but results differ by less than one order of magnitude. Significant fracture

flow, typically the controlling factor on flow in wells producing from the Diablo Plateau aquifer to the north on the Diablo Plateau (Kreitler and others, 1987), did not appear to influence either aquifer test conducted on well 22.

Wells 72 and 73 Aquifer Tests

Two aquifer tests were conducted during November and December 1989 using well 73 as the pumping well and well 72, located 50 ft (15 m) south of well 73, as the observation well. These two wells, located along the southern boundary of the principal study area immediately west of the main county road (fig. 1), are completed in the saturated zone of the Hueco Bolson silt and sand aquifer.

Well 72, designed as an observation well (fig. 7), was originally cored from a depth of 21 ft (6.4 m) to a total depth of 609 ft (185.6 m) (for a description of lithologies encountered, see Gustavson, 1990). Well 73 was drilled and completed as a production well. After a production screen was installed in well 73, the well was cored from 570 ft (174 m) to a total depth of 740 ft (225 m) to determine the thickness of bolson strata and the nature of uppermost Cretaceous strata in the principal study area (fig. 7). Cretaceous shales were encountered at a depth of 718 ft (219 m) (Gustavson, 1990). A 3-horsepower submersible pump was installed at a depth of 565 ft (172 m) in well 73.

Water levels in both wells show semidiurnal fluctuations with maximum ranges of 0.7 ft (0.21 m) and 1.5 ft (0.46 m) for wells 72 and 73, respectively (figs. 3b, c, and 8a). Measured water level at the start of both aquifer tests was 361.5 ft (110 m) below ground surface (3,733.5 ft [1,140 m] above sea level) in well 72. Measured water level for well 73, located only 50 ft (15 m) north of well 72 and at the same ground elevation (4,095 ft [1,248 m]), was 15.5 ft (4.7 m) lower, at 377.1 ft (115 m) below ground surface (3,718 ft [1,133 m] above sea level).

The most reasonable explanation for this discrepancy in measured water level is that different drilling methods were used for the two wells. Well 72 was cored for all but 21 ft (6.4 m) of the

completed interval using relatively stiff HQ core rods. Well 73, however, was drilled with a tri-cone rock bit and relatively flexible drill rods over the entire length now completed. When the more flexible drill rods were used, the “walk,” or clockwise drift of the drill bit, would typically be greater than the drift experienced when the stiffer core rods were used. An apparent 15.6-ft (4.7-m) difference in measured water levels could result if the radius of the drift in well 73 (arbitrarily assuming one complete coil per 100 ft [30 m] drilling depth) was only 0.65 ft (0.2 m) greater than the radius of the drift of well 72. Thus, for mapping purposes, the measured water level in well 72 is considered more representative.

The first test ran from November 18 to November 20, 1989, with a constant discharge rate of approximately 10.8 gpm, or 2,118 ft³/d (59.9 m³/d). After approximately 40 hr of production, the 460V, three-phase generator used to power the submersible pump failed, which ended the aquifer test. The test was restarted at 17:00:51 hr on November 26 by pumping the well at a constant discharge rate of approximately 11.8 gpm, or 2,310 ft³/d (65.3 m³/d). Except for 5- to 10-min periods each morning when the generator was serviced (illustrated daily by brief water-level changes during drawdown phase), the drawdown phase of the aquifer test was run continuously until 09:20:21 hr on December 4, 1989. The aquifer test was terminated at this time because of geophysical surveys in progress adjacent to the well (ground noise from a generator would negatively impact geophysical surveys). Recovery was then monitored until 15:35:56 hr on December 18, 1989. Water-level fluctuation throughout the aquifer test in both wells is illustrated in figure 8a. No drawdown was observed in the observation well 72.

During the drawdown phase of the aquifer test, no effects of wellbore storage were observed in well 73; therefore, the Agarwal type-curve method was not used. In fact, the rate of initial drawdown was steeper than the rate represented by the Theis type curve (fig. 8b). Assuming confined conditions, drawdown data were matched to Walton's leaky type curve ($r/B = 0.5$). The continued increase in drawdown after 1 hr may be explained by effects of storativity within confining layers. (Walton's type curves are based on the assumption of zero storativity within the confining layer.)

The Jacob semilogarithmic approximation method was used for drawdown data (fig. 8c), and the Theis semilogarithmic approximation method and type-curve matching were used with recovery data (figs. 8d, e). Matches between recovery data and the Theis type curve differ between data from the early and late parts of the test (fig. 8e).

Semidiurnal water-level fluctuations in both wells (72 and 73) in combination with the reasonably good fit of drawdown data with Walton's leaky type curve ($r/B = 0.5$) would seem to indicate that the aquifer system is confined. The increased rate of drawdown seen over the last 80 hr of production (fig. 8b) may indicate the presence of a barrier to flow in well 73. The argument can be made, however, that these wells are producing from an unconfined aquifer because (1) no drawdown was observed in well 72, (2) there is an equally good fit between drawdown data and Neuman's type curves (Neuman, 1975) for unconfined aquifers with delayed yield, and (3) relatively thick sands are present.

Transmissivity calculations (table 3a), based on the assumption of confined or leaky conditions for well 73, range from 14.1 to 110.0 ft²/d (1.31 to 10.2 m²/d). Permeabilities (table 3b), based on a saturated thickness of 192.9 ft (58.8 m), range from 0.047 to 0.57 ft/d (0.0142 to 0.174 m/d). Transmissivities, based on the assumption of unconfined conditions, range from 24.6 to 22.9 ft²/d (2.28 to 2.13 m²/d), respectively (figs. 8f, g).

Well 91 Aquifer Test

Three aquifer tests were conducted on April 26 and April 28, 1989, at well 91, located south of the principal study area and immediately west of Campo Grande Mountain (fig. 1). Well 91 is completed in Lower Cretaceous strata of the Diablo Plateau aquifer in an area where Lower Cretaceous strata crop out within the Campo Grande fault trend. This well was originally drilled as an oil test by Haymon Krupp Oil and Land Co. and named the No. 1 Thaxton well. According to Albritton and Smith (1965), this well originally was drilled to test rocks of Paleozoic age but crossed thrust faults and never reached strata older than the Permian. The original well depth was

6,402 ft (1,951.3 m), but it now is plugged back to approximately 420 ft (128 m). The original construction of this well is unknown, but currently it has an 8-inch (20.3-cm) ID surface casing to an unknown depth. According to lithology logs from the well, the producing interval in this well is brown to dark-gray, fine-grained Cretaceous limestone. Measured water level is 317.25 ft (96.7 m) below land surface (3,727.8 ft [1,136 m] above sea level).

Water-level fluctuations during the tests conducted on April 28 are illustrated in figure 9a. Water was pumped by a 10-horsepower submersible pump powered by a portable 460V, three-phase generator at a discharge rate of approximately 32.4 gpm, or 6,353 ft³/d (179.9 m³/d). Because of electrical generator problems, the tests were conducted in several segments, the first on April 26 and the rest on April 28. Measured water level at the start of the aquifer test was 317.25 ft (96.7 m) below land surface with a water column of 94.73 ft (28.87 m) above the pressure transducer.

After repairs had been completed on the generator equipment, the well was again tested at two discharge rates, approximately 32.4 gpm, or 6,353 ft³/d (179.9 m³/d), and 12 gpm, or 2,310 ft³ (65.4 m³/d). The test, using a discharge rate of 6,353 ft³/d (179.9 m³/d), was started at 12:27:19 hr with an original water column of 94.31 ft (28.7 m). By 12:38:06 hr, 10 min and 47 sec after the test was started, the water column was drawn down to the transducer. The recovery phase was started at 12:39:06 hr and monitored until 13:10:26 hr, when the water column above the pressure transducer registered 94.9 ft (28.9 m), 100.6 percent of the original water column. The test was then repeated at a discharge rate of approximately 12 gpm, or 2,310 ft³/d (65.4 m³), starting at 13:17:08 hr. The recovery phase of this latest test was started at 16:16:01 hr and terminated at 16:25:01 hr when the water column above the transducer had recovered to a height of 92.11 ft (28.1 m).

The results of aquifer test analyses presented in table 3 are for the test conducted at a discharge rate of approximately 32.4 gpm, or 6,353 ft³/d (179.9 m³/d). Distinct changes in slope in both the drawdown and recovery segments of the curve (fig. 9a) suggest a change in wellbore geometry, and consequently in wellbore storage about 390 ft (118.9 m) below land surface. No

information was available concerning well-completion schematics for well 91. If the base of surface casing is located at a depth of 390 ft (118.9 m), if the well is open below this depth, and if the surface casing diameter is assumed to be less than the diameter of the wellbore, then this brief change in slope may simply result from increased wellbore volume from the surface casing to the open wellbore. The slope of water-level drawdown and recovery before and after reaching the 390-ft (118.9-m) level are essentially the same. This may suggest that inflow above and below the 390-ft (118.9-m) level is controlled by matrix flow.

Another possible explanation for the break is that the wellbore may intersect a fracture at this depth. The possible fracture is to some degree supported by well 91's proximity to the regional Campo Grande fault trend. Well 91 was the only well tested in the study that suggested the possible influence of fracture flow on well hydraulics.

Agarwal, Theis, and Walton type-curve matches and Jacob drawdown and Theis recovery semilogarithmic approximation methods are illustrated in figures 9b through 9f. Recovery data were fitted with Agarwal's type curve for $C_D = 10^5$ and $S = 20$ (fig. 9b). Estimated C_D value was $10^{5.1}$. The large positive skin effect suggests partial penetration of the aquifer or damaged wellbore conditions. It is most probable that, when this oil and gas exploration well was drilled, wellbore permeability within the fresh-water zone was damaged while drilling was done at greater than 6,000 ft (1,830 m).

Drawdown data from this aquifer test were matched with the Theis type curve (fig. 9c), whereas recovery data were matched with the Walton type curve $r/B = 0.075$ (fig. 9d). Although the drawdown curve showed a reasonably good fit with the Theis curve, the aquifer test was not long enough to include the longer-term drawdown pattern. On the other hand, the recovery data indicated a relatively steep rise in water level compared with the Theis curve, and only the latter part of the recovery could be fitted. Calculated transmissivities and permeabilities at this well were the highest of any of the eight wells tested (from both the Diablo Plateau and Hueco Bolson silt and sand aquifers). The estimates for transmissivity range from 5.96 to 290.0 ft²/d (0.55 to 26.9

m²/d). Permeability calculations range from 0.0058 to 2.82 ft/d (0.0018 to 0.861 m/d). Again, the maximum estimate is based on the Agarwal approach.

Well 94 Aquifer Test

Well 94 is an abandoned windmill located approximately 2,000 ft (610 m) south-southeast of Campo Grande Mountain (fig. 1). Prior to testing, the damaged windmill tower was removed, and 357 ft (109 m) of 2.5-inch (6.3-cm) production pipe was pulled from the well. On the basis of its depth and proximity to outcrops, this well is thought to produce from Lower Cretaceous strata of the Diablo Plateau aquifer. Initial plans called for testing the well with a 3-horsepower submersible pump, but the small wellbore diameter (less than 4 inches [10.2 cm]) required the use of a piston pump. The measured water level in this well was 294.0 ft (89.6 m) below ground surface (3,723 ft [1,135 m] above sea level). During testing the total depth of the well was approximately 360 ft (110 m), but the original well depth is not known due to caving.

Water-level fluctuations throughout the drawdown and recovery phases of the test are illustrated in figure 10a. Water-level fluctuations for 9 days (October 3 through October 12, 1989) following the test are illustrated in figure 3d. Water levels in this well show semidiurnal variations with maximum daily range of approximately 0.7 ft (0.2 m) during the monitor period from October 3 through October 12, 1989.

The aquifer test was started at 11:01:45 hr on October 1, 1989. Discharge during the test was approximately 1 gpm, or 202.1 ft³/d (5.7 m³/d). The drawdown phase was terminated after 5.68 hr of production; maximum drawdown in the wellbore was measured at 20.89 ft (6.4 m). The recovery phase of the aquifer test ended after another 6.3 hr, when the water level in the wellbore had recovered 22.76 ft (6.9 m), or 109% of the original drawdown.

Agarwal, Walton, and Theis type-curve matches and Jacob drawdown and Theis recovery semilogarithmic approximation methods are illustrated in figures 10b through 10f. The estimated dimensionless wellbore storage coefficient was $C_D = 10^{5.3}$. Recovery data are fitted with the

Agarwal type curve for $C_D = 10^5$ and $S = 20$. Similar to the other tests, only the later part of the recovery was fitted to the type curve. The early part could be affected by decreasing wellbore storage. Again, the somewhat higher transmissivities from the Agarwal approach may be due to leakage effects that are not accounted for by this method.

Drawdown data were matched with the Walton type curve $r/B = 0.4$, whereas recovery data were matched with the Walton type curve $r/B = 0.075$. Transmissivities calculated from this aquifer test range from 1.39 to 38.0 ft²/d (0.129 to 3.53 m²/d). With the exception of the Agarwal method results (38.0 ft²/d [3.53 m²/d]), the values for seven different solutions (table 3a) for transmissivity at this well are close, ranging from 1.39 to 3.54 ft²/d (0.129 to 0.329 m²/d). Values of permeability range from 0.026 to 0.714 ft/d (0.0080 to 0.218 m/d).

Well 98 Aquifer Tests

Field reconnaissance of well 98, located immediately north of the Camp Rice Reservoir 1, producing from the Hueco Bolson silt and sand aquifer, indicated that significant workover of the well would be required before an aquifer test could be performed. The initial inspection indicated that the well had an 8-inch (20.3-cm) steel surface casing down to a depth of approximately 200 ft (70 m), a measured water level of 200 ft (70 m), and an abandoned submersible pump at an unknown depth. After the submersible pump was removed, the well was reentered with a 7⁷/₈-inch-diameter (20.0-cm) drill bit so that the well could be cleaned out and deepened. At a depth of approximately 245 ft (74.7 m), a 20-ft-long (6.1-m), 5-inch-diameter (12.7-cm) brass production screen was encountered and removed from the well. The well then was deepened to 300 ft (91.4 m) and recompleted (see figure 11 for well schematic).

A series of seven aquifer tests were conducted: five from May 10 to May 12, 1989, a sixth from May 30 to May 31, 1989, and a final seventh test from September 14 to September 15, 1989. A high-viscosity drilling mud was required while the well was deepened to prevent the wellbore in the very loose and unconsolidated sediment from caving. Extensive well development then was

needed to remove the gel-based drilling muds from the wellbore and formation so that representative aquifer characteristics could be determined. Additional well development was performed over a 3-month period, and a seventh aquifer test (aquifer test 7) was conducted from September 14 to September 15, 1989, to determine whether all residual drilling mud (which inhibits ground-water inflow) had been removed. Results of the sixth and seventh aquifer tests are presented and compared below.

Water-level fluctuations from May 18 to May 30, 1989, are illustrated in figure 3e. Water levels in this well show semidiurnal fluctuations with a maximum daily range of approximately 3.5 ft (1.1 m). Water level in the well prior to the start of aquifer test 6 was measured at 204.18 ft (62.23 m) below land surface; the water column above the transducer was 86.46 ft (26.3 m). This starting water level was 4.18 ft (1.27 m) below the mean measured water level for this well (200 ft [61 m] below land surface, 3,544 ft [1,080 m] above sea level) due to pretest pumping to calibrate discharge rates.

The drawdown phase of aquifer test 6 was started at 22:24:10 hr and was stopped after 62.1 min when the water level reached 0.93 ft (0.28 m) above the transducer. The discharge rate throughout the drawdown phase was maintained at 5.9 gpm, or 1,155 ft³/d (32.7 m³/d). The recovery phase of the aquifer test ended after 4.67 hr, when the water column above the transducer stabilized at the mean measured water level.

Water-level variations for the complete aquifer test 6 are shown in figure 12a. Agarwal, Theis, and Walton type-curve matches and Jacob drawdown and Theis recovery semilogarithmic approximation methods are illustrated in figures 12b through 12f. Recovery data are fitted with the Agarwal type curve for $C_D = 10^5$ and $S = 20$ (fig. 12b). Estimated C_D value was $10^{4.2}$. Although the early part of the recovery followed Agarwal's type curve, a somewhat irregular curvature implies a large skin-effect parameter ($S = 20$). As a result, the matchpoint produces a low ΔP value and concomitantly a relatively high permeability estimate. Such a large positive skin effect could reflect partial penetration of the aquifer, a damaged wellbore, or retardation of inflow by drilling mud. The drawdown data were fitted with the Theis curve for elapsed times greater than 20 min

(fig. 12c). The later phase of recovery data was matched to the Walton type curve $r/B = 0.05$. Calculated transmissivities from aquifer test 6 for this well (table 3a) range from 1.15 to 59.0 ft²/d (0.107 to 5.48 m²/d). Calculated permeabilities (table 3b) range from 0.0115 to 0.59 ft/d (0.0035 to 0.18 m/d).

Aquifer test 7 was conducted from September 14 to September 15, 1989, to determine whether the well development throughout the summer of 1989 had removed the remainder of gel-based drilling muds from the saturated section. The drawdown phase of aquifer test 7 was started at 18:43:08 hr on September 14, 1989. Discharge rates were maintained at a constant 2.95 gpm, or 577.6 ft³/d (16.3 m³/d), throughout the aquifer test. Measured water level in the wellbore was 200.0 ft (60.9 m) with the water column above the pressure transducer recorded at 85.02 ft (25.9 m). The drawdown phase was terminated at 21:49:28 hr after 3.1 hr of production, when the water column above the transducer had been lowered to 0.12 ft (0.03 m). The subsequent recovery phase continued until 05:02:18 hr on September 15, when the water column above the transducer had recovered to 86.42 ft (26.3 m). Water-level fluctuations throughout the aquifer test are illustrated in figure 13a.

The same methods of analysis performed on the results of aquifer test 6 were used for test 7 (figs. 13b through 13f). Recovery data were fitted with Agarwal's type curve for $C_D = 10^5$ and $S = 20$. Estimated C_D value for aquifer test 7 was $10^{4.9}$. Figure 13b shows that only the recovery data between 4 min and 30 min have a 45° slope. The earliest part shows a steeper recovery than the comparable recovery in figure 12b. Most significantly, however, the irregular curvature (fig. 13b) does not fit well with the Agarwal type curve. No Theis or Walton type curves could be matched to the drawdown data, indicating the dominating influence of wellbore storage during the drawdown phase. The late part of the recovery data was matched with the Walton type curve $r/B = 0.075$ (fig. 13d). Transmissivity values for aquifer test 7 range from 0.64 to 33.0 ft²/d (0.060 to 3.07 m²/d) (table 3a). Permeability calculations range from 0.0064 to 0.33 ft/d (0.0020 to 0.101 m/d) (table 3b).

Well development conducted on this well between aquifer tests 6 and 7 did not result in any obvious enhancement of hydraulic properties for this well. The potential effects of long-term development on well hydraulics are not known.

Well 99 Aquifer Test

An aquifer test conducted as part of these investigations was performed on well 99, an abandoned windmill located just below the breached Cavett Lake Dam on Arroyo Alamo, west of the principal study area (fig. 1). The test was conducted from November 9 to November 12, 1988, in the Hueco Bolson silt and sand aquifer. The original well construction for this well is unknown. The well has a 6-inch (15.2-cm) ID surface casing to an unknown depth (thought to be less than 40 ft [12.2 m] on the basis of a conversation with its owner) and a measured total depth of 230.54 ft (70.3 m), with a measured water level prior to pumping of 140 ft (42.7 m).

Water-level fluctuations monitored in this well following the aquifer test (fig. 3f) are semidiurnal and have a daily range of almost 2.5 ft (0.76 m). Average water level is 140 ft (42.7 m) below land surface (3,705 ft [1,129 m] above sea level). The test was started at 10:55:15 hr on November 9 by pumping the well at a constant discharge rate of approximately 0.74 gpm, or 144.4 ft³/d (4.1 m³/d), using a piston pump. The drawdown phase of this aquifer test was terminated 115.25 min after the start of the test and subsequent recovery phase of the test was monitored for 56.0 hr, until water level had recovered to 62.18 ft (18.9 m) above the pressure transducer, or 99.1 percent of original measured water level. Figure 14a illustrates the water-level response throughout the aquifer test.

Agarwal, Theis, and Walton type curves are shown in figures 14b through d. Jacob drawdown and Theis recovery semilogarithmic approximation methods are illustrated in figures 14e and f, respectively. In this aquifer test, essentially all of the drawdown was from wellbore storage. Thus, no match was possible using the Theis type curves. The early part of the recovery shows a steeper water-level rise than what would be expected from the Agarwal type curve (fig.

14b). Recovery data were fitted with Agarwal's type curve for dimensionless storage $C_D = 10^5$ and skin effect $S = 10$ (fig. 14b). Estimated C_D value was $10^{5.3}$. Recovery data were also matched with the Walton type curve $r/B = 0.5$ (fig. 14c). The positive skin effect of $S = 10$ indicates either damaged wellbore conditions that restricted inflow of formation water into the well or partial penetration of the well in only part of the aquifer. Calculated transmissivities (table 3a) for well 99 range from 0.23 to 3.09 ft²/d (0.021 to 0.287 m²/d). Permeability calculations (table 3b) range from 0.0037 to 0.049 ft/d (0.0011 to 0.015 m/d).

Well 107 Slug Test

An aquifer test was conducted at well 107, the Tierra Del Sol windmill, on September 30, 1989. Well 107 is an abandoned windmill located approximately 6,000 ft (1,829 m) southeast of Arroyo Alamo Dam no. 3. This well is completed in the Hueco Bolson silt and sand aquifer. The original well construction is unknown except for the 4-inch (10.2-cm) surface casing. Upon arrival at this windmill, production equipment included 368.7 ft (112.4 m) of sucker rods (parted at the surface) and the same amount of 2-inch (5.1-cm) production pipe. The fan on the tower had been severely damaged, apparently by high winds. All sucker rods and production pipe were removed from the well. Well 107 has a total depth (as reported by driller) of 450.0 ft (137.2 m). Attempts to lower a 4-inch (10.2-cm) submersible pump below 40 ft (12.2 m) were unsuccessful because of either a downhole obstruction or wellbore diameter reduction.

Measured water level in well 107 was 347.1 ft (105.8 m) below land surface (3,855 ft [1,175.0 m] above sea level). A test was attempted from September 17 to September 19 using a piston pump with a maximum discharge rate of approximately 1 gpm, or 192 ft³/d (5.45 m³/d). After 24 hr of pumping, the water level in the well had been lowered by less than 5 ft (1.5 m), all of which could be attributed to wellbore storage. As previously discussed, the completion of this well did not allow for production equipment capable of higher discharge rates and therefore a slug

test (Ferris and Knowles, 1954; Cooper, Bredehoeft, and Papadopulos, 1967; Papadopulos, Bredehoeft, and Cooper, 1973; Bouwer and Rice, 1976; and Kipp, 1985) was performed.

The slug test began at 16:51:37 hr on September 30, 1989. To start the test, approximately 100 gal, or 13.4 ft³ (0.38 m³), of water were poured into the well as rapidly as possible (hence the term "slug"). Water level rose 108.37 ft (33.0 m) in 4.3 min after the start of the slug. The water level drained back to 351.9 ft (107.2 m), equivalent to 95.6 percent recovery, within 58 min. Water-level variations throughout the slug test are illustrated in figure 15a.

Recovery curves using the methods described by Ferris and Knowles (1954) and Cooper and others (1967) are illustrated in figures 15b and c, respectively. The method of Bouwer and Rice (1976) for analyzing slug test data from unconfined aquifers (using AQTESOLV) was also conducted for comparative purposes (fig. 15d). Transmissivity values for well 107 range from 3.6 to 81.4 ft²/d (0.334 to 7.56 m²/d). Permeability calculations range from 0.035 to 0.791 ft/d (0.0107 to 0.241 m/d). The type curves described by Cooper and others (1967) also provide a method for estimating the storage coefficient of the well. On the basis of the type curve designated as the best fit for this well, a storage coefficient of 10⁻⁵ was calculated. This method provides possible storage coefficients only within the range of 10⁻¹ to 10⁻⁵. The program AQTESOLV, however, provides a much greater range of type curves and storage coefficients, 10⁰ to 10⁻¹⁰, for matching with data sets. Matching the recovery data from well 107 with the type curve having a storage coefficient that equals 10⁻⁸ provides, at least visually, a much better type curve fit than does the curve for 10⁻⁵ (fig. 15e). The results of analysis of transmissivity and permeability for this slug test are given in table 3c.

Well 126 Slug Test

An aquifer test was conducted December 7 to 8, 1988, at well 126, located in the center of the principal study area (fig. 1). This monitoring well was drilled in 1986 as part of regional characterization studies for the TLLRWDA. It was reentered during 1988 and core was taken to a

depth of 675 ft, where Cretaceous shales were encountered. The well was completed in the Hueco Bolson silt and sand aquifer (fig. 16).

Measured water level in well 126 was 478.9 ft (146.0 m) below land surface (4,178 ft [1,273 m] above sea level). An aquifer test was conducted from December 7 to December 8, 1988, and used a piston pump with a maximum discharge rate of approximately 0.74 gpm, or 144.4 ft³/d (4.09 m³/d). After 26 hr of pumping, the water level in the well had been lowered by less than 3 ft (0.9 m), all of which could be attributed to wellbore storage. Because these were the same conditions as were experienced in well 107, plans were made to perform a slug test to evaluate the water-bearing characteristics of this well.

The slug test began at 10:00:18 hr on September 13, 1989. To start the test, approximately 104 gal, or 14.2 ft³ (0.40 m³), of water was injected into the well. The initial water level prior to injection of water was 478.9 ft (146.0 m) below land surface. Water level rose 44.867 ft (13.67 m) in 12.5 min. The test ended after another 60.6 min, when 100 percent recovery of the original water level had been achieved.

The results of this slug test were noticeably different from the results obtained from well 107 (compare fig. 17a with 15a). Approximately 521 sec into the recovery phase of the test at well 126, a significant delay in recovery was encountered (fig. 17a). This delay clearly divides the period of recovery into two phases, to be referred to as the early phase and the late phase.

The early phase of recovery was analyzed with the same methods used to analyze data from the slug test at well 107. Transmissivity values (table 3c) for this well range from 3.96 to 34.4 ft²/d (0.367 to 3.20 m²/d) for the early phase and from 11.7 to 49.0 ft²/d (1.09 to 4.55 m²/d) for the late phase. Results of analysis for permeability (table 3c) for the early and late phases range from 0.033 to 0.284 ft/d (0.010 to 0.087 m/d) and from 0.097 to 0.405 ft/d (0.0295 to 0.123 m/d), respectively. A storage coefficient of 10⁻⁵ was calculated on the basis of the matched type curve.

The delay anomaly in recovery makes analysis of the late phase of this test more problematic. Development of slug-test procedures and analytical methods has dealt with some causes for deviation of a data curve from a type curve. Papadopulos and others (1973) and Kipp (1985), for

example, discuss possible effects of wellbore storage, skin factors, or inertial effects. Analysis of the recovery curve from well 126 with solutions for these factors did not, however, indicate that these are potential factors in the recovery delay.

The early phase of recovery did result in a reasonable fit with type curves, whereas the late phase did not. Using the method described by Ferris and Knowles (1954) to analyze the late phase, after the delay in recovery, does not yield reasonable results (fig. 17c). Separate analysis of early and late phases was also possible using the Bouwer and Rice (1976) method (figs. 17d and 17e). Any attempts, however, to match the late phase with the type curves of Cooper and others (1967) were clearly unreliable, and no calculations were made.

A clear understanding or explanation for the delay in recovery seen in the slug test was not possible with currently available information. A possible scenario that could explain this delay is the presence of an isolated high-permeability lens or fracture of finite extent at about 23 ft above the transducer (fig. 17a). Incomplete cementation of the casing could allow the water column to rise behind the well casing. As water is poured into the wellbore, the water-level rise is reduced when a high-permeability lens or fracture behind the casing is filled. Conversely, as the water level in the well drops below the fracture, water drains out of the pocket, resulting in a stationary water level. Retesting this well, perhaps with different volumes of water for injection, might provide some insight into this question.

Summary of Hydraulic Properties

Water levels in all the tested wells in the bolson and Cretaceous aquifers show semidiurnal fluctuations, representing the influence of barometric pressure variations. Semidiurnal variations are typical of confined and semiconfined aquifers.

Results of the aquifer tests at the different wells yielded transmissivities ranging from 0.19 to 290 ft²/d (0.018 to 26.9m²/d). Wells 22* and 98 yielded the only recovery data that fit the early part of the recovery (fig. 6b). Except for well 22, all other tests showed discrepancies in calculated

transmissivity greater than one order of magnitude. In these cases, the early part of the recovery showed a steeper rise in water level than would be expected for wellbore storage conditions reflected by the 45° slope of the type curves. On the other hand, the early part of the recovery is not as steep as the Theis curve, suggesting possible wellbore storage effects or a change in wellbore storage (table 3a). The Agarwal method gave transmissivities that were generally higher by one order of magnitude than estimates from the other methods used. As discussed previously, the Agarwal method overestimates transmissivity because it neglects potential leakage. Type-curve matching for the recovery tests using Theis or Walton type curves were considered to yield more representative aquifer parameters than did the semilog approximations. In general, results from these methods agree reasonably well. Cretaceous wells 22 and 22* at the principal study area had the lowest permeabilities of 0.028 and 0.0064 ft/d (0.0085 to 0.002 m/d) respectively, whereas wells 91 and 94, located along the Campo Grande fault, had higher permeabilities of 0.067 and 0.235 ft/d (0.02 to 0.072 m/d). Bolson well 99 near the Cavett dam, southwest of the principal study area, showed the lowest permeability of 0.0056 ft/d, whereas well 73 had the highest permeability of approximately 0.414 and 0.127 ft/d (0.126 and 0.039 m/d). Well 73 is located at the southwest corner of the principal study area. A slug test in well 126, located just south of the principal study area, indicated similar permeabilities ranging from 0.136 to 0.405 ft/d (0.0415 to 0.123 m/d), on the basis of the method of Cooper and others (1967), for confined aquifers. Aquifer tests in well 98 and a slug test in well 107 yielded permeabilities ranging from 0.029 to 0.791 ft/d (0.0087 to 0.241 m/d) for bolson deposits south of the Campo Grande fault.

HYDRAULIC-HEAD DISTRIBUTION

Regional ground-water flow in the area is inferred from a potentiometric surface map constructed from measured water levels of the Diablo Plateau, Hueco Bolson silt and sand, and Rio Grande alluvium aquifers in the study area (fig. 18). We assumed that the three hydrostratigraphic units are hydrologically connected. The composite potentiometric surface (fig.

18) shows a regional hydraulic gradient from the Diablo Plateau toward the Rio Grande, representing recharge and discharge areas, respectively, in the regional flow system. However, water-level elevations in several wells, located near the Campo Grande fault trend (Diablo Plateau wells 91, 94, and 116, and wells 72/73 and 99) are higher than those measured in wells 22 and 126, located in the principal study area. There is a relatively steep southwest gradient between the Diablo Plateau and the principal study area and a relatively gentle low northward gradient from the area along the Campo Grande fault trend toward the principal study area (fig. 18).

The potentiometric high near the Campo Grande fault (figs. 2 and 18) possibly suggests recharge along the Cretaceous outcrop near the Campo Grande fault. However, because of the high potential of evapotranspiration and the great depth to the water table below land surface in the Hueco Bolson, there is a low probability that infiltrating water would reach the water table even in the Cretaceous outcrops along the fault (Scanlon and others, 1990a, b). Alternatively, the relatively high hydraulic heads near the fault could be an extension of the high hydraulic heads from the eastern Diablo Plateau. This explanation implies the existence of a transmissive preferential ground-water flow path from the eastern Diablo Plateau toward the west, south of the study area. The latter interpretation of hydraulic-head data is consistent with interpretation of the spatial distribution of total dissolved solids (TDS) and tritium concentrations (fig. 19). Well 114 along the eastern escarpment shows relatively low TDS and high tritium concentration, and TDS values in wells 91, 94, 113, and 116 are much lower than those in wells 22 and 126 at the study area (Fisher and Mullican, 1990). Except for wells 22, 116, and 126, wells in Cretaceous strata (fig. 19) show tritium concentrations above detection limit (0.8 tritium units [TU]), indicating some recent recharge water. The high tritium concentrations in well 114 suggest rapid recharge, possibly along faults and fractures in the vicinity of the escarpment. Cretaceous strata in this area are extensively fractured in association with the dome structure of the Finlay Mountains. Tritium concentrations decrease away (fig. 19) from the eastern Diablo Plateau (Finlay Mountains) toward the Campo Grande fault, suggesting increasing ground-water ages along the flow path.

MODELING OF REGIONAL GROUND-WATER FLOW

Flow modeling was designed to test explanations of the regional flow regime in the vicinity of the study area. The planar, finite-difference model extends from the Diablo Plateau in the north toward the Rio Grande to the south (fig. 18). The northwest and southeast boundaries of the model were chosen perpendicular to the course of the Rio Grande, where interpreted head contours approximately parallel the river. Although the three aquifer units in the area, the Diablo Plateau aquifer, the Hueco Bolson silt and sand aquifer, and the Rio Grande alluvium aquifer, have different vertical and lateral distributions, available hydraulic head data for the different units do not overlap. The model incorporates the different hydrologic units in a single layer with distinct lateral permeability zones. Simulated hydraulic heads were compared with the constructed composite map of hydraulic head as a basis for adjusting the permeability distribution of the model.

Conceptual Model of Ground-Water Flow

We assume that the regional ground-water flow system is recharged on the Diablo Plateau by infiltration through fractures along arroyos; discharge occurs along the Rio Grande to the south. No recharge by infiltration is assumed to occur in arroyos or interarroyo areas within the Hueco Bolson. The different hydrostratigraphic units, the Diablo Plateau aquifer, the Hueco Bolson sand and silt aquifer, and the Rio Grande alluvium aquifer, are considered to be confined and hydraulically interconnected; regional ground-water flow can be described by a single potentiometric surface on the basis of measured hydraulic heads of the different aquifers.

Boundary Conditions

Recharge on the Diablo Plateau was represented by prescribed head conditions along the northeastern boundary. Similarly, discharge along the Rio Grande was represented by prescribed hydraulic heads equivalent to land-surface elevation along the Rio Grande channel. Boundary nodes do not exactly follow the stream course; however, this has negligible effects on the simulation results because of the relatively high permeability of the Rio Grande alluvium. The northwest and southeast boundaries of the model were considered no-flow boundaries. The model includes only recharge on the Diablo Plateau and discharge along the Rio Grande. By assigning prescribed heads in the planar model, lateral recharge is assumed to occur along the model boundary on the Diablo Plateau which, in fact, is a ground-water flow divide. However, recharge occurs locally on the plateau by infiltration through fractured Cretaceous rocks exposed at or near the surface along arroyos. However, because of lack of detailed information on recharge rates and recharge locations, prescribed hydraulic head conditions were used with artificially reduced transmissivities of Cretaceous rocks on the Diablo Plateau. This approach is considered a reasonable approximation since the focus of the study is on ground-water flow in the Hueco Bolson.

Delineation of Permeability Zones

Twelve zones of differing permeability in the model are delineated on the basis of the overall geologic setting, information on depositional environments, and hydraulic characteristics inferred from the overall head distribution. In general, initial estimates of transmissivities for the different facies (table 4) are based on aquifer test results in wells throughout the study area (table 3). The boundaries of permeability zones and assigned values of transmissivities were adjusted on a trial-and-error basis.

Diablo Plateau aquifer

Within the Diablo Plateau aquifer, four permeability zones were distinguished:

(1) Kreitler and others (1987) indicated that transmissivities for the Cretaceous strata on the Diablo Plateau range from 0.32 to 6,700 ft²/d (0.029 to 622 m²/d) and have a mean value of 21 ft²/d (1.9 m²/d), on the basis of aquifer tests conducted in wells to the northeast of this study area. Those wells occur along major regional flexure trends and thus may encounter somewhat higher transmissivities than those in the Diablo Plateau in the present study area. Using the mean value of transmissivity did not give reasonable results in initial flow simulations. This is due to the fact that by representing recharge on the Diablo Plateau with prescribed hydraulic heads, too much ground water enters the model along the northern boundary. Recharge occurs through fractures along arroyos. Consequently, recharge water is restricted by artificially reducing transmissivity in some areas. Cretaceous strata on the Diablo Plateau are subdivided into a low-transmissivity area in the west (zone 1) and a high-transmissivity area in the east (zone 2), representing the Finlay Mountains (fig. 20; table 4).

(2) Cretaceous strata that crop out locally near the Campo Grande fault were assumed to have somewhat higher permeabilities associated with fractures. The aquifer test in well 91 ($T = 24.1$ ft²/d [2.24 m²/d]) suggested the presence of a fracture, whereas no fracture could be inferred in tests at well 94 ($T = 3.54$ ft²/d [0.329 m²/d]). This particular permeability facies (zone 6) includes the area just north of the main fault trace of the Campo Grande fault (fig. 20), where Cretaceous strata crop out locally. Bolson deposits markedly thicken as Cretaceous strata dip to depths as great as 800 ft (240 m) to the northeast and are downfaulted to depths of several thousand feet to the southwest (fig. 2). Also, Cretaceous strata dip along the strike of the fault to the northwest and southeast, away from the outcrops that are south and southwest of the principal study area (near wells 91, 94, and 116).

(3) Cretaceous rocks were also tested at the principal study area at great depth (between 600 and 800 ft [180 and 240 m] below land surface) in well 22 and have relatively low transmissivities of 0.19 and 0.81 ft²/d (0.018 and 0.075 m²/d). At this well, the overlying bolson deposits were unsaturated. A permeability facies is included in the model (zone 5), south of the Diablo Plateau escarpment, representing relatively low permeability Cretaceous rocks. Overlying bolson sediments in this zone were assumed to be hydrologically insignificant.

(4) Near the Diablo Plateau escarpment, the regional dip of Cretaceous strata changes from a northeast to a southwest direction, reflecting a flexure in the vicinity of the escarpment. The escarpment also represents a significant drop in land-surface elevation. The observed steep hydraulic gradient in the vicinity of the escarpment indicates potential vertical flow in the subsurface associated with the topographic relief. However, the model is a planar, single-layer representation of the aquifers that can only represent horizontal flow. Projecting the hydraulic gradient into the horizontal plane results in a steeper hydraulic gradient than that which is actually observed. This apparently steeper gradient in the vicinity of the escarpment is represented in the planar model by an area of relatively low transmissivity of the Cretaceous strata. Topographic gradients in the vicinity of the Finlay Mountains, part of the Diablo Plateau east of the principal study area, are not as steep as those farther to the west, implying a smaller vertical-flow component and concomitantly a lower hydraulic gradient. Thus, transmissivities along the escarpment in the eastern part (zone 4) are assumed to be higher than those along the escarpment further to the west (zone 3).

Hueco Bolson silt and sand aquifer

The Hueco Bolson silt and sand aquifer was subdivided into three permeability zones:

(1) Bolson deposits north of the Campo Grande fault were tested in wells 73 (T = 80.0 ft²/d [7.42 m²/d]) and 126 (T = 28.4 ft²/d [2.60 m²/d]), indicating relatively permeable bolson deposits. These two wells may be characteristic of a sand-dominated deposit, perhaps representing a fluvial

channel. Well 126 is located along the axis of the basin in the extension of the major canyon cutting into the Diablo Plateau northeast of the principal study area. This suggests that a sand-rich deposit with relatively high transmissivities coincides with the basin axis north of the Campo Grande fault (zone 9) (fig. 18). Well 73 is located just south of the basin axis and its relatively high transmissivity may represent a tributary sand channel to the main east-west channel along the basin axis (or may be part of a broad braided stream channel along the basin axis).

(2) Well 99, located near the fault, yielded a relatively low transmissivity of 0.35 ft²/d (0.033 m²/d). This well may be characteristic of sand-poor bolson deposits adjacent to the sand channels.

(3) South of the Campo Grande fault, bolson deposits were tested in wells 98 (T = 6.13 ft²/d and 2.87 ft²/d [0.570 and 0.267 m²/d]) and 107 (T = 12.0 ft²/d and 81.4 ft²/d [1.11 and 7.56 m²/d]). These bolson deposits in the main graben are several thousand feet thick, but only the upper part is assumed to have significant permeability. Furthermore, it is assumed that the upper bolson deposits thin toward the east and are represented by decreasing transmissivities from west to east (zone 10).

Rio Grande alluvium aquifer

Transmissivities of the Rio Grande alluvium have been reported to range from about 4,500 to 20,700 ft²/d (418 to 1,923 m²/d) in the El Paso area. Data from the Fort Hancock area are not available, but transmissivities can be assumed to be somewhat lower (1,000 ft²/d [93 m²/d]) on the basis of lower overall ground-water production in the area (zone 11).

Additional permeability zones

(1) The Campo Grande fault displaces Cretaceous rocks that crop out locally against bolson deposits to the south (fig. 2). Along the strike of the fault, Cretaceous strata also dip to greater depth, and saturated bolson deposits are continuous across the fault in the northwestern part and the southeastern part of the study area. The central fault segment south of the principal study area

may therefore act as a barrier (zone 12) between the Cretaceous rocks and the bolson deposits to the south.

(2) North of the Campo Grande fault, where bolson deposits pinch out against Cretaceous strata (fig. 2), the contact area between the two aquifer units is assumed to be represented by a low-permeability zone (zone 8). Drill cores from wells 73 and 126 indicated low-permeability shales in the uppermost part of the Cretaceous strata. This permeability zone also includes mud-rich bolson deposits adjacent to the main sand channel. The aquifer test in well 99 located just north of the fault yielded relatively low transmissivity for the bolson sediments.

(3) Information on hydraulic properties for Cretaceous rocks and/or bolson deposits in the eastern part, south of the escarpment, is not available. However, extrapolated head contours in this area suggest transmissivities that are different from Cretaceous strata near the Campo Grande fault or those on the Diablo Plateau. This particular area is designated an individual permeability facies (zone 7), representative of both Cretaceous rocks and possible saturated bolson deposits.

Discussion of Simulation Results

In a series of steady-state flow simulations, transmissivities of the different permeability zones were varied to evaluate the main controls on computed hydraulic heads. Generally, transmissivities were changed by less than a factor of 5 from representative values that were based on results from the aquifer tests. In addition, effects of the spatial transmissivity distribution on simulated heads were tested by minor modifications of the different permeability zones.

Figure 21 shows the best representation of the regional flow system. Transmissivities assigned to the different permeability zones are generally consistent with measured values (fig. 20) (table 4). The simulated distribution of hydraulic heads agrees reasonably well with the interpreted potentiometric surface (fig. 18) and reproduces the main features: the potentiometric high extending from the eastern part of the Diablo Plateau toward the Campo Grande fault and the potentiometric low area in the vicinity of the principal study area. On the basis of a series of steady-state

simulations it was found that the main controls of the regional flow pattern are the (1) preferential recharge in the eastern part of the Diablo Plateau (Finlay Mountains), (2) relatively high permeability of Cretaceous strata along the Campo Grande fault, (3) relatively high permeability of bolson deposits along the basin axis north of the Campo Grande fault, which are separated from the Cretaceous strata along the Campo Grande fault by a low-permeability zone, and (4) displacement of permeable Cretaceous- strata at the central part of the Campo Grande fault against bolson deposits to the south (fig. 18), which acts as a low-permeability zone for ground-water flow toward the Rio Grande.

Minor discrepancies between simulated heads (fig. 21) and measured hydraulic heads (fig. 18) could not be resolved by modifying transmissivities and/or facies distributions in the model. Measured hydraulic heads in well 72/73 are 3,729 ft (1,137 m), whereas simulated heads are below 3,700 ft (1,128 m). Because of the relatively high transmissivities measured in well 72/73, it was assumed that its location is within the main sand channel, although well 72/73 is located somewhat south of the basin axis. It is possible that sands encountered in well 73 represent a smaller tributary sand channel perpendicular to the main channel along the basin axis; thus, the effective average transmissivity value assigned to the corresponding model element may be lower than the value used in the simulation (fig. 21). Another possible way to expand the potentiometric high near the Campo Grande fault is to increase flow rates from the eastern Diablo Plateau toward the fault by increasing overall transmissivity of permeability zones 2, 9, and 10. However, this results in higher simulated heads in the eastern part than those observed in wells 91 and 94.

The relatively steep gradient between Cretaceous well 22 (3,644 ft [1,111 m]), at the principal study area, and nearby bolson well 126 (3,702 ft [1,128 m]) could not be reproduced. It is likely that the observed head difference between bolson and Cretaceous strata near the principal study area is due to restricted vertical hydraulic communication between the two aquifers, which is not accounted for in the planar model. The potential for reduced hydraulic communication between the Cretaceous and bolson aquifers was supported by observations during drilling of well 22. While the bolson section from 500 to 590 ft (152 to 180 m) was being cored in well 22, the

annular water level appeared to remain constant at approximately 500 ft (152 m) below land surface, similar to the water level measured in well 126. After Cretaceous strata were penetrated, however, water levels fell for several days, finally reaching a constant level of 592 ft (180.4 m) below land surface. This drop suggests that water level in Cretaceous rocks may be as much as 100 ft (30 m) below that in the bolson at well 22.

The valley in the potentiometric surface in the study area (fig. 18) can be explained by preferential drainage through relatively permeable bolson deposits along the basin axis to the west and southwest. However, if hydraulic heads are markedly lower in Cretaceous strata than in bolson sediments in the study area, which suggests limited hydraulic communication, a similar draining mechanism is required for the Diablo Plateau aquifer. Preferential drainage within the Cretaceous strata may be controlled by faults or fractures associated with the Laramide thrust fault in the area (Collins and Raney, 1990).

Simulated heads in the southeastern part of the study area, near wells 107 and 111, are somewhat higher than observed ones. This discrepancy may be due to the chosen no-flow boundary condition along the left side of the model. The relatively low hydraulic heads near the principal study area imply drainage along a relatively permeable zone toward the west and to the southwest across the Campo Grande fault (fig. 18). Because of the no-flow boundary, all the ground-water flow is channeled through a relatively narrow zone across the fault trace (fig. 20). As a result, the simulated head contours in the southwestern part of the model are deflected toward the Rio Grande. If the model extended farther to the northwest, the ground-water flow across the Campo Grande fault trace in the western part could be distributed over a broader area, and simulated head contours might not show as much deflection to the south as those indicated in figure 21.

The distribution of flow vectors calculated for each model element is illustrated in figure 22. The length of the vectors are logarithmically scaled with the plot of the maximum-velocity vector (specific discharge $q = 1.77$ ft/d [0.54 m/d]) equal to the size of a grid element. The distribution of computed fluxes indicates a preferential flow path from the eastern Diablo Plateau toward the

Campo Grande fault to the southwest. Along the Campo Grande fault, the flow vectors show a more northwesterly direction parallel to the central part of the fault segment. In the eastern part of the fault zone in the study area, ground-water flow continues to the southwest toward the Rio Grande. The vectors indicate some diffraction of flow at the southeastern edge of the barrier (zone 8), representing the central segment of the fault (fig. 20). Ground-water flow, from the Cretaceous strata along the Campo Grande fault to the north toward the principal study area, appears greatly restricted by a low-permeability zone (zone 6). Ground-water flow at the principal study area is to the west and southwest across the northwestern fault segment toward the Rio Grande. Fluxes along the interpreted sand channel are relatively high, indicating that the potentiometric low at the principal study area results from preferential drainage from the high-permeability bolson deposits along the axis of the basin north of the Campo Grande fault (fig. 22).

Modeling results indicate that ground water from the bolson aquifer south of the Campo Grande fault drains into the high-permeability Rio Grande alluvium aquifer where flow is more parallel to the stream (fig. 22). The assumed transmissivity for the alluvium is two orders of magnitude higher than that for the adjacent bolson (table 4); thus the volumetric flow rate in the alluvium is much higher than that in the bolson. The addition of ground water from the bolson aquifer to the alluvium may therefore have no significant effect on the water chemistry of the Rio Grande alluvium aquifer.

Flow velocity and travel times computed by the ground-water flow model, using an assumed range of porosities for Cretaceous and bolson strata, are strongly dependent on the accuracy of regional transmissivity estimates assigned to the different permeability zones (fig. 20). Transmissivities based on aquifer tests are representative only of the aquifer rock volume in the immediate vicinity of the well. Because of lack of recharge estimates for the Diablo Plateau, only a prescribed-head boundary condition was applied in the model; thus, a proportionate increase or decrease of transmissivity for the different permeability zones would not change hydraulic-head distribution (fig. 21) and flow pattern (fig. 22) for steady-state simulation, although the magnitude of flow velocity would differ. Model calibration evaluated sensitivity to transmissivities, which

were modified as little as possible from values inferred from the aquifer test results. However, calculated flow velocities and travel times (figs. 21, 22) are compared with water chemistry data, as discussed below.

Relationship between Ground-Water Flow and Water Chemistry

As discussed above, the distribution of total dissolved solids and tritium concentrations assisted in the construction and interpretation of the potentiometric surface map (fig. 18). Tritium concentration above detection limit in wells 91 and 94 (fig. 19) suggested a flow path from the eastern Diablo Plateau to the south toward the Campo Grande fault. On the basis of calculated fluxes for each model element in figure 22, travel times were estimated assuming representative porosities along the flow path. For the distance between the eastern escarpment (Finlay Mountains) to well 94 (5 mi; 8 km), calculated travel times range from 32 to 320 yr, assuming effective porosities of 2.5 and 25 percent, respectively, along the flow path (fig. 22). Assuming that the observed tritium in well 94 originates from recharge along the escarpment near the Finlay Mountains and ground water flows mainly through low-porosity Cretaceous rocks, one would expect detectable tritium in the ground water about 5 mi (8 km) away from the recharge zone (at well 94) after 32 yr, because original tritium concentrations in the recharge water would have decreased by radioactive decay (half-life of 12.4 years).

Ground-water travel times calculated along a flow path from the central part of Diablo Plateau to the study area (fig. 21), for a distance of about 6 miles (9.6 km), range from 204 to 2,040 yr, assuming effective porosities of 2.5 and 25 percent, respectively. Thus, no tritium concentration can be expected in water samples from wells near the study area (fig. 19). However, transmissivities assigned to the permeability zones on and near the escarpment are based on limited data; simulated hydraulic heads are not very sensitive to transmissivities along the western escarpment and do not constrain the lower limit of hydraulic properties. Consequently,

transmissivities in that area may be lower by a factor of 10 or more than those used in the flow simulation (figs. 21, 22), resulting in much longer travel times toward the study area.

The calculated carbon-14 age from well 126 (28,817 yr) at the principal study area is much greater than the calculated travel time from the recharge area on the plateau to the principal study area (Fisher and Mullican, 1990). However, carbon-14 ages from wells on the Diablo Plateau, representing the recharge area, range from less than 1,000 yr, indicating recent recharge, to as much as 13,000 yr. The presence of detectable tritium in wells with carbon-14 ages greater than 1,000 yr was attributed to mixing of older ground water with recent recharge water (Fisher and Mullican, 1990). Assumptions used for the carbon-14 age calculations can produce a significant range in the age (Fisher and Mullican, 1990); thus, the utility of carbon-14 data may be limited in calibrating travel-time calculations in a numerical model.

The inferred flow associated with the distribution of total dissolved solids (fig. 19) agrees in some areas with the simulated flow pattern (fig. 22). Relatively low TDS values are found along the preferential flow paths from the eastern Diablo Plateau to the south toward and along the Campo Grande fault. Furthermore, well 98 shows lower TDS values than do wells 22 and 126 in the study area. Although the Campo Grande fault acts as a low-permeability barrier, its transmissivity (zone 8) is assumed to be higher than that of the low-permeability zone 6 (table 5) that separates the Cretaceous rocks along the fault from the sand-rich bolson deposits north of the fault. The diffraction of flow vectors at the southeastern edge of the barrier (zone 8) indicates a relatively high-velocity flow path from the eastern escarpment toward well 98 (fig. 22).

The transmissivities of the sand-rich bolson deposit along the axis of the basin (zone 7, fig. 20), north of the fault, are relatively high (table 3) and imply a potential for relatively rapid groundwater flow (fig. 22). However, recharge to this area is greatly restricted, compared with that to the eastern part of the model. Consequently, ground water that has been in contact with the aquifer rock near the principal study area for a longer time may be reflected in the higher TDS (fig. 19).

Implication of Paleohydrologic Conditions

Late Quaternary evolution of the Rio Grande valley resulted in the incision of the stream bed between 25,000 and 10,000 yr ago (Gile and others, 1981) by as much as 200 ft (60 m). Within the last 10,000 yr, the base level of the Rio Grande remained stationary. This suggests that water levels were significantly higher in the Hueco Bolson in the recent geologic past than at present. It can be assumed, however, that water levels on the Diablo Plateau may not have been significantly higher than those of today because additional ground water on the plateau would have been discharged through springs and seeps along the escarpment.

The possibility that hydraulic heads are still responding to the Quaternary changes in geomorphology (i.e., transient conditions) can be precluded on the basis of relatively rapid ground-water flow (fig. 22), particularly in the eastern part of the study area. That is, the observed hydraulic heads represent steady-state flow conditions. Calculated ground-water travel times in the eastern part of the model were low, as indicated by relatively young ground water with detectable tritium concentrations in wells 91 and 94 (fig. 19). However, in the central part of the regional study area, carbon-14 age dates suggest that ground water is as much as 28,000 yr old (Fisher and Mullican, 1990), which implies that these waters were recharged prior to the Quaternary Rio Grande incision.

Note that the contours of total dissolved solids show only minor deflection across the Campo Grande fault trace (fig. 19), whereas the simulated flow pattern indicates near-parallel flow along the fault (fig. 22), oblique to the TDS contours. Prior to the Rio Grande incision, water levels in the vicinity of the Campo Grande fault may have been as much as 100 ft higher than those observed today, resulting in a thicker saturated bolson section across the fault. The fault may have acted much less as a barrier to flow than is inferred for the present (figs. 21, 22), and regional ground-water flow was probably more in a northeast-southwest direction across the fault, parallel to the TDS contours.

Carbon-14 ages of water samples from wells south of the Campo Grande fault (well 98: 6,090 yr; well 107: 14,747 yr; well 111: 6,914 yr) are noticeably younger than those at the principal study area (well 126: 28,718 yr) (Fisher and Mullican, 1990). Water levels prior to the Rio Grande incision can be expected to have been much closer to land surface, particularly near the river, than those observed today. In addition, recharge rates in the past were probably higher than rates of today because of a wetter climate. The lower evapotranspiration potential and the shorter travel time for infiltrating surface water to reach the water table in the recent geologic past (>10,000 yr) may explain these relatively young ground waters south of the Campo Grande fault. Lateral ground-water flow was significantly reduced in the past due to a lower hydraulic gradient in the Hueco Bolson associated with the higher base level of the Rio Grande. Local infiltration in the Hueco Bolson may therefore have dominated the ground-water chemistry in this area.

EVALUATION OF GROUND-WATER RESOURCES, HUDSPETH COUNTY

Water Usage

The main water usage within the regional study area is irrigation of cropland near the Rio Grande. Both diverted river water and ground water have been used for this purpose. Surface water from the Rio Grande was first appropriated for irrigation in 1918 (Young, 1981). Since then, various treaties and contracts have served to distribute waters from the Rio Grande for irrigation. The current agreement, the Rio Grande Federal Irrigation Project, has failed to appropriate any primary water rights from the Rio Grande to the Fort Hancock District. Fort Hancock does, however, have secondary rights to return flow and surplus waters (Young, 1976).

Because of severe drought conditions in the Rio Grande drainage basin from 1951 to 1957, the amount of water available for irrigation dropped from an average 354,000 acre-ft per annum (1941 to 1950) to 44,000 acre-ft per annum (1951 to 1957) (Young, 1981). This reduction in available water for irrigation resulted in the drilling of 148 irrigation wells in 1954 in the Hudspeth

Valley (the Rio Grande valley from the El Paso–Hudspeth county line to where the Guayuca Arroyo enters the Rio Grande near the site of Old Fort Quitman) to supplement available river water. During 1954, 27,000 acre-ft of ground water was produced to irrigate approximately 12,000 acres. High salinity and low capacity resulted in the abandonment of 50 of these wells by 1955 (Lyerly, 1957).

Using data from Alvarez and Buckner (1980), Young (1981) calculated that for the five Hudspeth Valley 7.5-minute quadrangles (PD 48-33, PD 48-41, PD 48-42, PD 48-50, and PD 48-51) adjacent to the Rio Grande, salt content of waters used to irrigate in 1955 ranged from 4.14 to 7.55 tons per acre-ft. These values indicate very high sodium hazard and exceed recommended limits of TDS for irrigation water. Davis and Leggat (1965) reported that the salt content averaged 5.34 tons per acre-ft in 56 wells tested in Hudspeth County.

Young (1976) reported that the Fort Hancock Water Control and Improvement District, established in 1952, served 154 customers in the community in 1975. Recorded average annual water usage by the Fort Hancock municipality ranged from 6.5 million gal in 1965 to 10,530,460 gal in 1970 (Young, 1976). Records indicate that as of 1986, 195 customers were served and the water usage for the year was 16,100,000 gal. Fort Hancock used well 108 (TWC # 48-42-404) as the municipal supply well during 1988–89 (table 5; fig. 1). This well probably is producing from both Rio Grande alluvial deposits and the Hueco Bolson deposits. Although quality of water from this well is better than that of water from wells previously used (48-42-702 and 48-42-708), it still fails to meet drinking water standards set by the Texas Department of Health for maximum acceptable levels of sulfate (300 mg/L recommended; 469 mg/L measured May 1, 1989) and TDS (1,000 mg/L recommended; 1,511 mg/L measured May 1, 1989). Young (1976) concluded that with rare exception, the quality of ground water in the Fort Hancock area is poor and would require treatment to remove dissolved inorganic solids. He also stated that ground water from Rio Grande alluvial deposits is probably contaminated by recharging irrigation waters containing pesticides, herbicides, and fertilizers and also would require treatment for use as drinking water.

Water Supply

The Texas Water Commission (TWC) and the Texas Department of Water Resources (TDWR) have divided Hudspeth County into three major aquifer subregions and two minor aquifer subregions with regard to ground-water resources (TDWR, 1984). The major aquifers include Rio Grande alluvial deposits, Red Light Bolson deposits, and Salt Basin alluvial deposits. The two minor aquifer subregions include the Victorio Peak and Bone Springs limestone aquifers of the Dell City Irrigation District and a local area of Capitan Limestone along the Hudspeth-Culberson county line (TDWR, 1984). Previous water and resource studies focused on the economically important surface water in the Rio Grande and ground water in adjacent alluvium (Leggat, 1962; Peckham, 1963; Davis and Leggat, 1965; Alvarez and Buckner, 1980).

Within a 10-mi (16.1-km) radius of the study area, however, TDWR (1984) did not map a major or minor aquifer system. Previous investigations of the hydrology of West Texas generally failed to identify ground-water resources within the Hueco Bolson of Hudspeth County. Smith (1956) located no water wells in the Hueco Bolson of Hudspeth County. Leggat (1962) identified four water wells within the area examined by Smith (1956) and described them as yielding small to moderate quantities of water too highly mineralized for municipal use. Well U-8 was the most promising water supply well, with a reported discharge rate of 50 gpm (272 m³/d) and TDS of 2,160 mg/L (Leggat, 1962). This well was probably used by the Soil Conservation Service during the construction of the Arroyo Alamo Reservoir no. 3 flood control dam and abandoned after completion of the structure. Davis and Leggat (1965, their plate U1) indicated six water wells in the Hueco Bolson of Hudspeth County, four of which are within 10 mi (16.1 km) of the study area, and simply stated that the wells probably produced from Cretaceous Cox sandstone. Gates and Stanley (1976) reported that the discovery of significant usable ground-water resources from Cretaceous strata was unlikely. They cited poor water quality due to slow water circulation, low permeabilities, and the presence of soluble minerals.

As part of this investigation, 16 water wells and 1 spring producing from saturated sections within Hueco Bolson silts and sands and Cretaceous limestones and sandstones have been located, tested, and sampled within a 10-mi (16.1-km) radius of the study area (table 5).

Within the hydrologic study area, ground water is used to meet ranching, irrigation, and municipal needs. Ground-water requirements for ranching are met by wells that typically yield fresh to slightly saline waters from low-transmissivity formations. Windmills, pump jacks, and submersible pumps are used to produce water in isolated areas of the Hueco Bolson and Diablo Plateau. Wells are usually separated by several miles, and pipelines are often used to distribute the water to various impoundments for watering livestock. Dirt tanks have also been constructed by some of the ranchers across minor drainages to catch and hold precipitation runoff (fig. 23). The seasonal evaporation rate (relatively high in summer, low in winter) and permeability of sediments lining the tanks (sand, silt, or clay) dictate the duration that surface water is available for livestock.

Current and potential water resources in the area of the principal study area are minimal. The highest sustainable discharge rate of any well tested during this study was equal to 12 gpm, or 2,351 ft³/d (66.6 m²/d), measured at well 91. All well waters sampled during this study exceed maximum acceptable concentration levels for one or more of the following: total dissolved solids, sulfates, chlorides, or nitrates. Due to the heterogeneity of the Hueco Bolson strata and the limited number of wells, it is unlikely that a new significant water resource of acceptable water quality will be identified from bolson strata within the regional study area. The potential for new water resources from Cretaceous limestones is more problematic. There is always the potential in such a hydrologic system for a well-connected open fracture system that could significantly, but locally, enhance the hydraulic conductivity. To date, only one possible fracture has been identified from aquifer tests in the study area (well 91). As has been documented in the Dell City Irrigation District, however, the probability of intersecting productive fracture systems in any given well is 0.01 to 0.1 (Logan, 1984). The great depth to Cretaceous strata beneath the study area and much of the bolson (300 to 700 ft), the high cost to lift water from these depths, and the previous failure

to locate a high-transmissivity fracture system, suggest that future efforts to explore for such resources will be limited.

CONCLUSIONS

Regional and local hydrologic studies, performed as part of investigations for a low-level radioactive waste repository in Trans-Pecos Texas, indicate that ground-water resources in the vicinity are limited by two key factors: (1) costs of drilling and completing wells and of producing water at depths typically greater than 400 ft (122 m) and (2) very low productivity of aquifers. On the basis of nine aquifer tests and two slug tests, we found that representative transmissivities of aquifers producing from bolson and Cretaceous strata range from approximately 0.19 to 290.0 ft²/d (0.018 to 26.9 m²/d); corresponding permeabilities range from 0.0015 to 2.82 ft/d (0.0005 to 0.861 m/d).

A composite potentiometric surface was mapped on the basis of measured water levels in all available wells, assuming that the three aquifer units, (1) the Diablo Plateau aquifer, (2) the Hueco Bolson silt and sand aquifer, and (3) the Rio Grande alluvium aquifer area, are hydrologically connected. Ground water in the area of the principal study area is found at depths of 361 ft (110 m) and 478 ft (146 m) in Hueco Bolson silts and sands and 592 ft (180 m) in Cretaceous limestones. Interpretation of selected hydrochemical data assisted in the interpretation of the regional potentiometric surface map. The constructed potentiometric surface indicates regional ground-water flow recharging on the Diablo Plateau and flowing to the south and southwest discharging along the Rio Grande.

A numerical flow model was constructed for the study area to help interpret controls on the potentiometric surface. Through a series of steady-state simulations, it was found that the main controls of the regional flow pattern are (1) greater recharge in the eastern part of the Diablo Plateau (Finlay Mountains) than in the western part, (2) relatively high permeability of Cretaceous strata along the Campo Grande fault, (3) relatively high permeability of bolson deposits along the basin

axis north of the Campo Grande fault, which are separated from the Cretaceous strata along the Campo Grande fault by a low-permeability zone, and (4) displacement of permeable Cretaceous strata at the central part of the Campo Grande fault against bolson deposits to the south, which acts as a low-permeability zone for ground-water flow toward the Rio Grande.

The inferred distribution of permeability zones causes a greater flow rate along a trend from the eastern Diablo Plateau toward Cretaceous outcrops along the Campo Grande fault than beneath the study area, creating the observed potentiometric high. The relatively low hydraulic heads at the study area are caused by preferential drainage along relatively permeable bolson deposits to the west and southwest toward the Rio Grande. Data on water chemistry, particularly tritium, TDS, and, to a lesser extent, carbon-14 ages, generally support the interpreted flow pattern. Some discrepancies between flow interpretation based on chemical data and physical data may be related to paleohydrologic phenomena associated with the incision of the Rio Grande during Quaternary time.

ACKNOWLEDGMENTS

This research was funded by the Texas Low-Level Radioactive Waste Disposal Authority under contract number IAC(90-91) 0268. The conclusions of the authors are not necessarily approved or endorsed by the Authority.

Special acknowledgments are given to the local residents of the Fort Hancock community for their help in locating, testing, and sampling water wells in the area. Dennis Walker, Joe Galvan, and the late Scott Wilkey have continually assisted in various ground-water investigations, and to them we extend our special thanks. Byrl Binkley and R. C. Corona were our drillers and well pullers. Their patience in dealing with our special demands has been appreciated.

Hydrologic investigations described in this report were conducted under the technical supervision of A. R. Dutton. The study benefited from discussions with him concerning aquifer test analysis.

The report was reviewed by A. R. Dutton and T. F. Hentz, and edited by Amanda R. Masterson and Bobby Duncan. Word processing was by Melissa Snell and Lucille Harrell. Illustrations were drafted by Richard L. Dillon, Wade Kolb, Joel C. Lardon, Kerza Prewitt, and Maria E. Saenz.

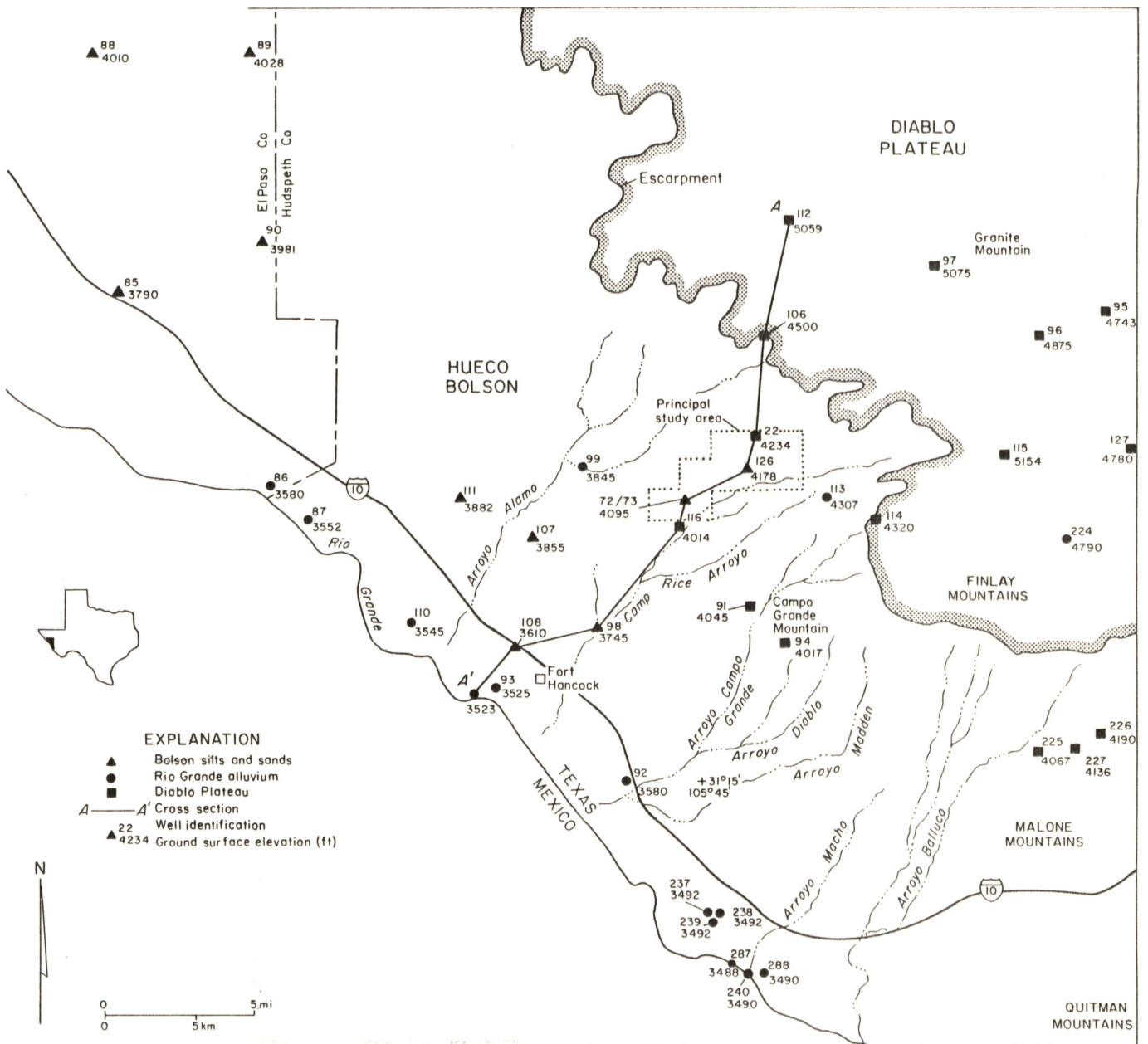
REFERENCES

- Agarwal, R. G., Al-Hussainy, Rafi, and Ramey, H. J., Jr., 1970, An investigation of wellbore storage and skin effect in unsteady liquid flow: I. Analytical Treatment: Society of Petroleum Engineers Journal, v. 10, no. 3, p. 279–290.
- Albritton, C. C., Jr., and Smith, J. F., Jr., 1965, Geology of the Sierra Blanca area, Hudspeth County, Texas: U.S. Geological Survey, Professional Paper 479, 131 p.
- Alvarez, H. J., and Buckner, A. W., 1980, Ground-water development in the El Paso region, Texas, with emphasis on the resources of the lower El Paso Valley: Texas Department of Water Resources, Report 246, 346 p.
- Bouwer, Herman, and Rice, R. C., 1976, A slug test method for determining hydraulic conductivity of unconfined aquifers with completely or partially penetrating wells: Water Resources Research, v. 12, no. 3, p. 423–428.
- Collins, E. W., and Raney, J. A., 1990, Description and Quaternary history of the Campo Grande fault of the Hueco Basin, Hudspeth and El Paso Counties, Trans-Pecos Texas: The University of Texas at Austin, Bureau of Economic Geology, contract report prepared for the Texas Low-Level Waste Disposal Authority under Interagency Contract Number IAC (90-91) 0268, 61 p.
- Cooper, H. H., Jr., Bredehoeft, J. D., and Papadopoulos, I. S., 1967, Response of a finite-diameter well to an instantaneous charge of water: Water Resources Research, v. 3, no. 1, p. 263–269.
- Cooper, H. H., and Jacob, C. E., 1946, A generalized graphical method for evaluating formation constants and summarizing well field history: American Geophysical Union Transactions, v. 27, p. 526–534.
- Davis, M. E., and Leggat, E. R., 1965, Reconnaissance investigations of the ground-water resources of the Upper Rio Grande Basin, Texas: Texas Water Commission Bulletin 6502, 213 p.
- Duffield, G. M., and Rumbaugh, J. O., III, 1989, Geraghty & Miller's AQTESOLV Aquifer Test Solver, Version 1.00, 135 p.
- Ferris, J. G., and Knowles, D. B., 1954, The slug test for estimating transmissibility: U.S. Geological Survey, Ground Water Notes No. 26, 7 p.
- Fisher, R. S., and Mullican, W. F., III, 1990, Ground-water hydrochemistry in the southeastern Hueco Bolson and southwestern Diablo Plateau, Trans-Pecos Texas: The University of Texas at Austin, Bureau of Economic Geology, contract report prepared for the Texas Low-Level Radioactive Waste Disposal Authority under Interagency Contract Number IAC (90-91) 0268, 66 p.

- Fogg, G. E., and Senger, R. K., 1985, Automatic generation of ground-water flow nets using numerical models: *Ground Water*, v. 23, no. 3, p. 336–344.
- Frind, E. O., and Matanga, G. B., 1985, The dual formulation of flow for contaminant transport modeling, 1. Review of theory and accuracy aspects: *Water Resources Research* vol. 21, no. 2, p. 159–169.
- Gates, J. S., and Stanley, W. D., 1976, Hydrologic interpretation of geophysical data from the southeastern Hueco Bolson, El Paso and Hudspeth Counties, Texas: U.S. Department of the Interior Geological Survey, Open-File Report 76-650, 37 p.
- Gile, L. H., Hawley, J. W., and Grossman, R. B., 1981, Soils and geomorphology in the Basin and Range area of southern New Mexico—guidebook to the Desert Project: New Mexico Bureau of Mines and Mineral Resources Memoir 39, 222 p.
- Gustavson, T. C., 1990, Sedimentary facies, depositional environments, and paleosols of the late Tertiary Fort Hancock Formation and the Tertiary–Quaternary Camp Rice Formation, Hueco Bolson, West Texas: The University of Texas at Austin, Bureau of Economic Geology, contract report prepared for the Texas Low-Level Radioactive Waste Disposal Authority under Interagency Contract Number IAC (90-91) 0268.
- Hantush, M. R., 1956, Analysis of data from pumping tests in leaky aquifers: *American Geophysical Union Transactions*, v. 37, no. 6, p. 702–714.
- Henry, C. D., and Price, J. G., 1985, Summary of the tectonic development of Trans-Pecos Texas: The University of Texas at Austin, Bureau of Economic Geology Miscellaneous Map No. 36, 8 p.
- Hill, R. T., 1900, Physical geography of the Texas region: U.S. Geological Survey, Topographic Atlas, folio no. 3, p. 8.
- Kipp, K. L., Jr., 1985, Type curve analysis of inertial effects in the response of a well to a slug test: *Water Resources Research*, v. 21, no. 9, p. 1397–1408.
- Knorr, D. B., and Cliett, T., 1985, Proposed groundwater recharge at El Paso, Texas, *in* Asano, T., ed., *Artificial recharge of groundwater*: California State Water Resources Control Board, Sacramento, California, and Department of Civil Engineering, University of California, Davis, California, p. 425–480.
- Kreitler, C. W., Raney, J. A., Nativ, Ronit, Collins, E. W., Mullican, W. F., III, Gustavson, T. C., and Henry, C. D., 1987, Siting a low-level radioactive waste disposal facility in Texas, volume four—geologic and hydrologic investigations of State of Texas and University of Texas lands: The University of Texas at Austin, Bureau of Economic Geology, report prepared for the Texas Low-Level Radioactive Waste Disposal Authority under Interagency Contract Number IAC (86-87)-1790, 330 p.

- Kruseman, G. P., and De Ridder, N. A., 1983, Analysis and evaluation of pumping test data (3d ed.): Wageningen, The Netherlands, International Institute for Land Reclamation and Improvement, Bulletin 11, 200 p.
- Larkin, T. J., and Bomar, G. W., 1983, Climatic atlas of Texas: Austin, Texas Department of Water Resources Publication LP-192, 151 p.
- Leggat, E. R., 1962, Development of ground water in the El Paso District, Texas, 1955–1960, Progress Report No. 8: Texas Water Commission, Bulletin 6204, 56 p.
- Logan, H. H., 1984, A ground-water recharge project associated with a flood protection plan in Hudspeth County, Texas—supportive geologic applications: Texas Christian University, Master's thesis, 110 p.
- Lyerly, P. J., 1957, Salinity problems in the El Paso area, *in* Duisberg, P. C., ed., Problems of the Upper Rio Grande, an arid zone river: U.S. Commission for Arid Resource Improvement and Development, Publication No. 1, p. 55–64.
- Meyer, W. R., 1976, Digital model for simulated effects of ground-water pumping in the Hueco Bolson, El Paso area, Texas, New Mexico, and Mexico: U.S. Geological Survey, Water Resources Investigations 58-75, 31 p.
- Mullican, W. F., III, Kreitler, C. W., Senger, R. K., and Fisher, R. S., 1989, Truly deep saturated zone investigations at the proposed low-level radioactive waste disposal site for Texas, *in* Proceedings of the Third National Outdoor Action Conference on Aquifer Restoration, Ground Water Monitoring, and Geophysical Methods: Dublin, Ohio, National Water Well Association, p. 447–461.
- Myers, B. N., 1969, Compilation of results of aquifer tests in Texas: Texas Water Development Board, Report 98, 532 p.
- Neuman, S. P., 1975, Analysis of pumping test data from anisotropic unconfined aquifers considering delayed yield: Water Resources Research, v. 11, no. 2, p. 329–342.
- Neuman, S. P., and Witherspoon, P. A., 1970, Finite element method for analyzing steady seepage with a free surface: Water Resources Research, v. 6, no. 3, p. 889–897.
- Orton, R. B., 1964, The climate of Texas and adjacent Gulf waters: Washington, D.C., U.S. Department of Commerce, Weather Bureau, 195 p.
- Papadopoulos, J. S., Bredehoeft, J. D., and Cooper, H. H., Jr., 1973, On the analysis of “slug test” data: Water Resources Research, v. 9, p. 1087–1089.
- Peckham, R. C., 1963, Summary of the ground-water aquifers in the Rio Grande Basin: Texas Water Commission, Circular No. 63–05, 16 p.
- Ramey, H. J., Jr., 1970, Short-time well test data interpretation in the presence of skin effect and wellbore storage: Journal of Petroleum Technology, January, p. 97–104.

- Sayre, A. N., and Livingston, P., 1945, Ground-water resources of the El Paso area, Texas: U.S. Geological Survey, Water-Supply Paper 919, 190 p.
- Scanlon, B. R., and Richter, B. C., 1990a, Analysis of unsaturated flow based on chemical tracers (chloride, ^{36}Cl , ^3H , and bromide) and comparison with physical data, Chihuahuan Desert, Texas: The University of Texas at Austin, Bureau of Economic Geology, contract report prepared for the Texas Low-Level Radioactive Waste Disposal Authority under Interagency Contract No. IAC (90-91) 0268, 56 p.
- Scanlon, B. R., Wang, F. P., and Richter, B. C., 1990b, Analysis of unsaturated flow based on physical data related to low-level radioactive waste disposal, Chihuahuan Desert, Texas: The University of Texas at Austin, Bureau of Economic Geology, contract report prepared for the Texas Low-Level Radioactive Waste Disposal Authority under Interagency Contract No. IAC (90-91) 0268.
- Slichter, C. S., 1905, Observations on the ground waters of Rio Grande Valley: U.S. Geological Survey, Water-Supply Paper 141, 83 p.
- Smith, R. E., 1956, Ground water resources of the El Paso District, Texas, Progress Report No. 7: Texas Board of Water Engineers, Bulletin 5603, 33 p.
- Sundstrom, R. W., and Hood, J. W., 1952, Results of artificial recharge of the ground-water reservoir at El Paso, Texas: Texas Board of Water Engineers, Bulletin 5206, 19 p.
- Texas Department of Water Resources, 1984, Water for Texas—a comprehensive plan for the future: GP-4-1, v. 1, 72 p.
- Theis, C. V., 1935, The relation between the lowering of the piezometric surface and the rate and duration of discharge of a well using groundwater storage: American Geophysical Union Transactions, v. 16, p. 519–524.
- Thorntwaite, C. W., 1931, The climates of North America according to a new classification: Geographical Review, v. 21, p. 633–655.
- Van Everdingen, A. F., and Hurst, W., 1949, The application of the La Place transformation to flow problems in reservoirs: American Institute of Mining Engineers (AIME), Transactions, v. 186, p. 304–324.
- Walton, W. C., 1962, Selected analytical methods for well and aquifer evaluation: Illinois State Water Survey Bulletin, no. 49, 81 p.
- Young, P. W., 1976, Water resources survey of Hudspeth County: West Texas Council of Governments, 156 p.
- 1981, Evaluation of surface and ground irrigation water—the Lower El Paso Valley emphasizing Hudspeth County, Texas: West Texas Council of Governments, 219 p.



QA 12297

Figure 1. Location of water wells and spring (106) within regional hydrologic study area. Study area includes Rio Grande alluvium aquifer, Hueco Bolson silt and sand aquifer, and Diablo Plateau aquifer systems.

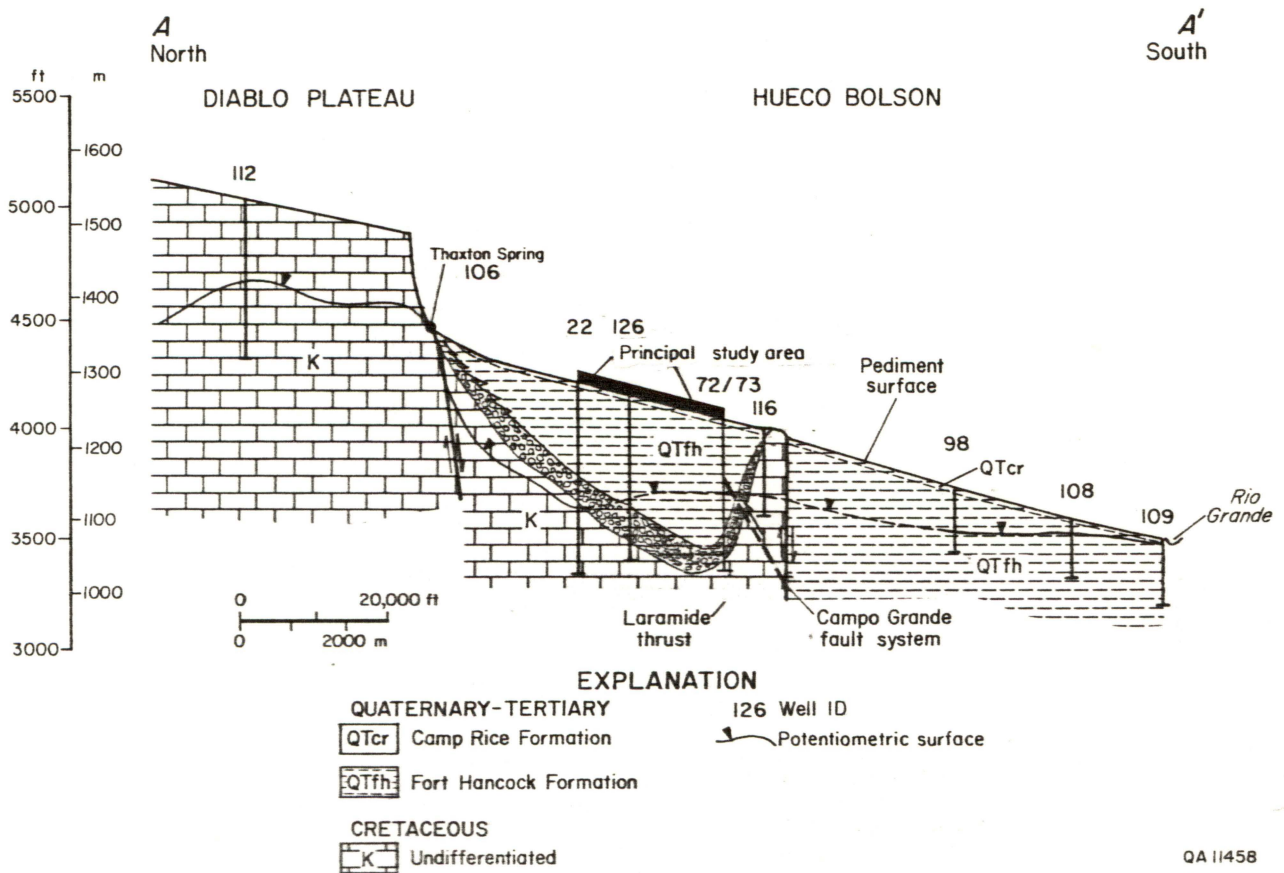


Figure 2. Hydrologic cross section illustrating relationship between potentiometric surface and stratigraphy from the Diablo Plateau to the Rio Grande. Location of cross section shown in figure 1.

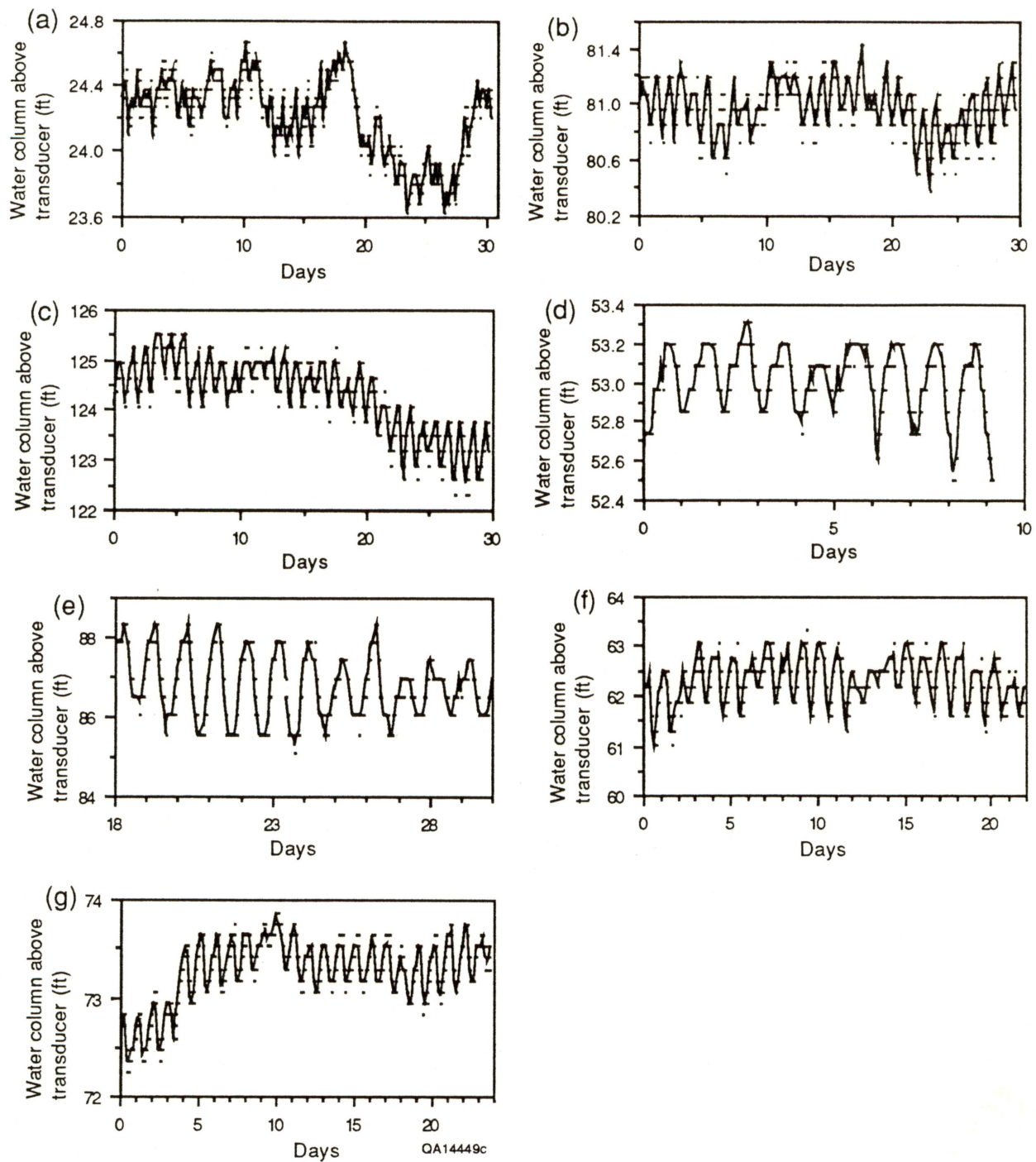


Figure 3. Fluctuations in water levels (a) in well 22 from November 8 to December 8, 1988, (b) in well 72 from December 18, 1989, to January 17, 1990, (c) in well 73 from December 18, 1989, to January 17, 1990, (d) in well 94 from October 3 to October 12, 1989, (e) in well 98 from May 18 to May 30, 1989, (f) in well 99 from November 11 to December 2, 1988, and (g) in well 126 from March 17 to April 9, 1989.

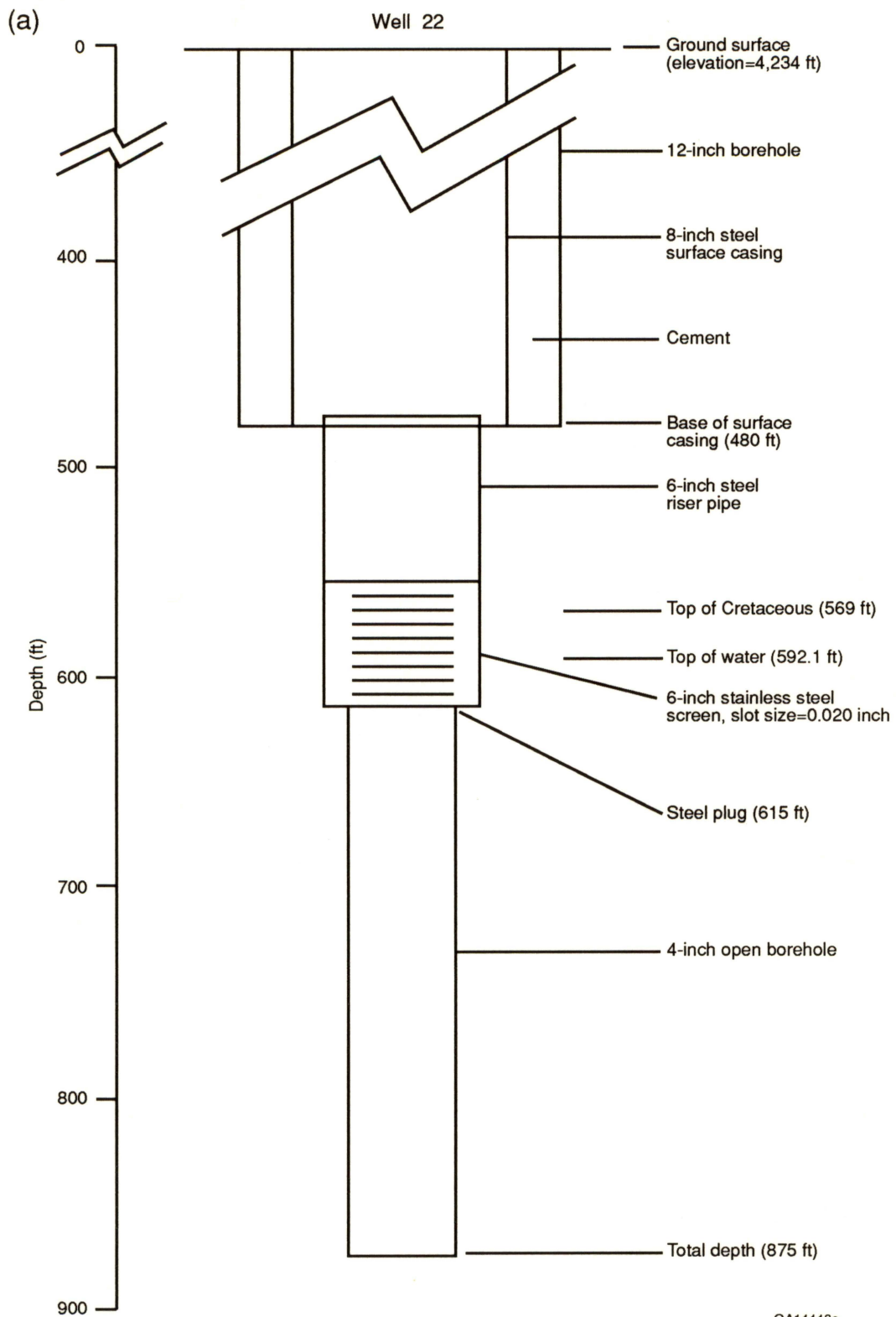


Figure 4. (a) Schematic diagram of well 22 during aquifer test conducted October 5, 1988. (b) Schematic diagram of well 22* after recompletion prior to testing conducted October 10–13, 1989.

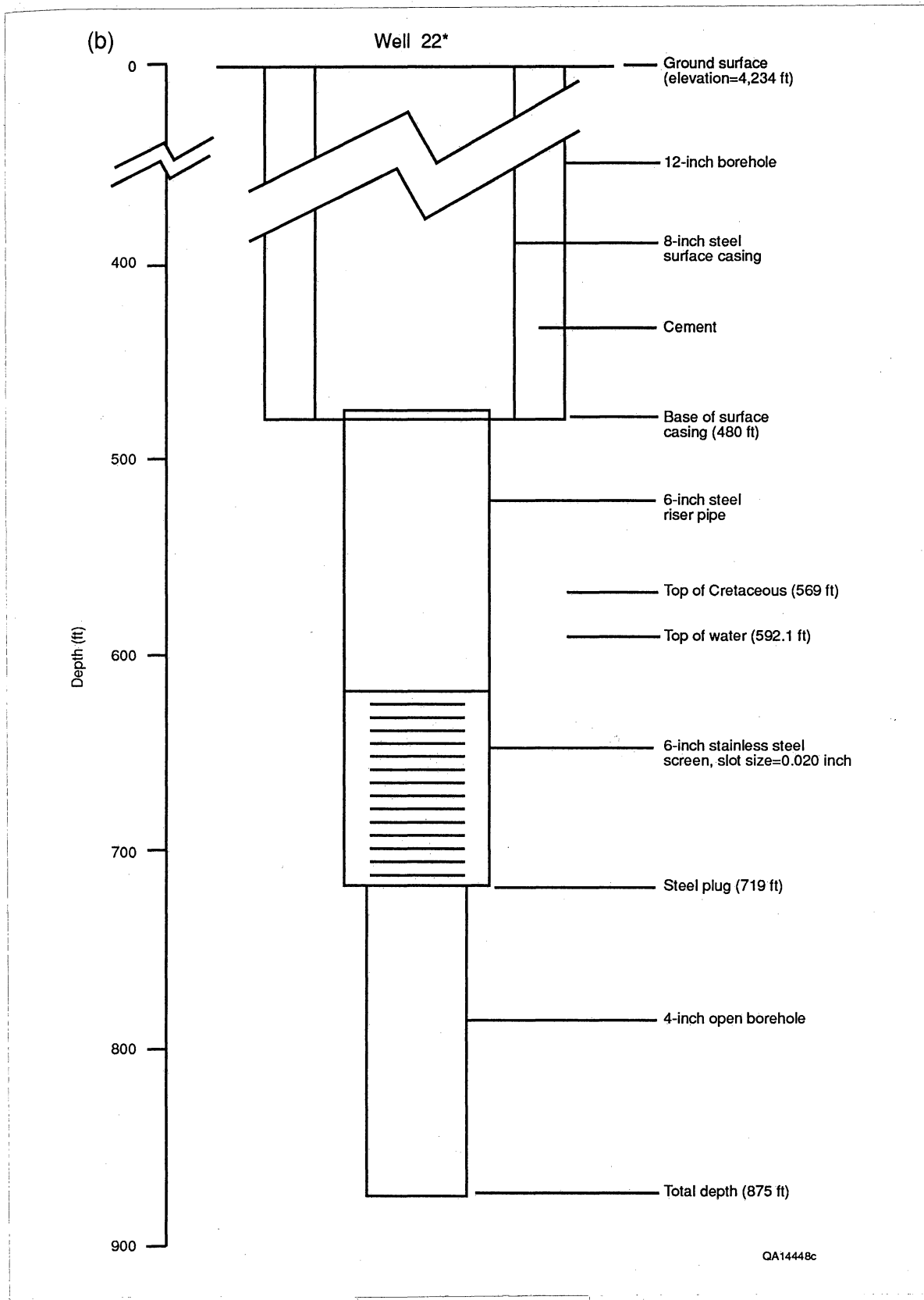


Figure 4. (cont.)

Figure 5. (a) Drawdown and recovery curves for aquifer test conducted in well 22 October 5–6, 1988. (b) Hydrologic test data during drawdown phase of aquifer test. This semilogarithmic presentation used in Jacob method of analysis. For this and subsequent figures, transmissivity and permeability values determined from this method are given in table 3. (c) Test data during recovery phase. This semilogarithmic presentation used in Theis method of analysis. (d) Test data during recovery phase. Logarithmic presentation used in matching test data with Agarwal's type curves. Hydraulic parameters used in type-curve matching include estimated dimensionless wellbore storage of $C_D = 10^{6.3}$ and skin effect (S) = 5. (e) Test data during drawdown phase. Logarithmic presentation used in matching test data with Theis type curve. Only data after first 40 min of drawdown were used to match curve. (f) Test data during recovery phase. Logarithmic presentation used in matching test data with Walton type curve $r/B = 0.6$.

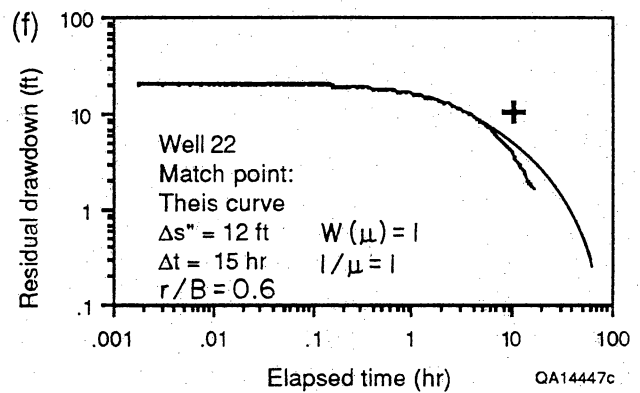
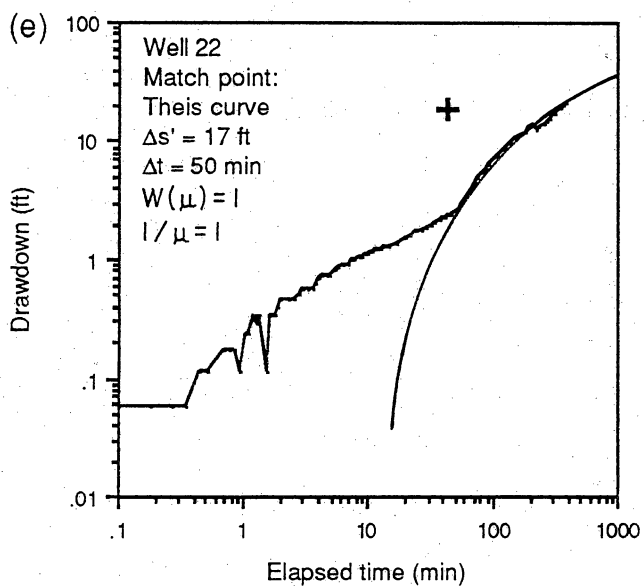
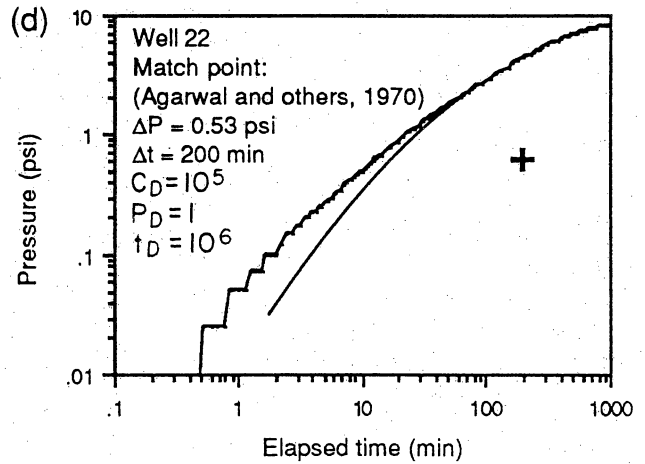
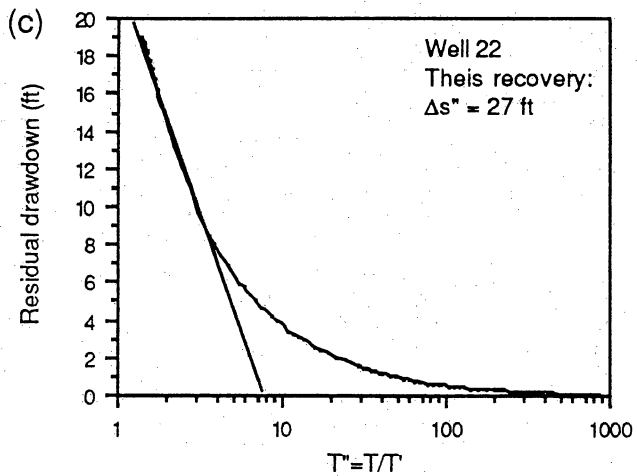
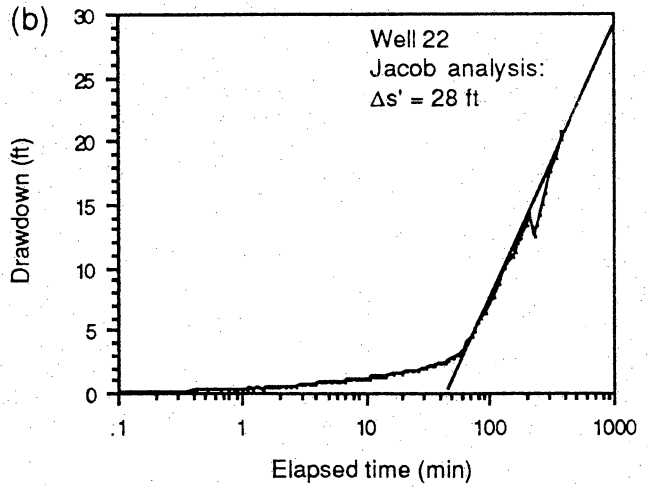
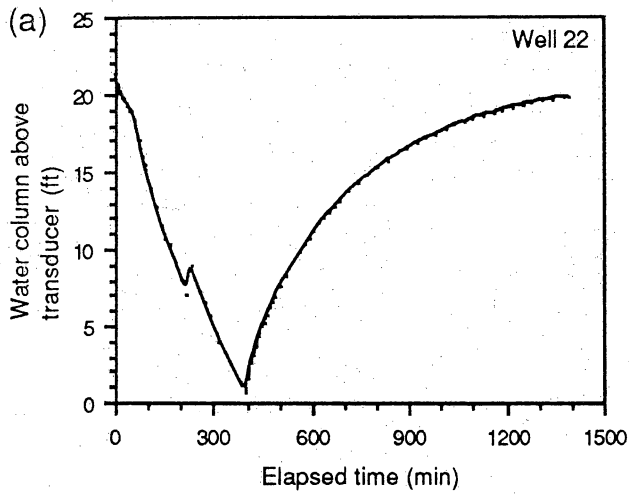
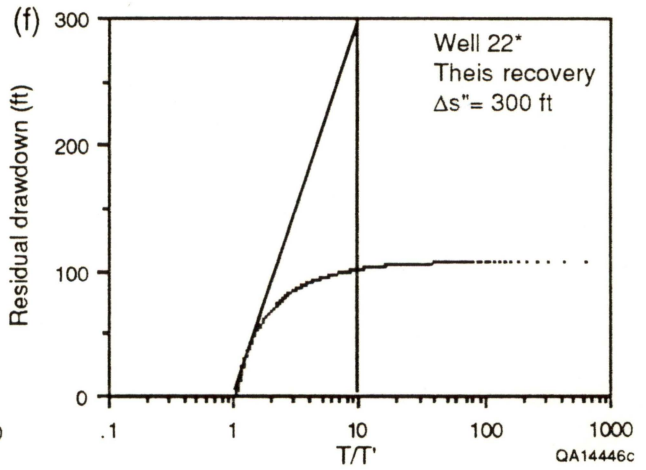
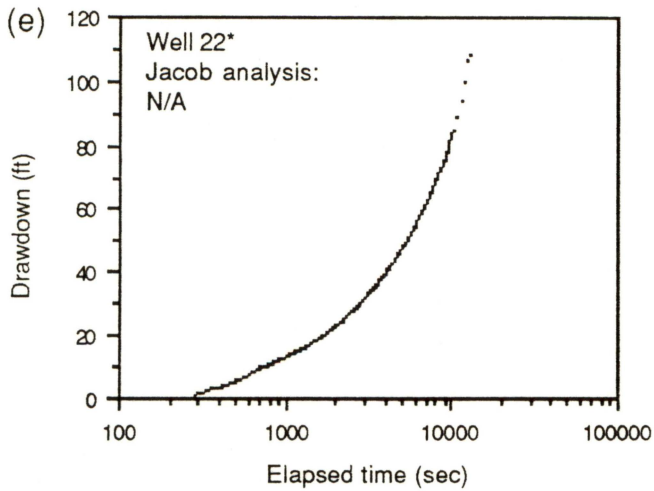
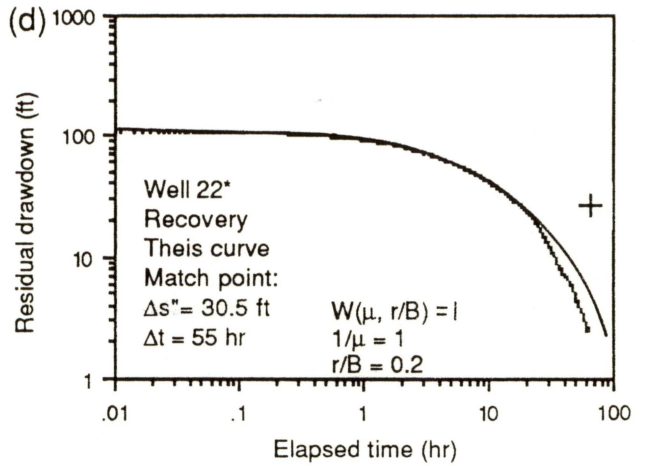
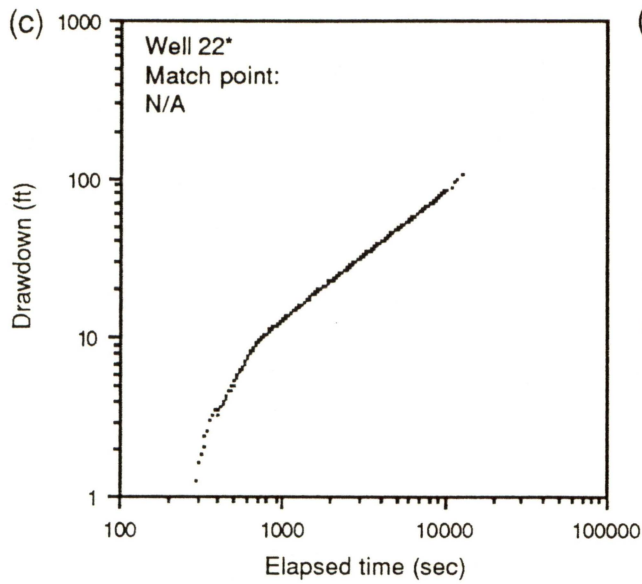
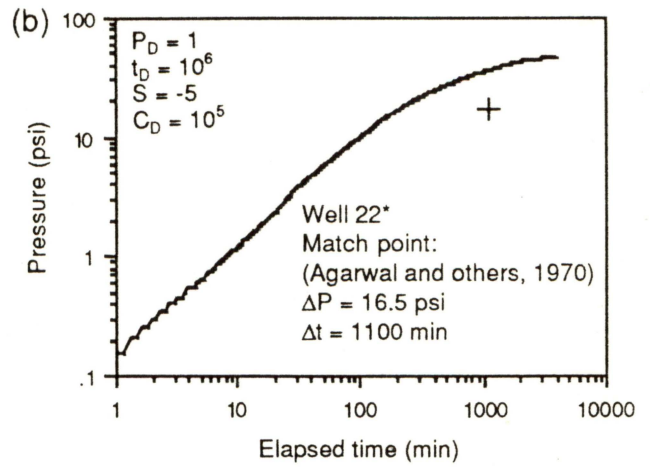
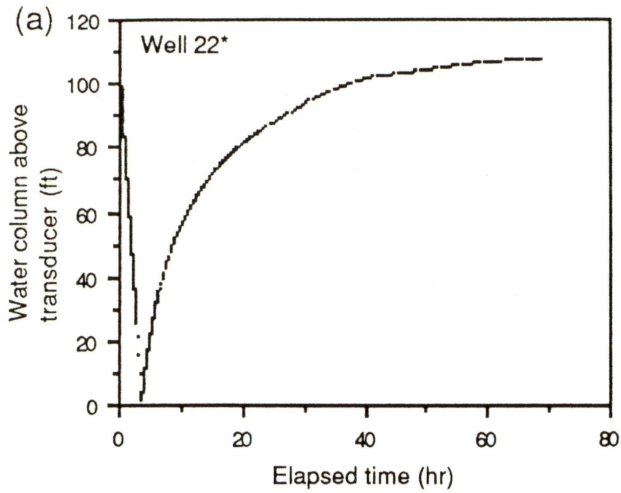


Figure 6. Aquifer test analysis for well 22* during October 10-13, 1989. (a) Drawdown and recovery curves. (b) Test data matched with Agarwal (1970) type curves. (c) Logarithmic presentation typically used for drawdown phase test data matched with Theis type curve. (d) Logarithmic presentation used in matching recovery phase test data with Walton type curve $r/B = 0.2$. (e) Semilogarithmic presentation used with drawdown phase test data and Jacob's semilogarithmic approximation method of analysis. (f) Semilogarithmic presentation of recovery phase test data used in Theis's method of analysis.



QA14446c

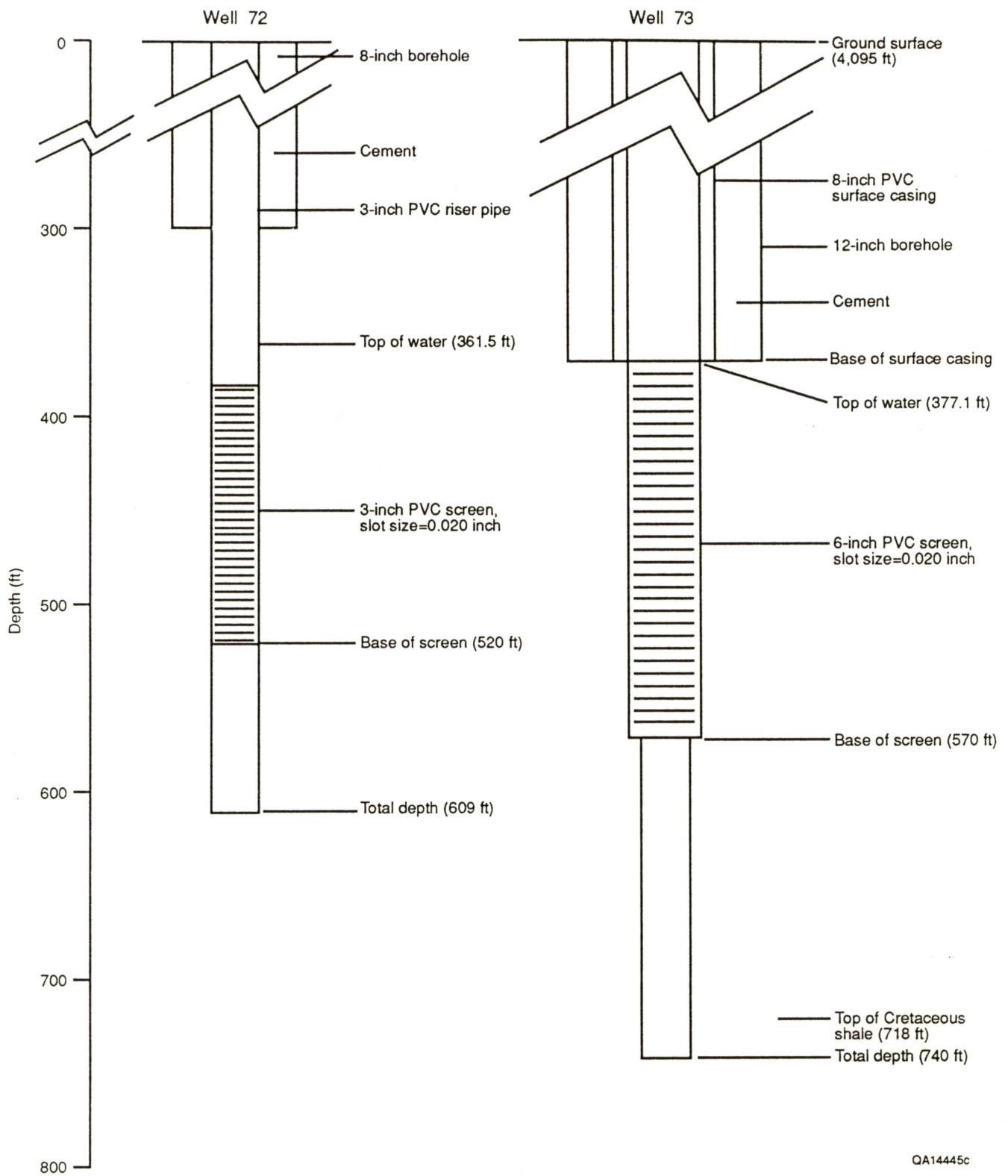
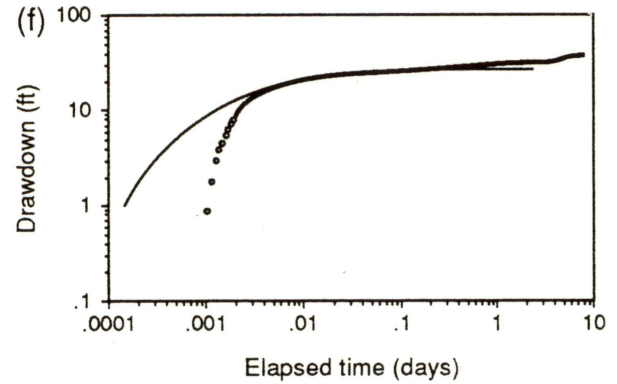
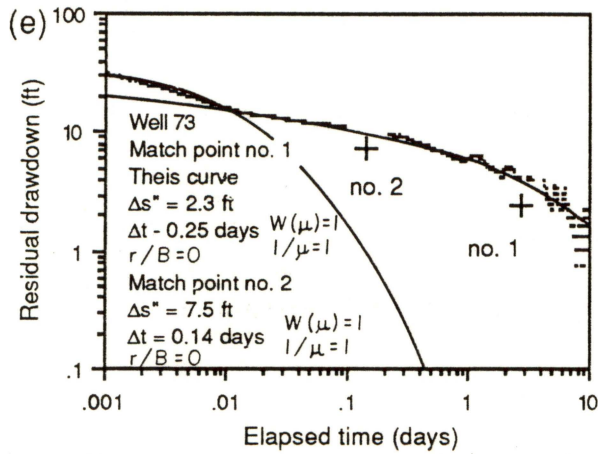
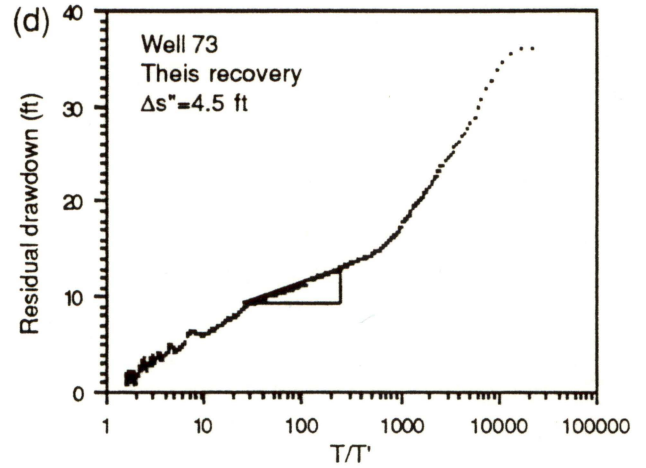
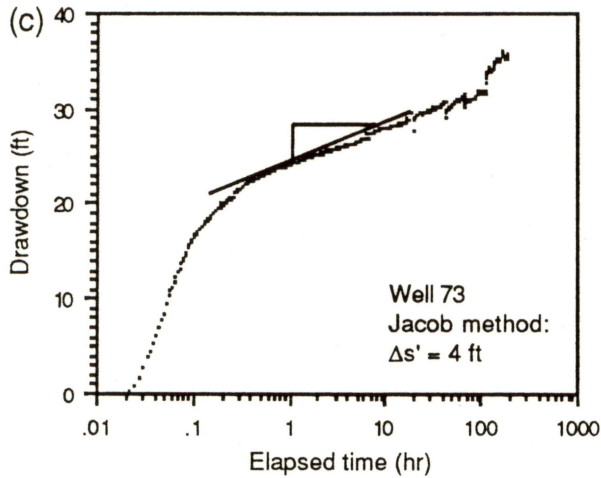
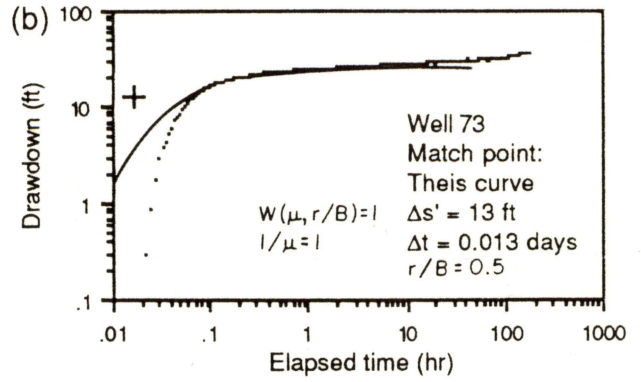
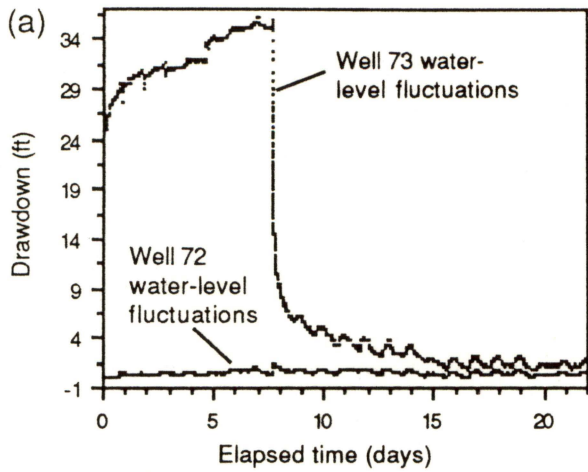


Figure 7. Schematic diagram of wells 72 and 73 during aquifer tests conducted during November and December, 1989.

Figure 8. (a) Drawdown and recovery curves for aquifer test conducted in well 73 using well 72, located 50 ft (15.2 m) away, as an observation well. This test was conducted from November 26 to December 18, 1989. (b) Hydrologic test data during drawdown phase of aquifer test of well 73. Logarithmic presentation used in matching test data with Walton type curve $r/B = 0.5$. (c) Semilogarithmic presentation used in Jacob method of analysis. (d) Semilogarithmic presentation of recovery phase test data used in Theis recovery method of analysis. (e) Logarithmic presentation of test data during recovery phase matched with Theis type curve. The logarithmic presentation was also analyzed with AQTESOLV program using Neuman method for unconfined aquifers with delayed yield. These match curves are for the (f) early and (g) late phase of the drawdown test, respectively.



QA 14444c

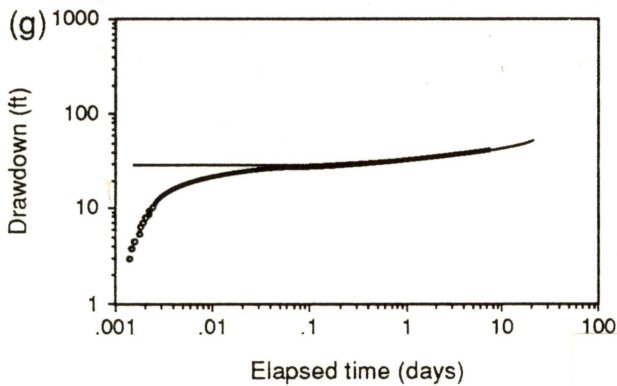
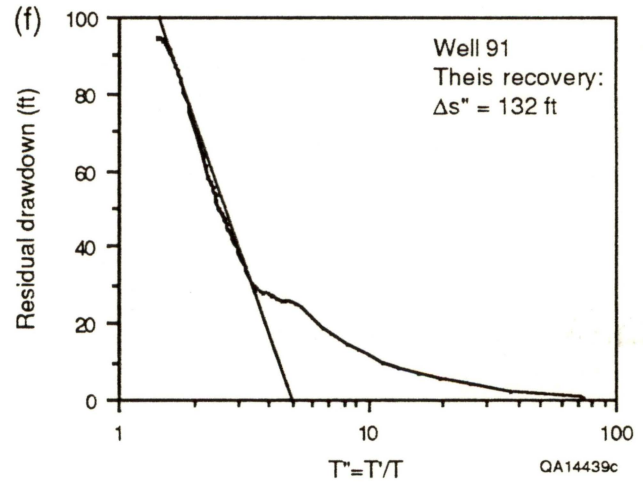
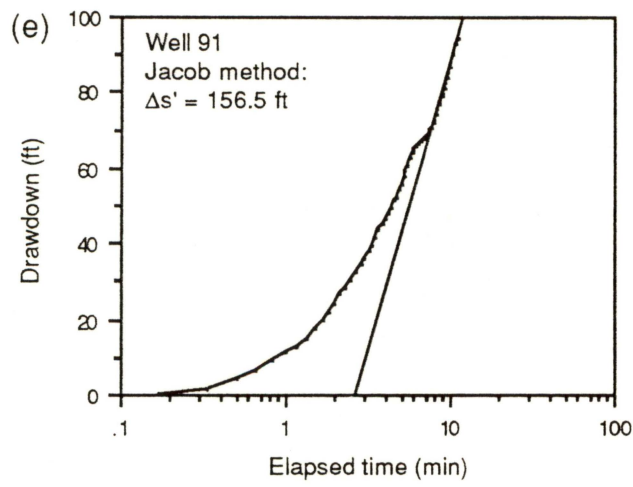
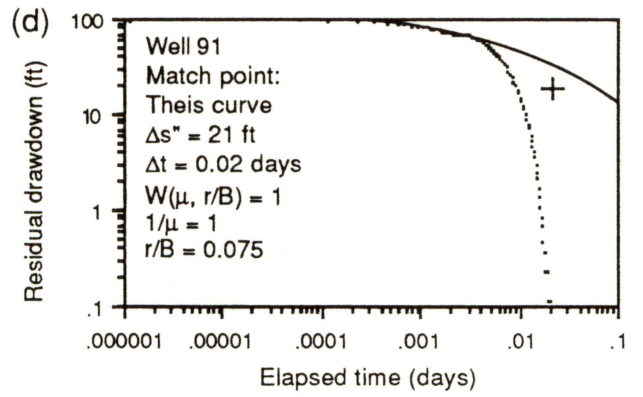
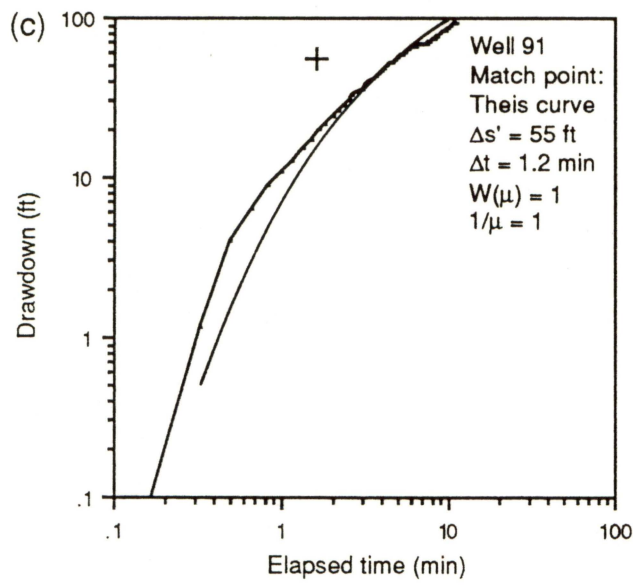
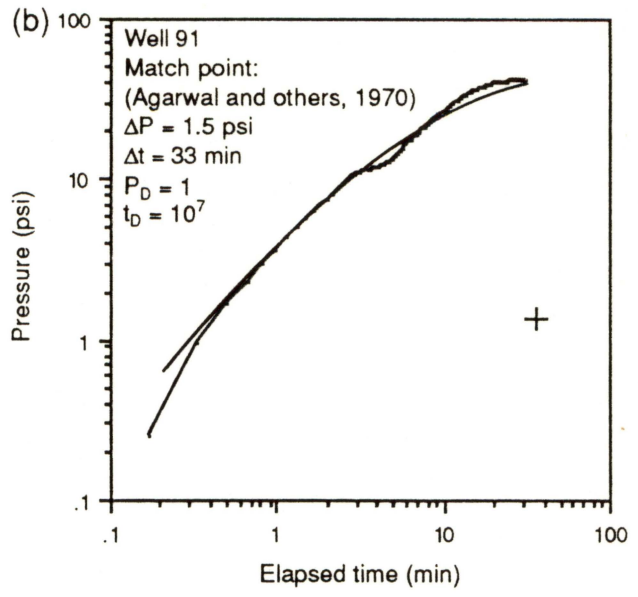
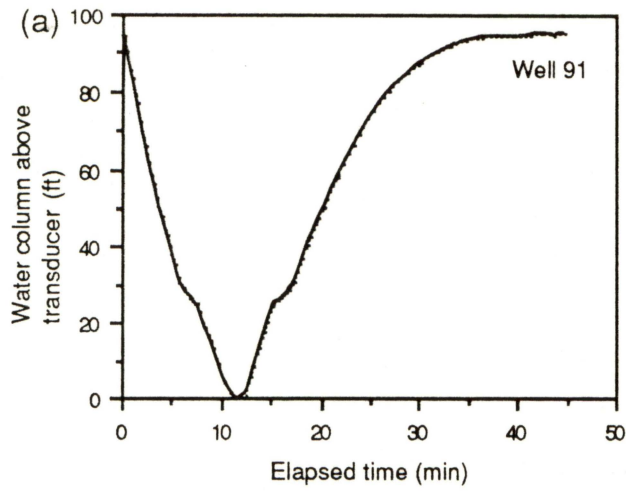
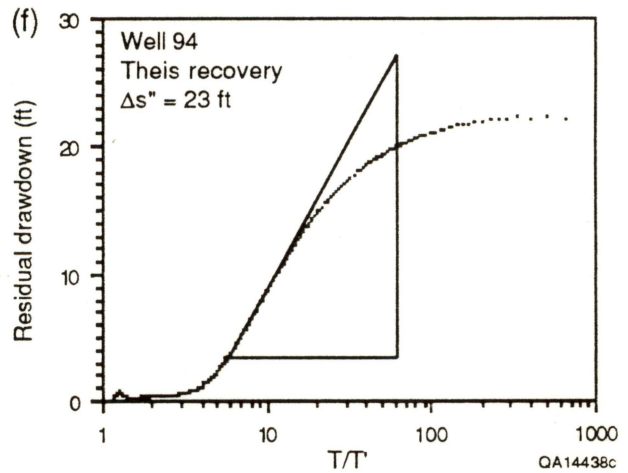
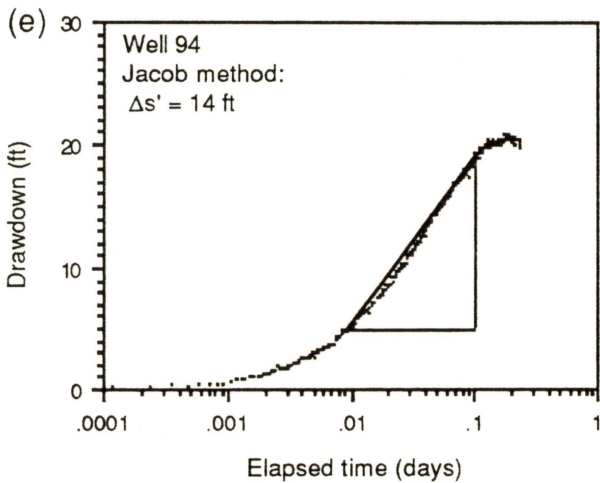
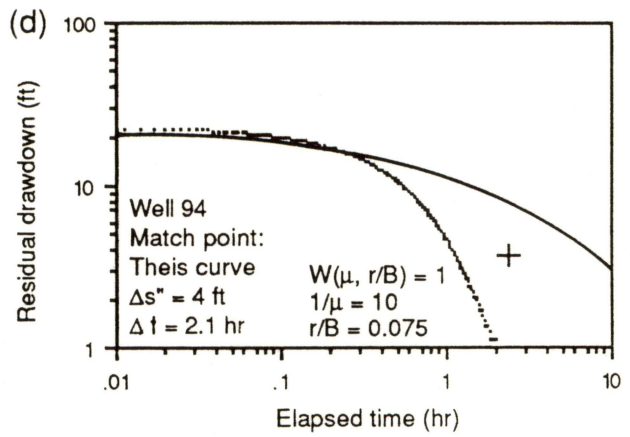
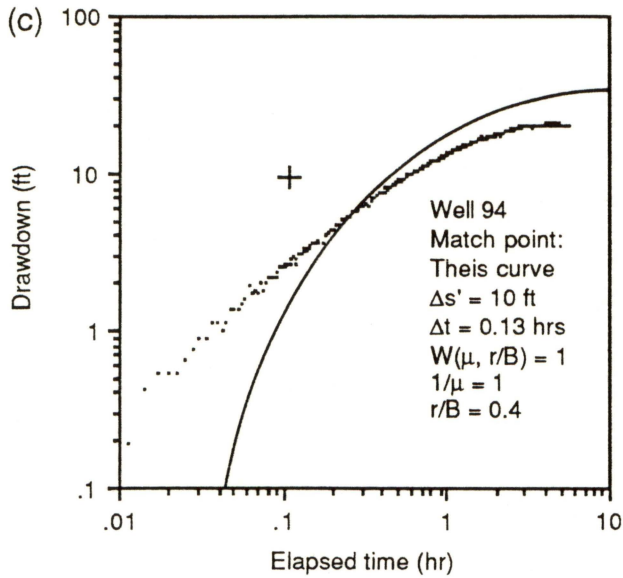
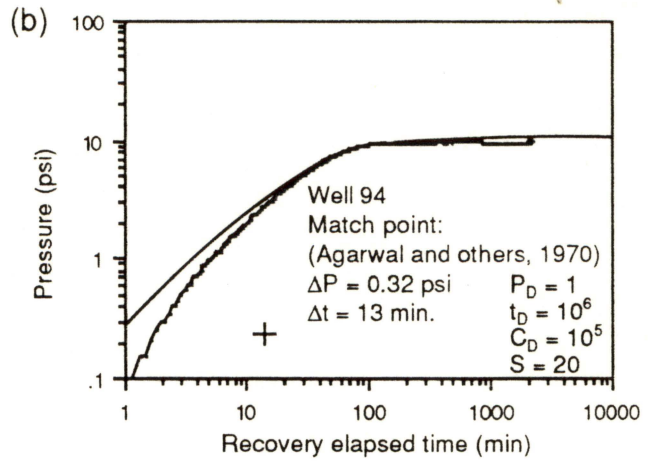
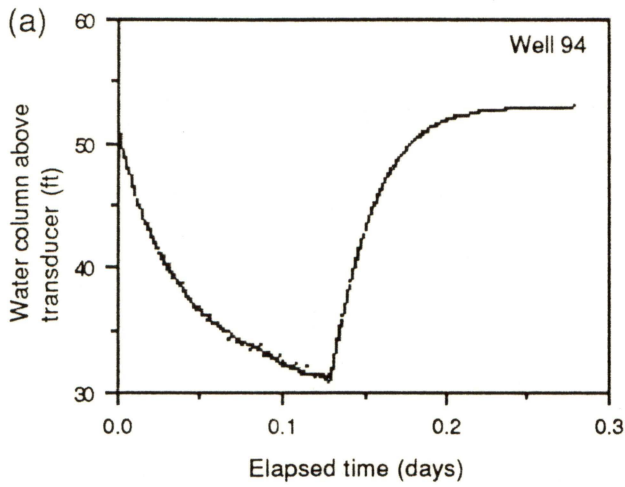


Figure 9. (a) Drawdown and recovery curves for aquifer test conducted in well 91 on April 28, 1989, (b) Logarithmic presentation of recovery phase used in matching test data with Agarwal type curves. Hydraulic parameters in type-curve matching include estimated dimensionless wellbore storage of $C_D = 10^{5.1}$ and skin effects $S = 20$. (c) Logarithmic presentation of test data during drawdown phase used in matching test data with the Theis type curve. (d) Logarithmic presentation of test data during recovery phase used in matching test data with Walton type curve $r/B = 0.075$. (e) Semilogarithmic presentation of test data during drawdown phase used in Jacob method of analysis. (f) Semilogarithmic presentation of test data used in Theis recovery method of analysis.



QA14439c

Figure 10. (a) Drawdown and recovery curves for aquifer test conducted in well 94 on October 1–October 3, 1989. (b) Logarithmic presentation of recovery test data used in matching test data with Agarwal's type curves. Hydraulic parameters in type-curve matching include estimated dimensionless wellbore storage of $C_D = 10^{5.3}$ and skin effects $(S) = 20$. (c) Logarithmic presentation used in matching test data with Walton type curve $r/B = 0.4$. (d) Logarithmic presentation used in matching test data with Walton type curve $r/B = 0.075$. (e) Semilogarithmic presentation used in Jacob method of analysis. (f) Semilogarithmic presentation used in Theis recovery method of analysis.



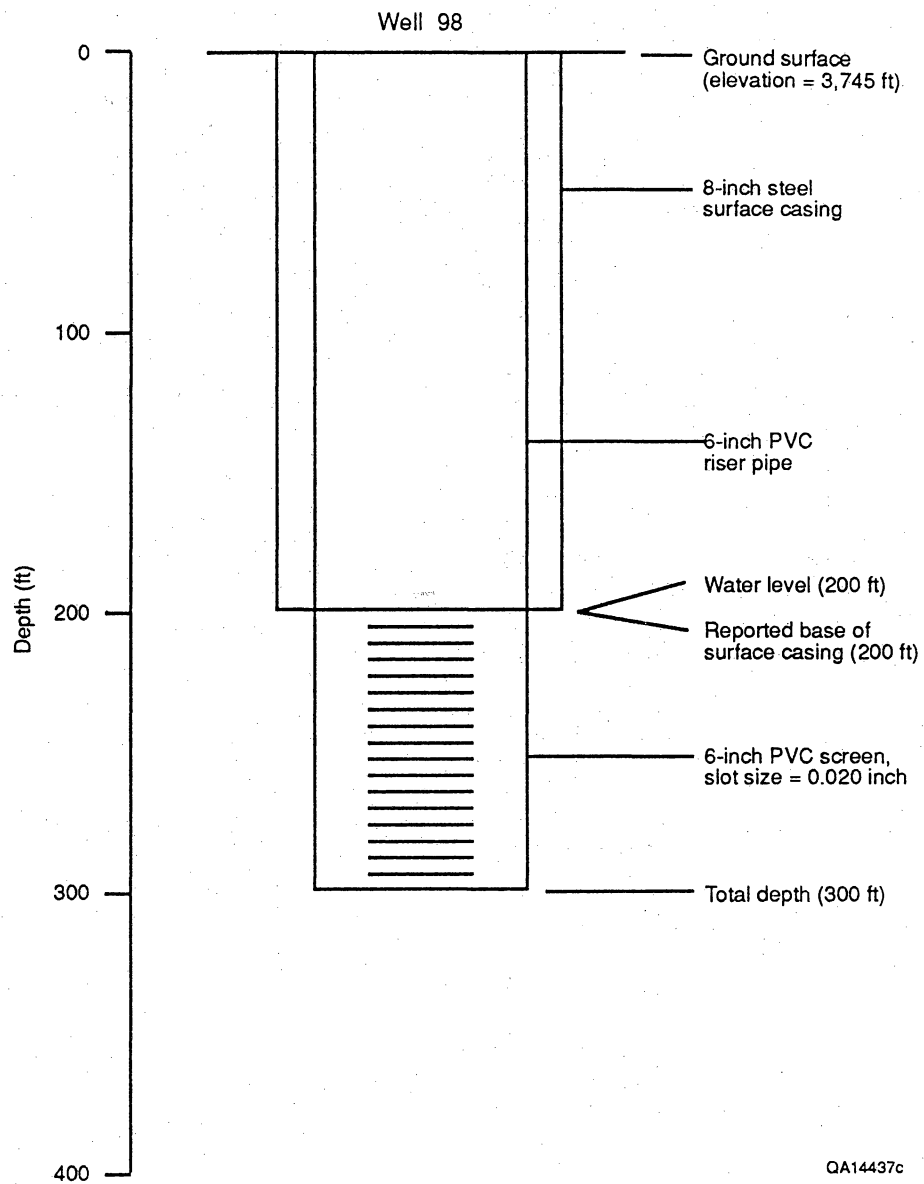
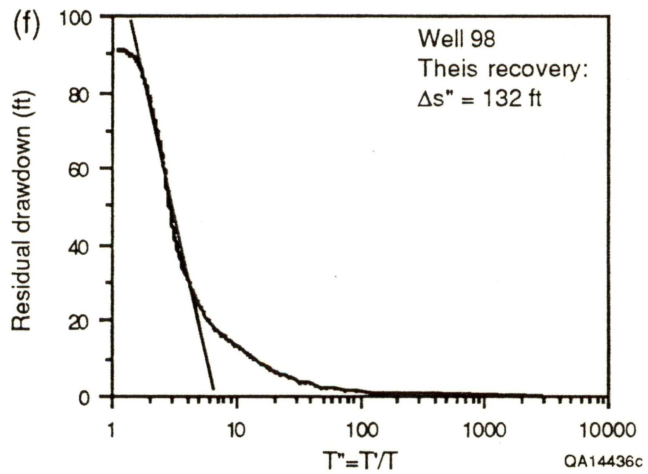
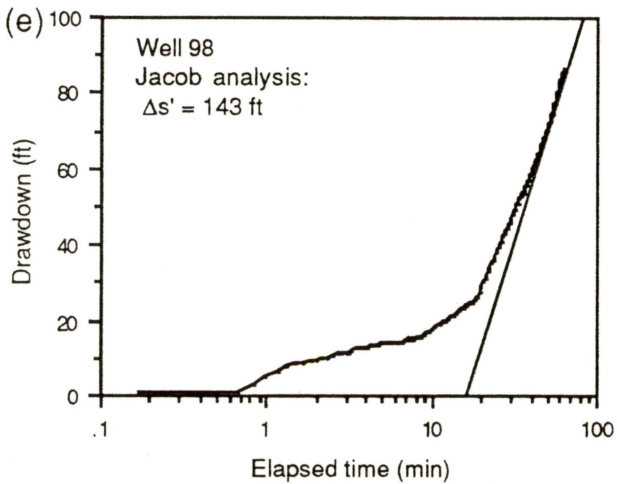
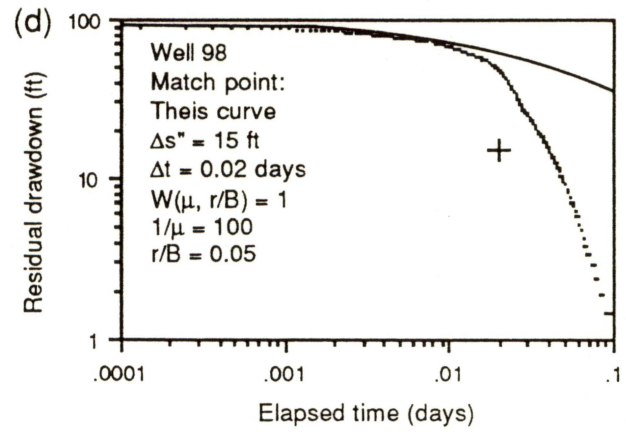
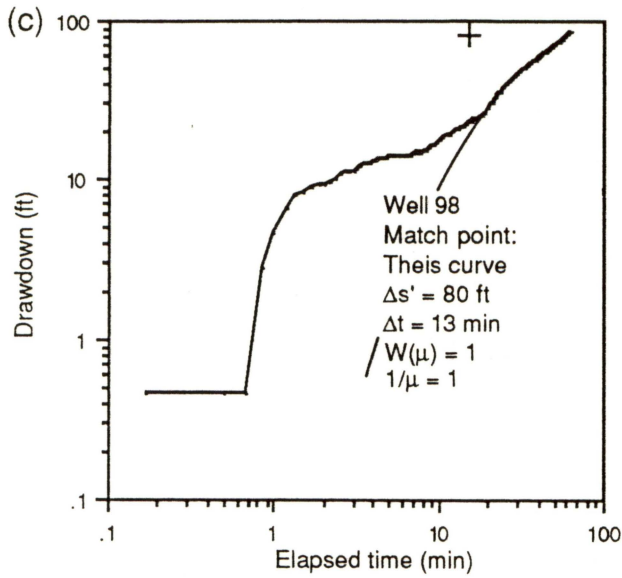
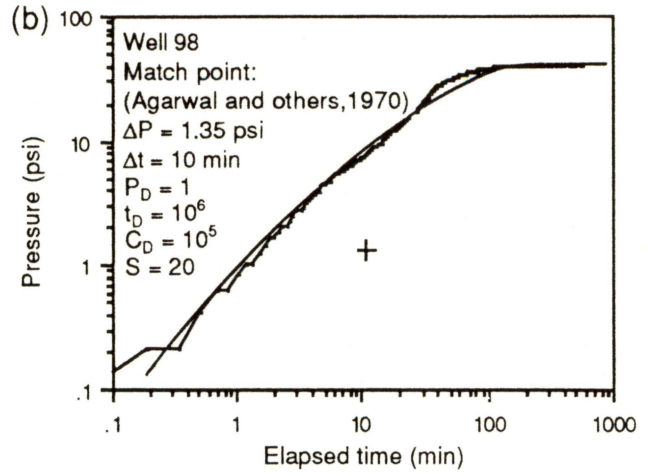
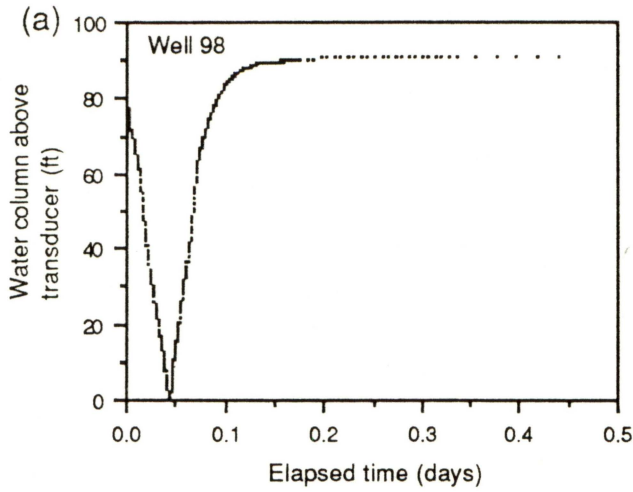


Figure 11. Schematic diagram of well 98 during aquifer tests conducted in May and September, 1989.

Figure 12. (a) Drawdown and recovery curves for aquifer test 6 conducted in well 98 May 30–31, 1989. (b) Logarithmic presentation of test data used in matching test data with Agarwal type curves. Hydraulic parameters used in type-curve matching include an estimated dimensionless wellbore storage of $C_D = 10^{4.2}$ and skin effects (S) = 20. (c) Logarithmic presentation used in matching test data with Theis type curves. (d) Logarithmic presentation used in matching test data with Walton type curve $r/B = 0.05$. (e) Semilogarithmic presentation used in Jacob method of analysis. (f) Semilogarithmic presentation used in Theis recovery method of analysis.



QA14436c

Figure 13. (a) Drawdown and recovery curves for aquifer test conducted in well 98* (after several periods of well development conducted in attempt to remove residual drilling muds from saturated section). Aquifer test conducted on September 14–15, 1989. (b) Logarithmic presentation used in matching test data with Agarwal type curves. Hydraulic parameters in type-curve matching include estimated dimensionless wellbore storage of $C_D = 10^{4.9}$ and skin effects (S) = 20. (c) Logarithmic presentation is typically used in matching test data with Theis or Walton type curves. In this case, however, wellbore storage and skin effects make attempts at type curve matching meaningless. (d) Logarithmic presentation used in matching test data with Walton type curve $r/B = 0.075$. (e) Semilogarithmic presentation used in Jacob method of analysis. (f) Semilogarithmic presentation used in Theis recovery method of analysis.

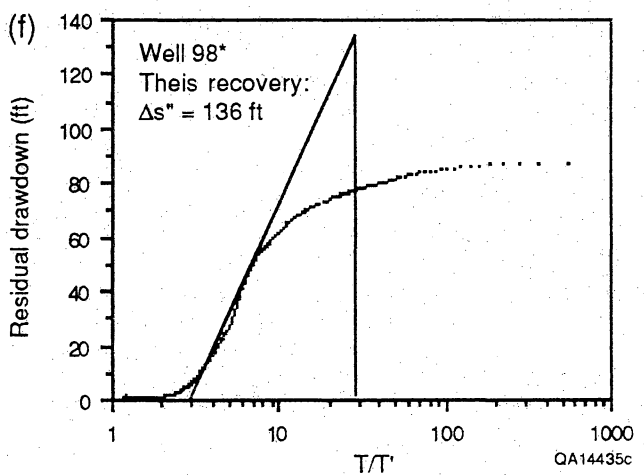
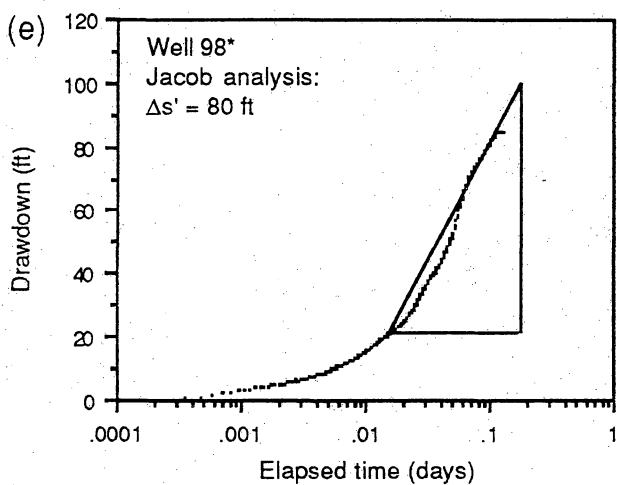
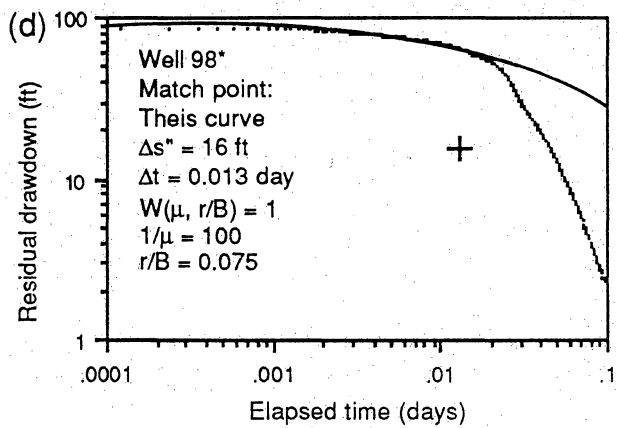
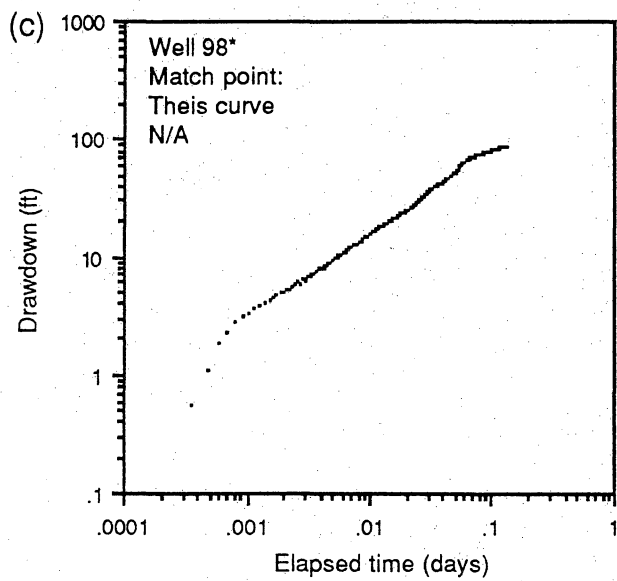
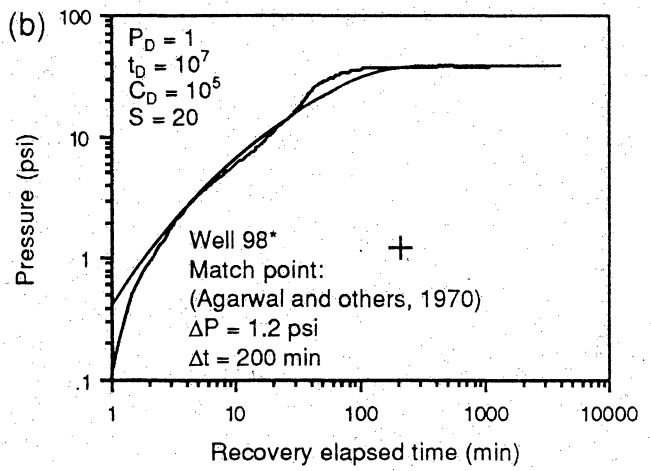
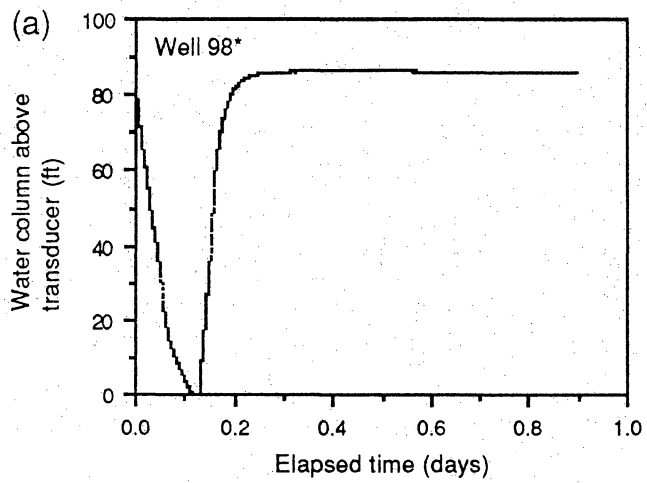


Figure 14. (a) Drawdown and recovery curves for aquifer test conducted in well 99. (b) Logarithmic presentation used in matching test data with Agarwal type curves. Hydraulic parameters used in type-curve matching include estimated dimensionless wellbore storage of $C_D = 10^{5.3}$ and skin effect (S) = 10. (c) Logarithmic presentation is typically used in matching test data with Theis or Walton type curves. In this case, however, wellbore storage and skin effects make attempts at type curve matching meaningless. (d) Logarithmic presentation used in matching test data with Walton type curve $r/B = 0.5$. (e) Semilogarithmic presentation used in Jacob method of analysis. (f) Semilogarithmic presentation used in Theis method of analysis.

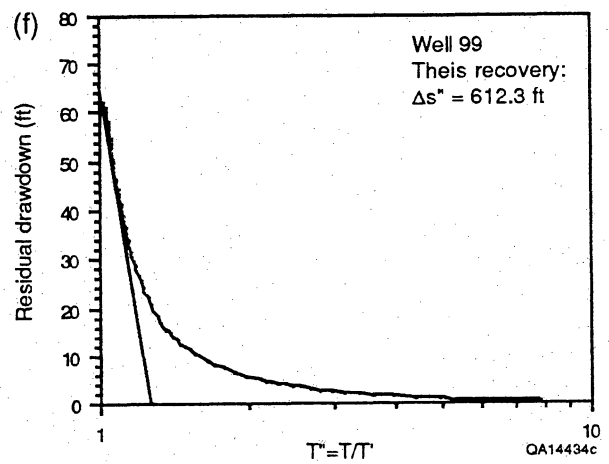
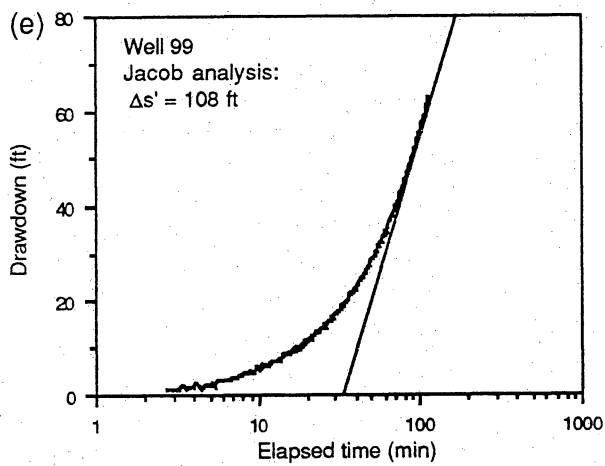
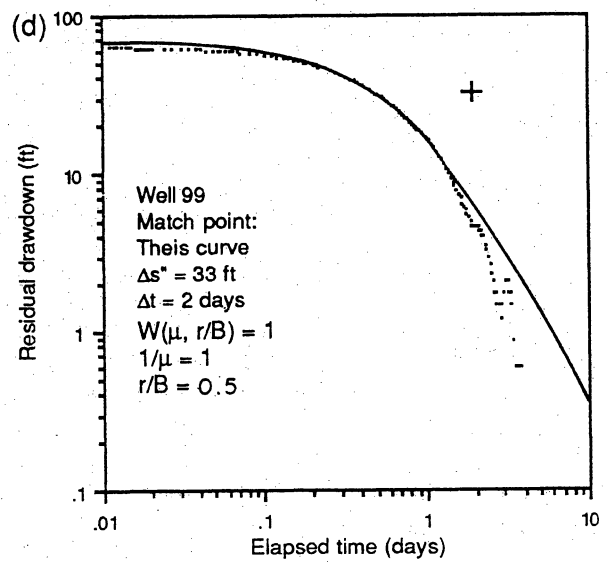
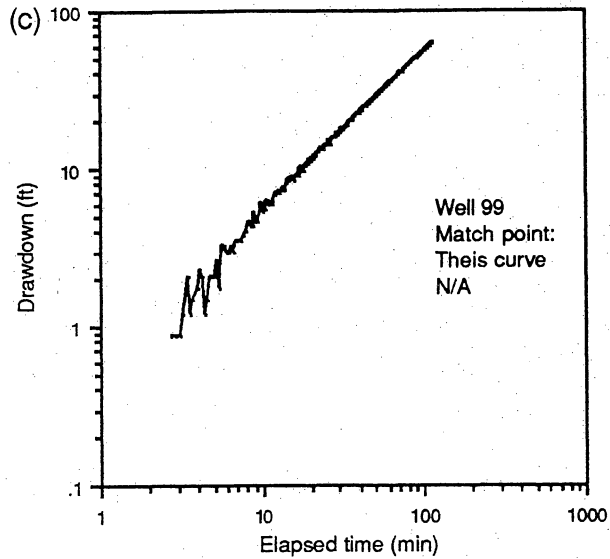
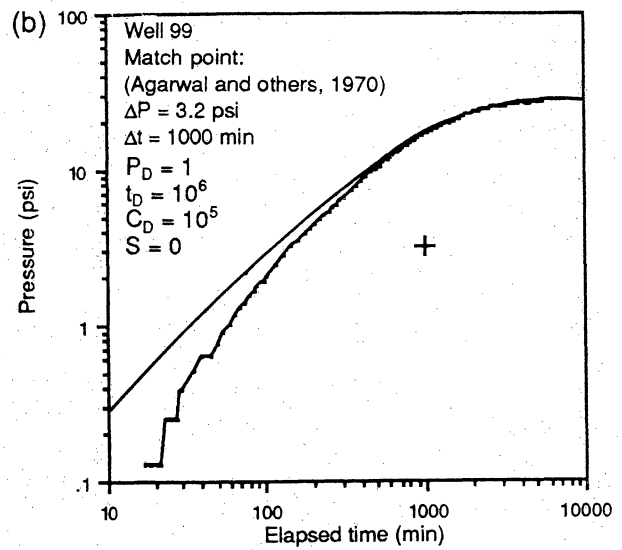
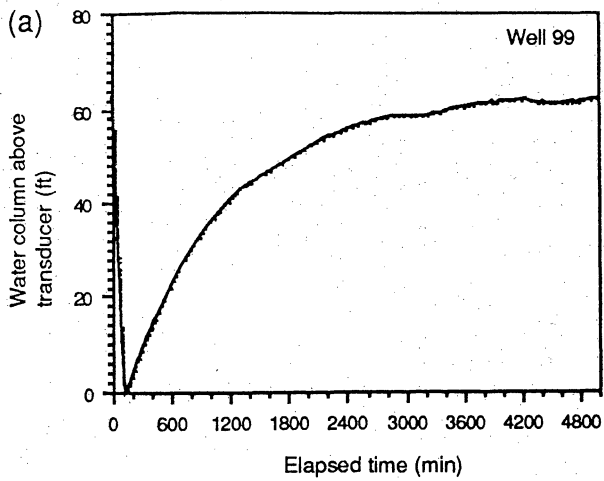
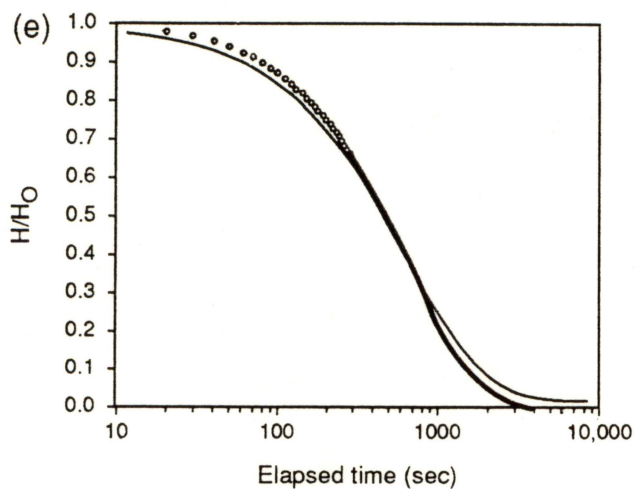
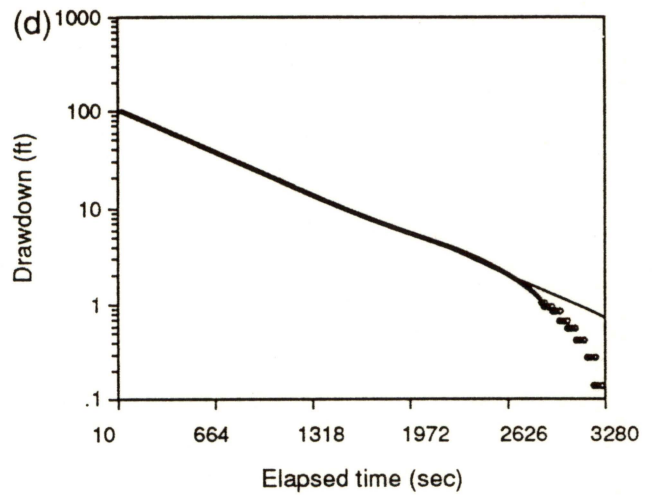
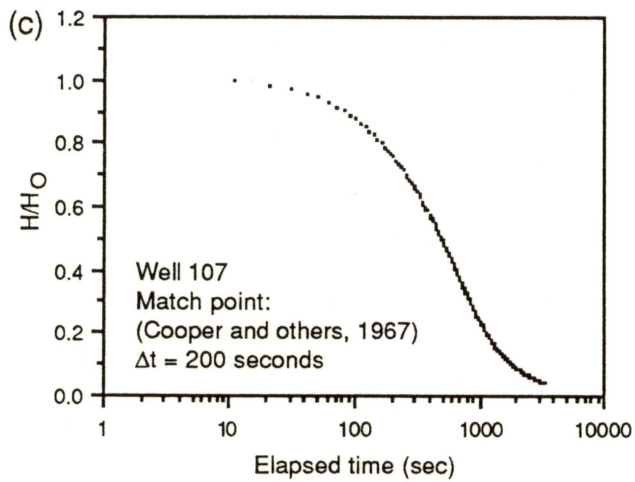
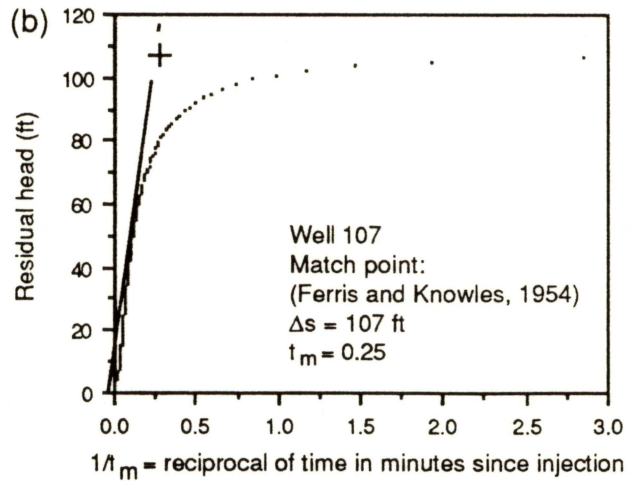
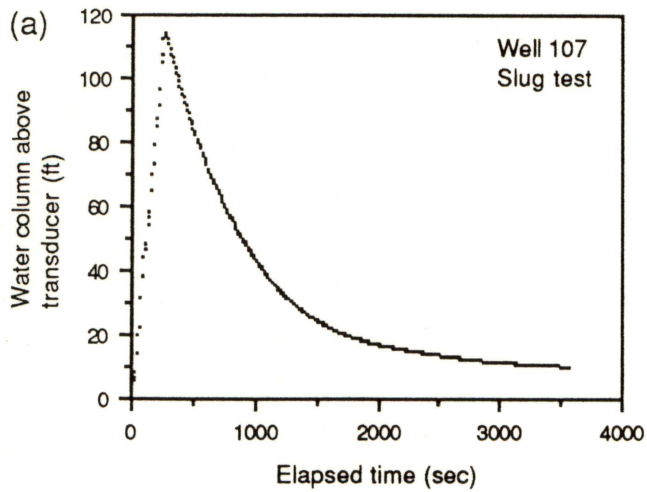


Figure 15. (a) Water-level fluctuations during slug test conducted in well 107 on September 30, 1989. (b) Linear presentation used in Ferris and Knowles (1954) method of analysis. (c) Semilogarithmic presentation used in Cooper and others (1967) type-curve matching. Type curve selected for matching was $S = 10^{-5}$. (d) Semilogarithmic presentation used in Bouwer and Rice (1976) method of analysis. (e) Semilogarithmic presentation generated by the program AQTESOLV using the methods described by Cooper, Bredehoeft, and Papadopulus (1967). This program enables the user a much greater range in type curves for matching. In this case the type curve selected for matching was $S = 10^{-8}$.



QA 14433c

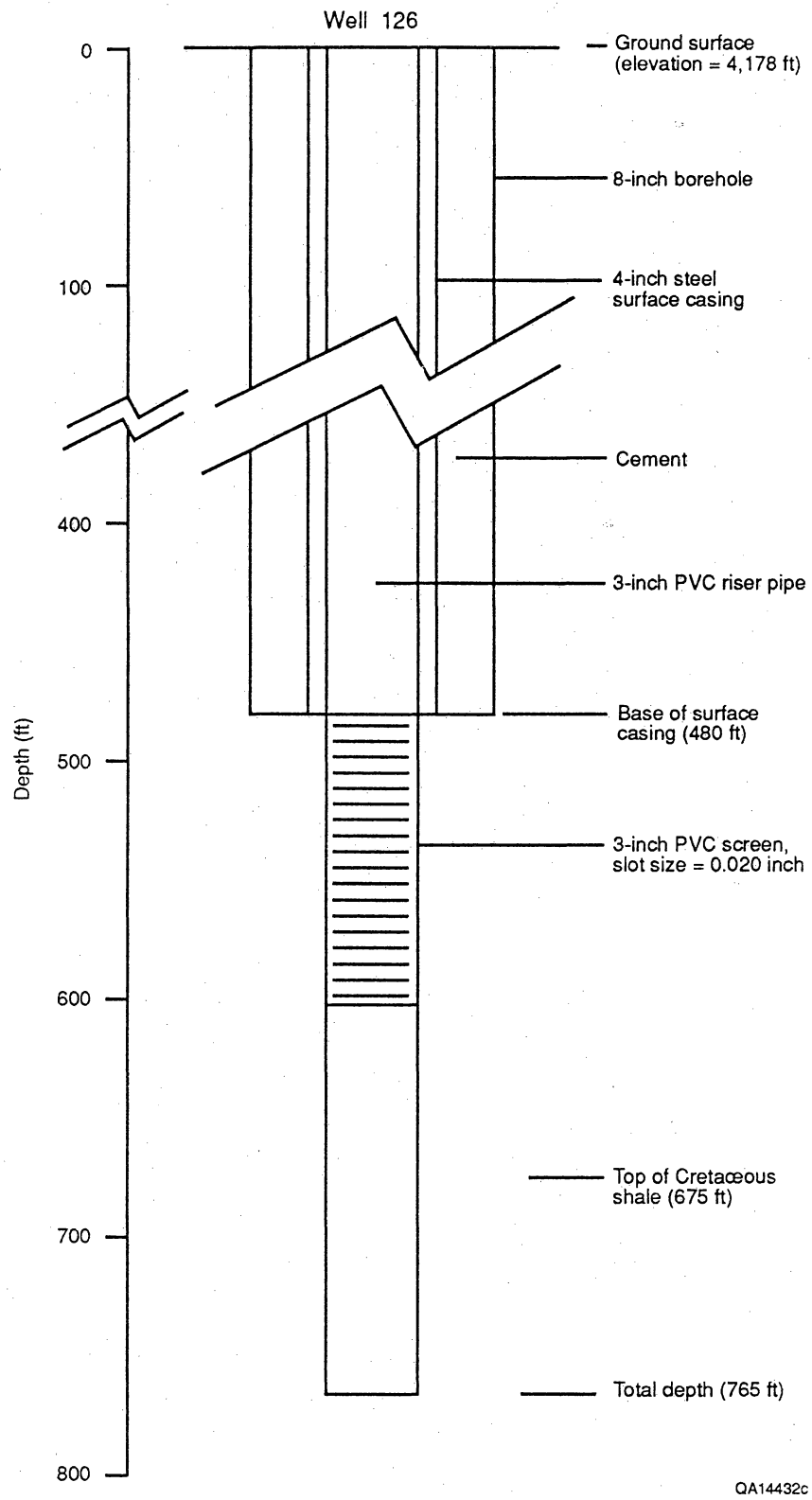
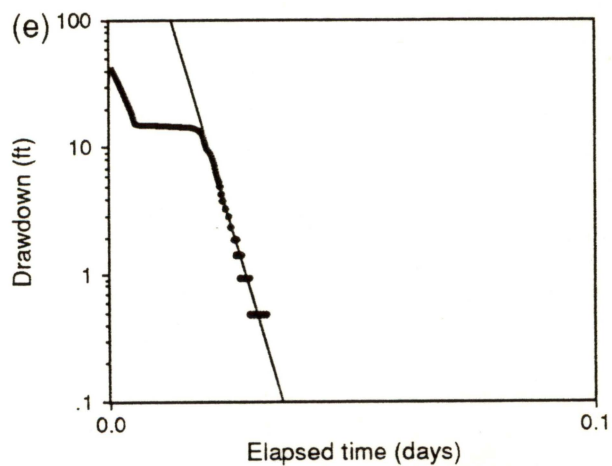
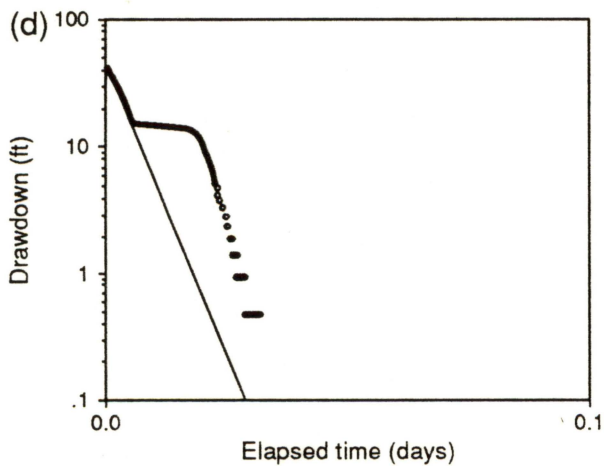
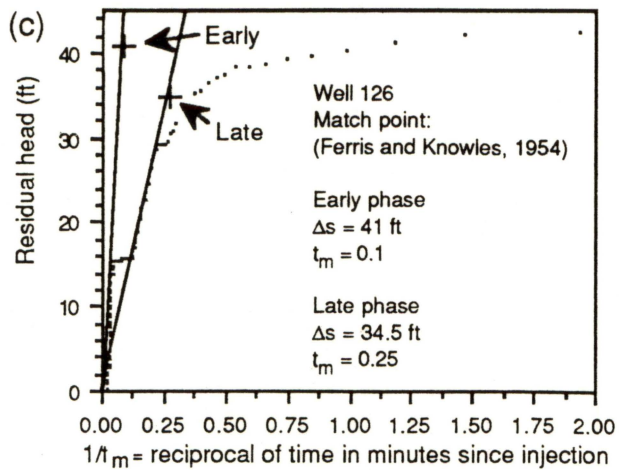
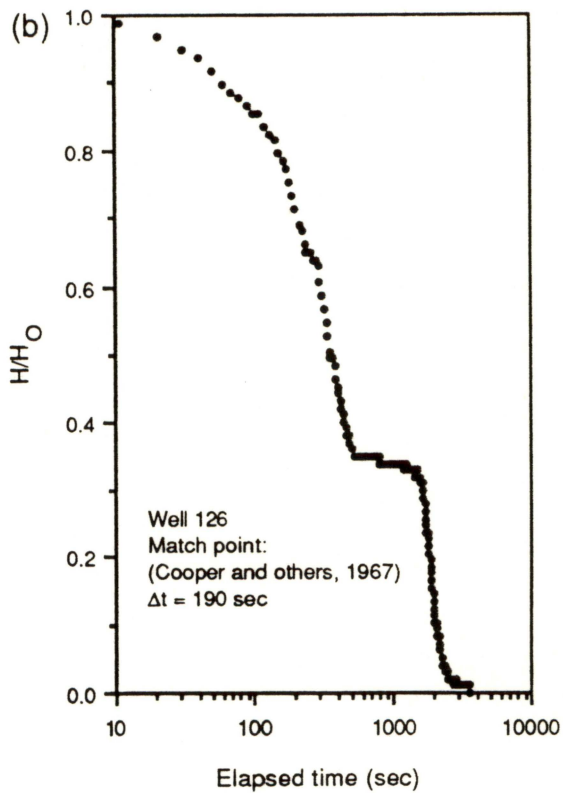
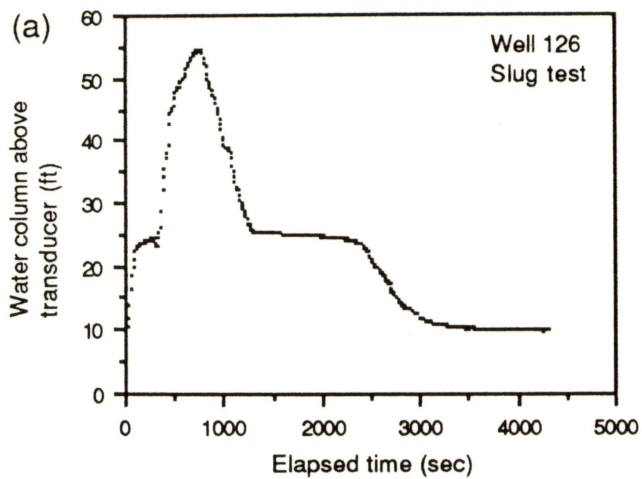


Figure 16. Schematic drawing of well 126 during slug test conducted on September 13, 1989.

Figure 17. (a) Water-level fluctuations during slug test conducted in well 126 on September 13, 1989. (b) Semilogarithmic presentation used in Cooper and others (1967) type-curve matching. Type curve selected for matching during early phase of recovery was $S = 10^{-5}$. No type curve matched with the late phase of recovery. (c) Linear presentation used in Ferris and Knowles (1954) method of analysis. In this case, both the early and late phases of recovery can be analyzed, and the solutions are presented in table 3. (d) Semilogarithmic presentation was used with Bouwer and Rice (1976) method of analysis for early phase of recovery. (e) Semilogarithmic presentation used in Bouwer and Rice (1976) method of analysis for late phase of recovery.



QA 14431c

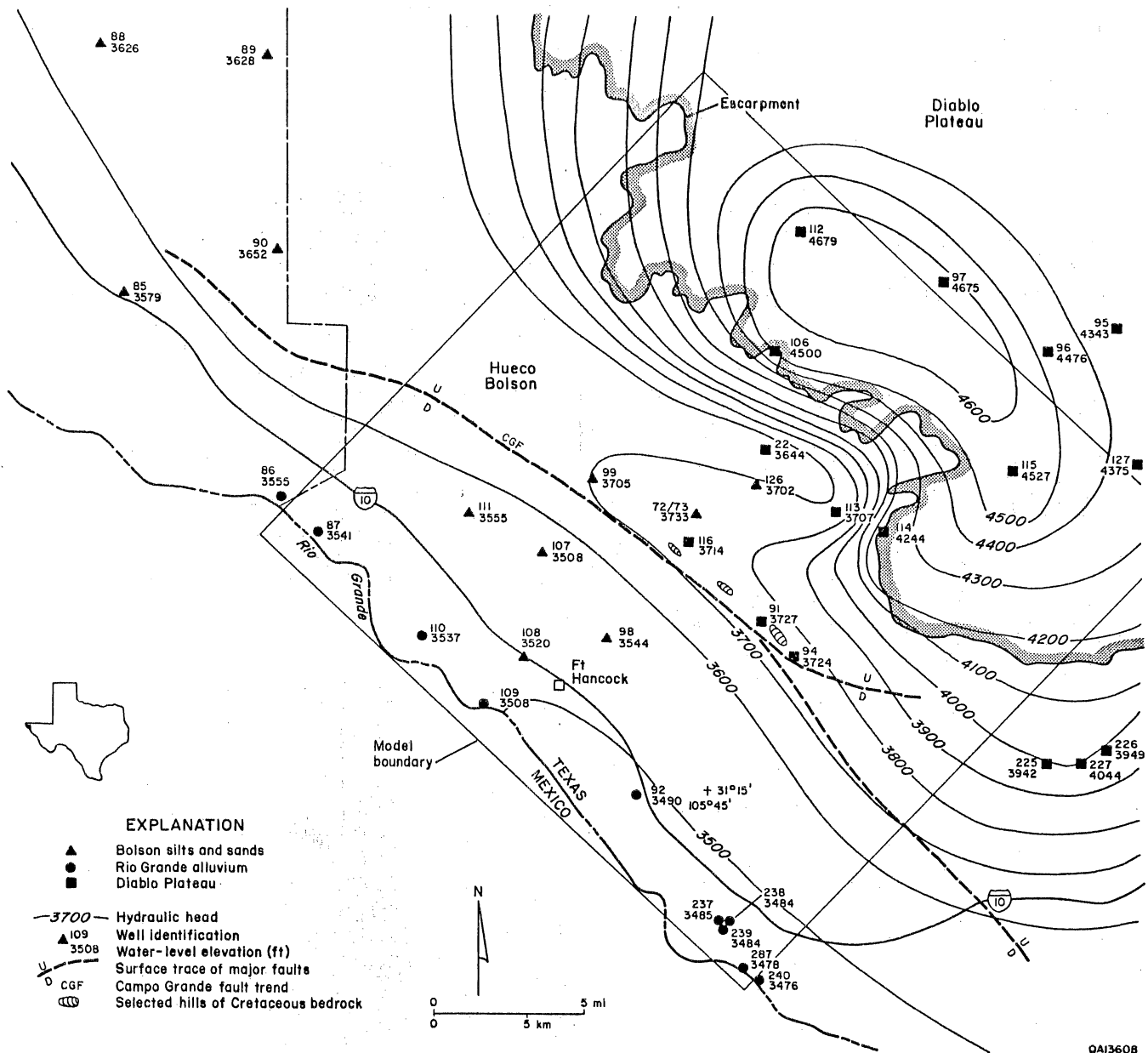
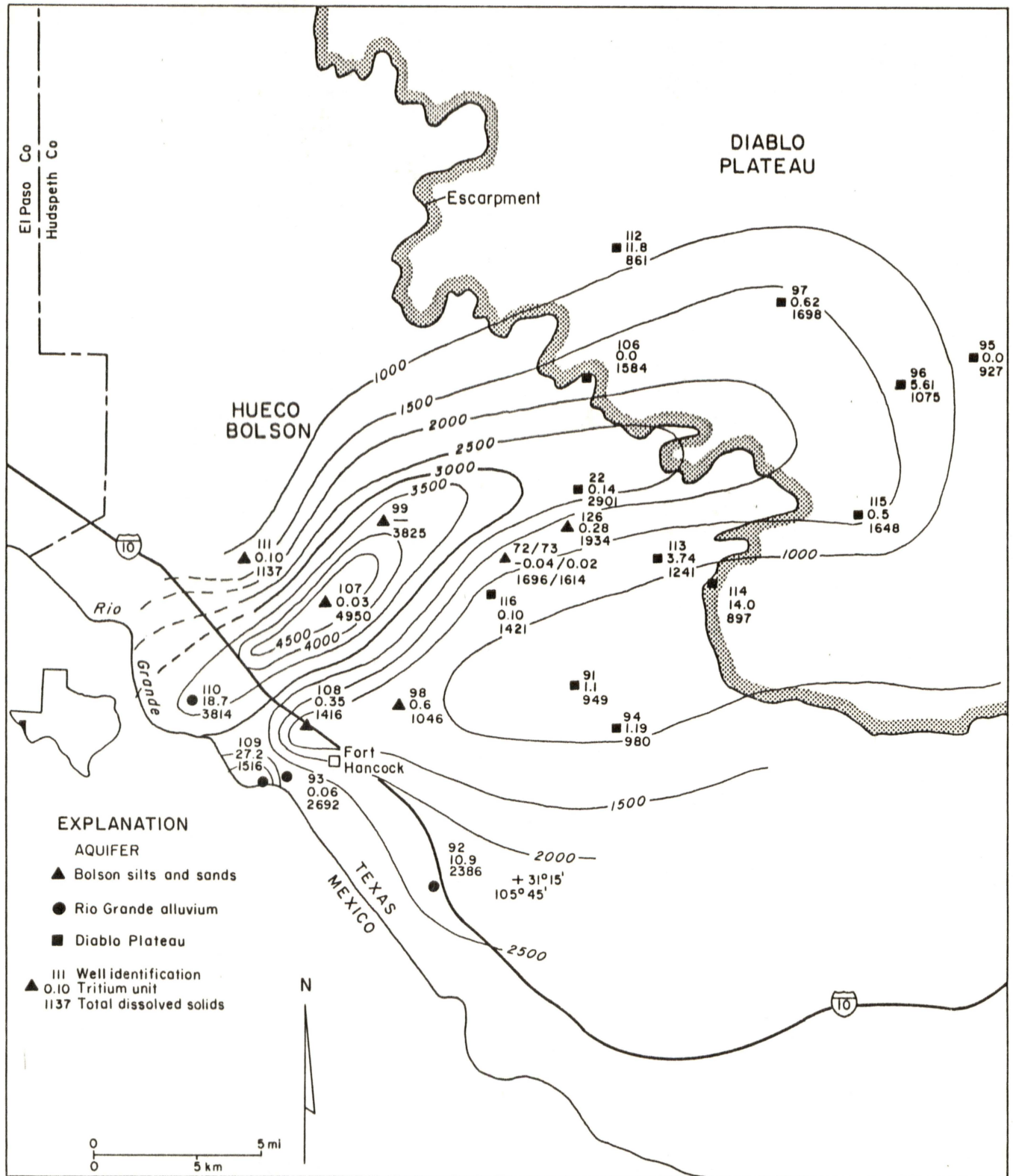
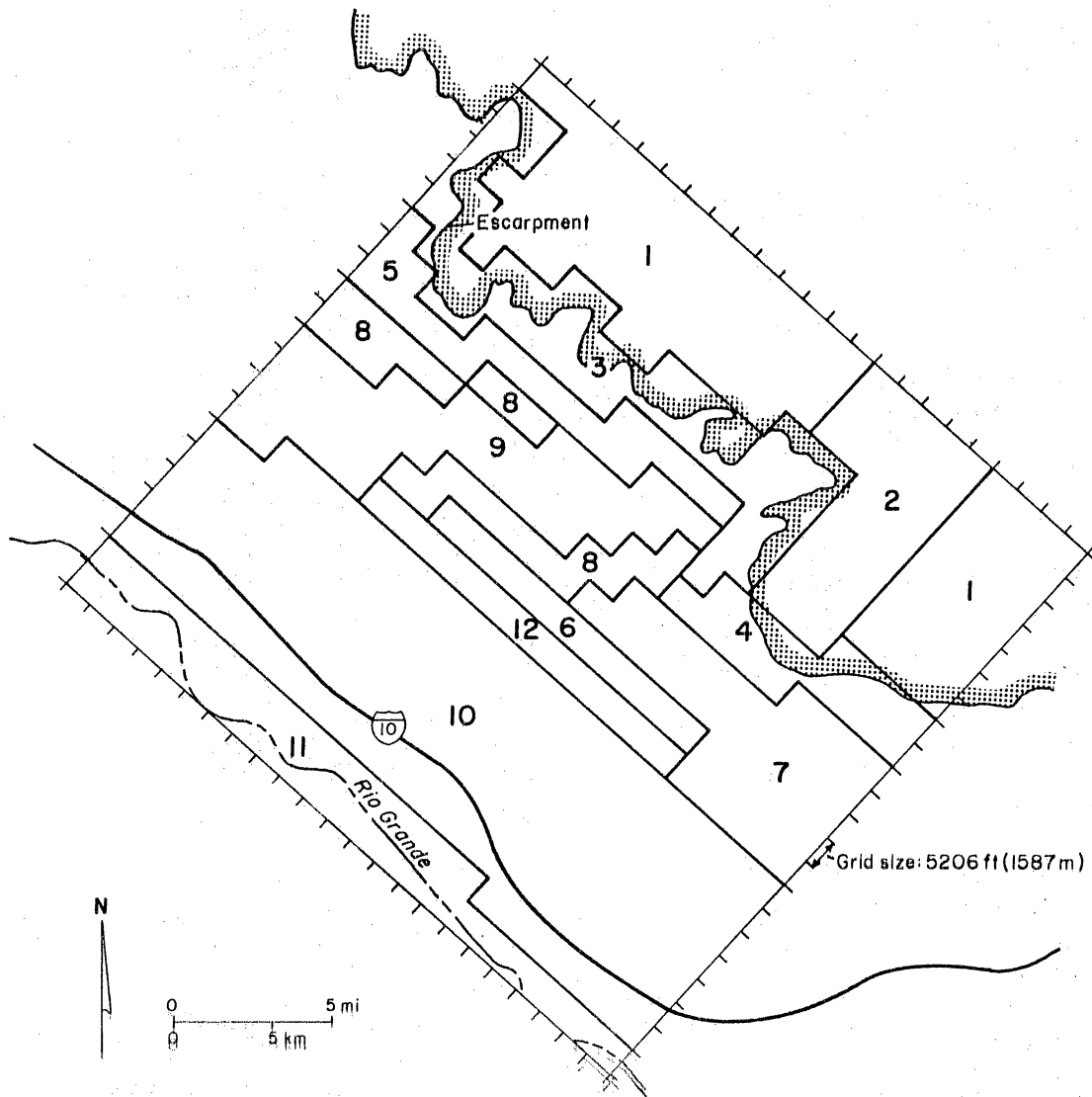


Figure 18. Potentiometric surface map of regional hydrologic study. The map also includes the Campo Grande fault and local outcrops of Cretaceous strata near the fault.



QA 14440

Figure 19. Distribution of total dissolved solids (TDS) and tritium concentrations of water samples collected at the wells in the area. The map assisted in the interpretation of the hydraulic-head data shown in figure 18.



EXPLANATION

Cretaceous	1	Diablo Plateau (west)	7	Cretaceous/bolson (east)
	2	Diablo Plateau (east)	8	Bolson (mud-rich)
	3	Escarpment (west)	9	Bolson (sand-rich)
	4	Escarpment (east)	10	Bolson south of Campo Grande fault
	5	Base of escarpment	11	Rio Grande alluvium
	6	Along Campo Grande fault	12	Campo Grande fault barrier

QA 14443

Figure 20. Delineation of permeability zones in the model area that are incorporated in the planar ground-water flow model. Transmissivity values assigned to the different zones for Simulation S-34 are listed in table 4.

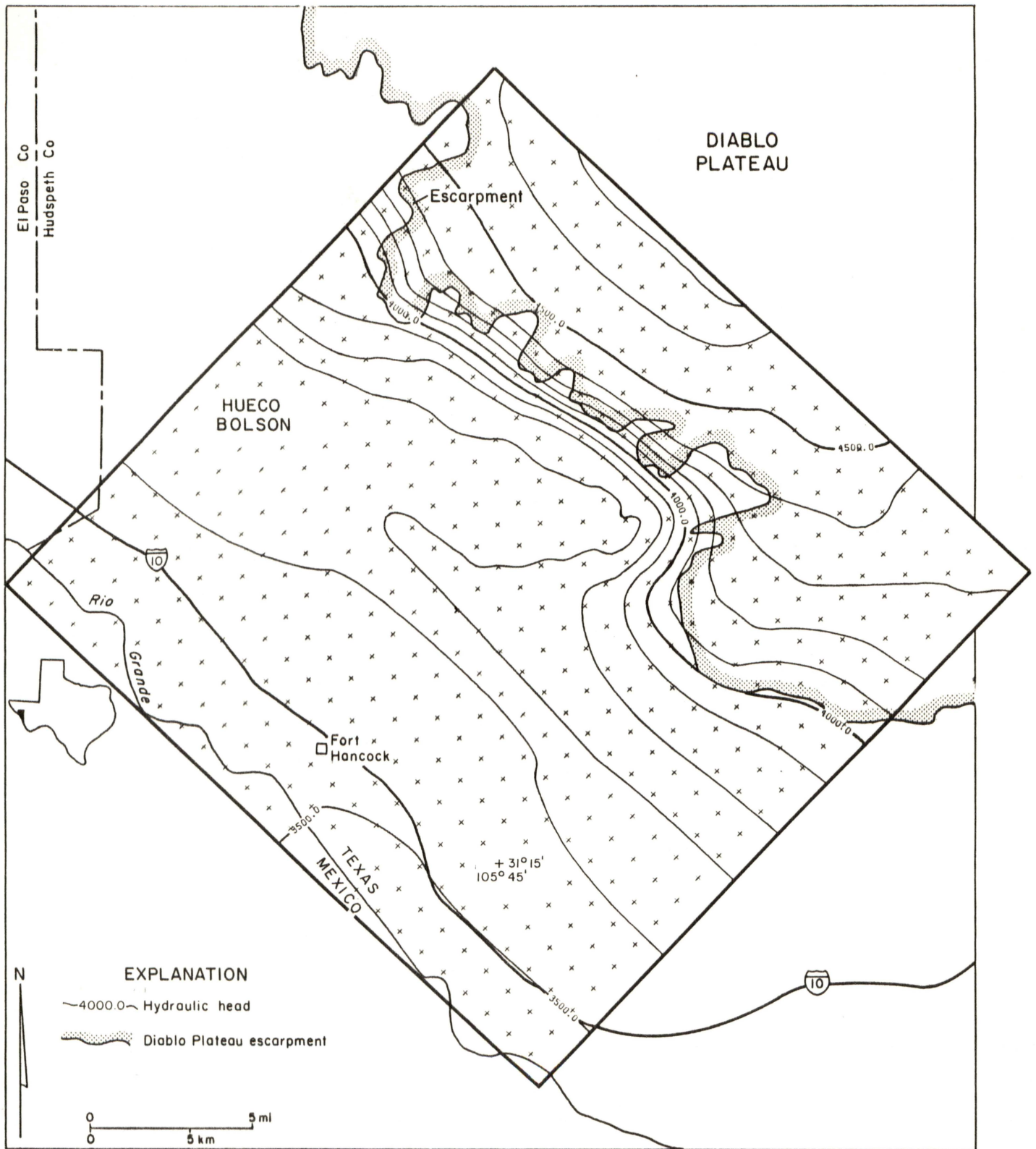


Figure 21. Distribution of simulated hydraulic heads for simulation S-34. The hydraulic head distribution shows the potentiometric high along the Campo Grande fault and relatively low heads near the principal study area.

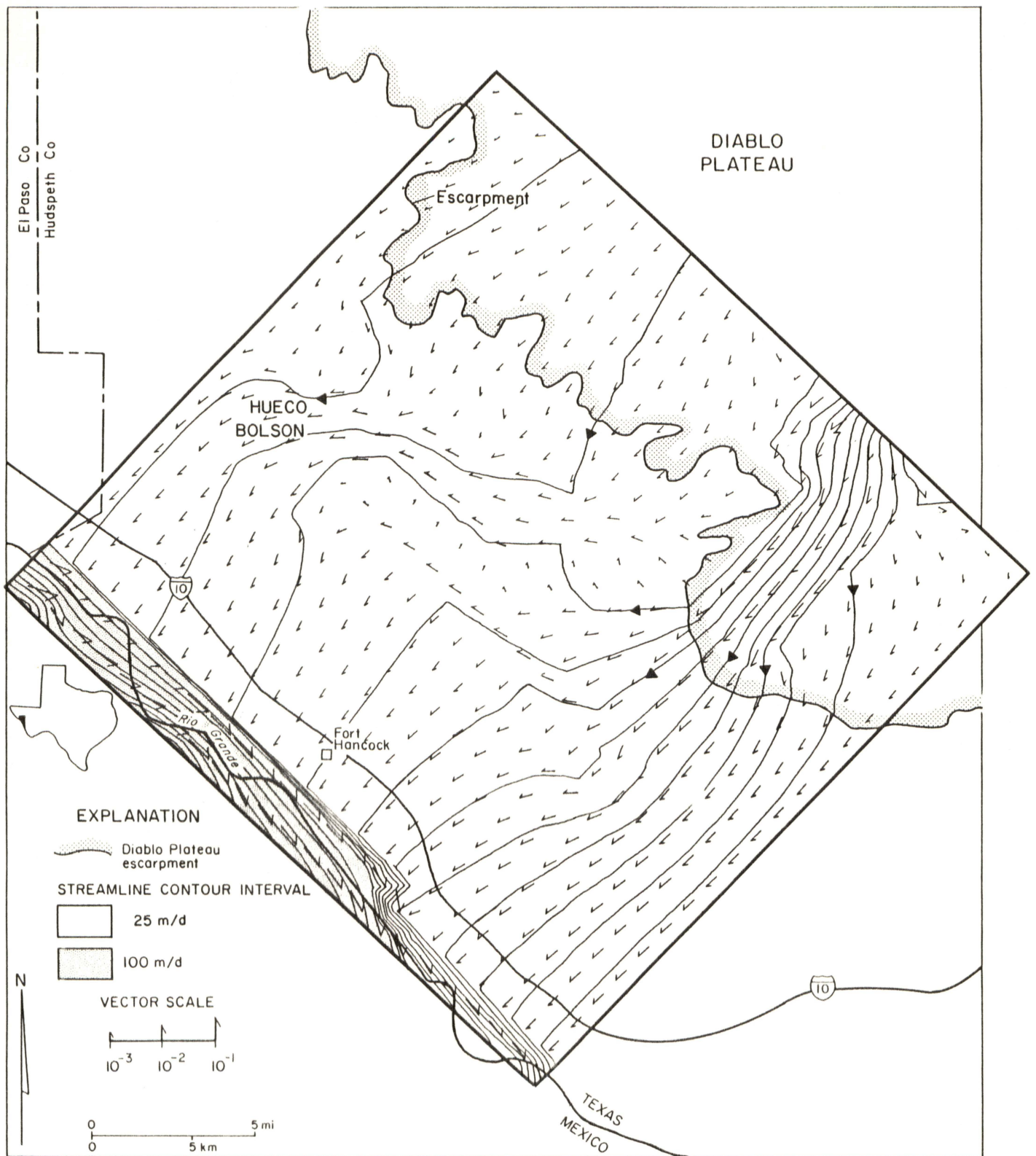


Figure 22. Streamlines and fluxes calculated for each element on the basis of simulation S-34. The streamlines delineate the regional flow pattern. The area between adjacent streamlines contain a volumetric flow rate of 25 m/d. The width of the stream tubes indicate the specific discharge, which is also represented by the length of the computed flow vectors. The two flow paths along which travel times were calculated are highlighted.

Figure 23. Photographs of dirt tank located west of study area were taken immediately before (upper photo) and after (lower photo) rainfall event in July 1988.

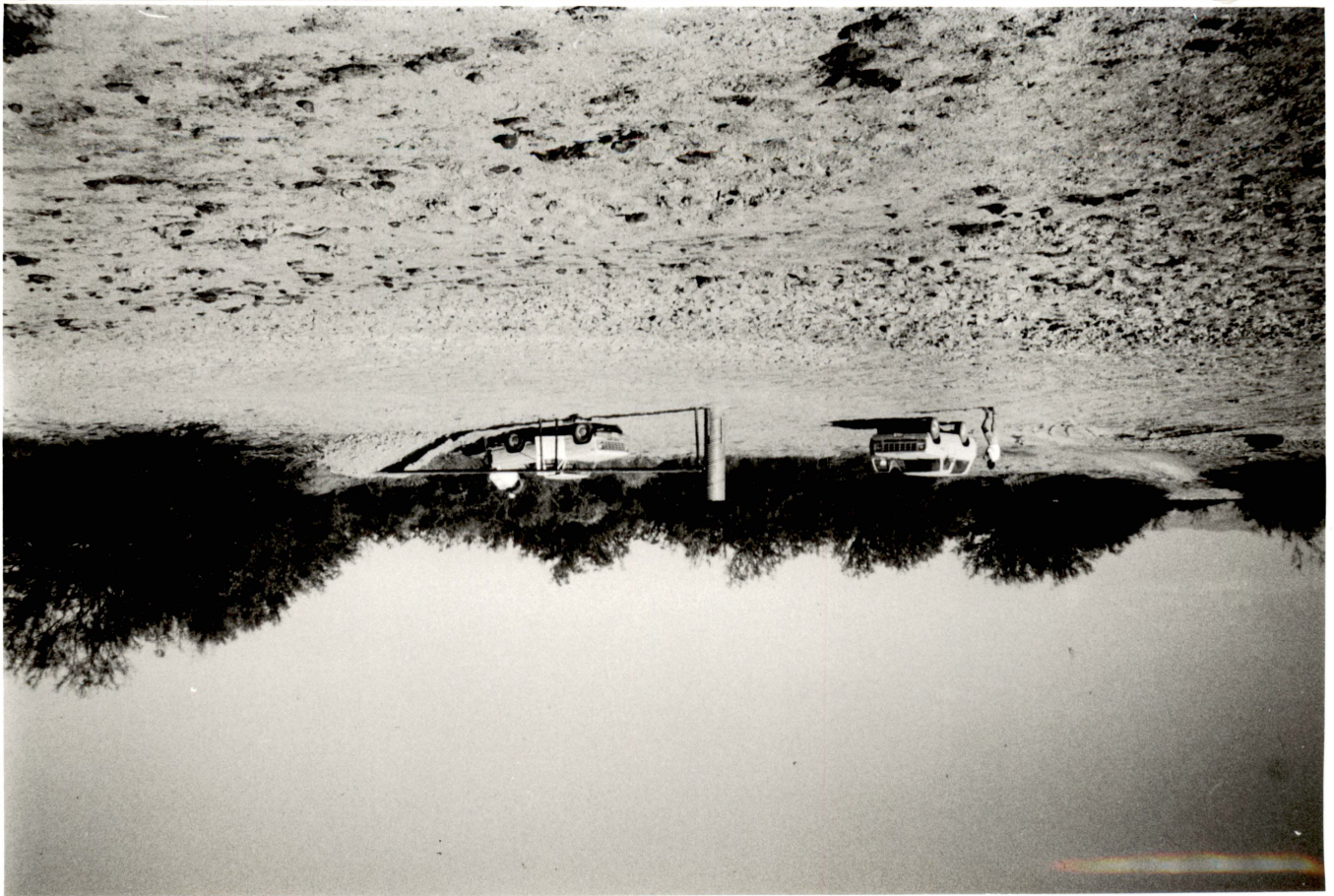


Table 1. Summary of pumping test results in bolson deposits. From Myers (1969).

TWC ID*	Lat/Long	Transmissivity (gpd/ft)	Storativity	Permeability (gpd/ft ²)	Aquifer**
48-15-201	31°51'42"/105°10'27"	15,300	—	60	L
NA	31°57'03"/106°36'41"	28,800	—	—	B
49-04-104	31°57'57"/106°36'58"	73,500	—	147	B
49-04-105	31°58'07"/106°36'30"	49,500	—	122	B
49-04-106	31°57'34"/106°36'42"	61,000	—	112	B
49-04-107	31°57'34"/106°36'42"	61,000	0.0007	230	B
49-04-108	31°58'54"/106°35'20"	47,600	—	2,380	B
49-04-112	31°59'32"/106°36'37"	20,000	—	118	SF
49-04-113	31°58'19"/106°37'05"	62,500	—	110	SF
49-04-114	31°58'54"/106°35'20"	23,200	—	263	B
49-04-115	31°58'19"/106°37'05"	62,500	—	110	SF
49-04-401	31°57'16"/106°36'22"	61,000	—	124	B
49-04-402	31°51'03"/106°36'42"	60,000	0.0007	127	B
49-04-403	31°56'17"/106°36'56"	140,000	—	1,770	B
49-04-404	31°56'18"/106°37'04"	46,400	—	252	B
49-04-405	31°56'17"/106°36'42"	121,000	—	1,020	RG
49-04-410	31°55'57"/106°36'43"	34,800	—	184	SF
49-04-411	31°55'56"/106°36'43"	104,000	—	758	B
49-04-412	31°55'57"/106°36'18"	150,000	—	1,780	B
49-04-415	31°55'37"/106°36'15"	110,000	—	—	B
49-04-417	31°55'56"/106°36'31"	155,000	0.001	—	B
49-04-418	31°55'55"/106°36'57"	87,000	0.0009	—	B
49-04-419	31°57'17"/106°36'40"	60,000	0.0006	129	B
49-04-420	31°55'57"/106°36'58"	150,000	—	1,830	B
49-04-421	31°55'50"/106°37'23"	29,700	—	75	SF
49-04-422	31°57'20"/106°36'22"	41,500	—	216	B
49-05-202	31°59'09"/106°25'34"	156,000	—	590	B
49-05-204	31°58'16"/106°25'27"	86,000	—	550	B
49-05-301	31°58'16"/106°24'31"	123,000	—	353	B
49-05-306	31°59'00"/106°53'27"	106,000	—	500	B
49-05-501	31°55'40"/106°25'29"	32,700	—	80	B
49-05-503	31°56'33"/106°25'24"	47,000	—	224	B
49-05-504	31°55'48"/106°26'33"	31,600	—	47	B
49-05-601	31°57'24"/106°24'23"	137,000	—	406	B
49-05-602	31°57'24"/106°23'28"	171,000	—	495	B
49-05-603	31°56'33"/106°24'22"	152,000	—	440	B
49-05-604	31°56'32"/106°23'27"	205,000	—	436	B
49-05-605	31°56'32"/106°22'32"	143,000	—	234	B
49-05-606	31°55'40"/106°24'26"	105,000	—	233	B
49-05-607	31°55'40"/106°23'26"	110,000	—	213	B

49-05-609	31°57'25"/106°22'25"	114,000	—	356	B
49-05-801	31°54'48"/106°26'23"	27,000	—	38	B
49-05-803	31°53'56"/106°25'22"	153,000	0.0006	298	B
49-05-901	31°54'48"/106°24'26"	114,000	—	303	B
49-05-902	31°53'58"/106°24'32"	105,000	—	223	B
49-05-903	31°54'51"/106°23'43"	175,000	—	231	B
49-05-906	31°54'44"/106°22'48"	176,000	—	284	B
49-06-401	31°57'25"/106°21'40"	135,000	—	—	B
49-13-202	31°52'13"/106°25'24"	70,000	—	137	B
49-13-204	31°50'25"/106°25'39"	37,500	—	—	B
49-13-301	31°52'12"/106°24'52"	200,000	0.0002	834	B
49-13-502	31°49'35"/106°25'18"	64,500	0.0005	134	B
49-13-512	31°49'38"/106°25'28"	82,600	0.026	173	B
49-13-605	31°49'34"/106°24'17"	73,000	—	982	B
49-13-608	31°48'11"/106°24'11"	97,000	—	151	B
49-13-609	31°47'40"/106°24'04"	145,000	—	228	B
49-13-610	31°47'52"/106°23'46"	60,400	—	130	B
49-13-702	31°45'42"/106°28'27"	83,600	0.0006	—	B
49-13-703	31°45'42"/106°28'10"	95,200	0.0006	—	B
49-13-705	31°45'42"/106°28'02"	95,200	0.0009	388	B
49-13-803	31°46'29"/106°26'54"	5,600	0.00005	183	B
49-13-807	31°47'13"/106°26'01"	107,000	0.001	—	B
49-13-810	31°46'53"/106°25'31"	39,400	0.0034	215	B
49-14-101	31°52'14"/106°22'21"	55,000	—	183	B
49-14-401	31°47'45"/106°22'21"	59,200	—	121	B
49-14-402	31°47'46"/106°21'21"	73,500	—	165	B
49-14-701	31°46'52"/106°21'35"	60,200	—	158	B
49-14-706	31°46'52"/106°20'38"	46,700	—	146	B

*Texas Water Commission identification number

**Explanation (as defined by Myers [1969])

B = Huecco Bolson deposits

L = Limestone

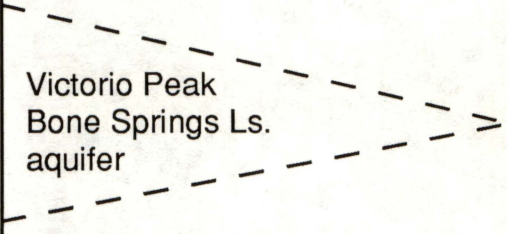
SF = Santa Fe deposits

RG = Rio Grande alluvium

NA = not applicable

— = Data not available

Table 2. Geologic and hydrologic units in study area.

Era	System	Unit	Hydrostratigraphic unit
Cenozoic	Quaternary	Alluvium	Rio Grande alluvial aquifer
	Tertiary	Santa Fe Fm. Hueco Bolson deposits	Hueco Bolson silt and sand aquifer
Mesozoic	Cretaceous	Kiamichi Fm. Finlay Fm. Cox Ss. Campagrande Fm. Bluff Mesa Fm.	Diablo Plateau aquifer
	Jurassic	Malone Fm.	
Paleozoic	Permian	Rustler Fm. Castile Fm. Victorio Peak Ls. Bone Springs Ls. Hueco Ls.	

QA 14458

Table 3a. Transmissivity results of aquifer test analyses for wells tested during study.

Well no.	Aquifer	Method of analysis for transmissivity (ft ² /d [m ² /d])				
		Agarwal	Theis (pumpage) (log-log)	Theis (recovery) (log-log)	Jacob (semilog)	Theis (recovery) (semilog)
22	D	12.5 (1.16)	0.45 (0.042)	0.64 (0.060)	0.63 (0.059)	0.65 (0.060)
22*	D	1.44 (0.134)	N/A	0.81 (0.075)	N/A	0.19 (0.018)
						0.22 (0.020) ^A
73	B	N/A	14.1 (1.31)	79.9 (7.42) ^c	100. (9.29)	94.0 (8.73)
			89.0 (8.27) ^A	24.5 (2.28) ^l	110. (10.2) ^A	89.0 (8.27) ^A
91	D	290.0 (26.9)	9.16 (0.85)	24.1 (2.24)	0.74 (0.069)	0.60 (0.056)
			11.0 (1.02) ^A		0.78 (0.073) ^A	0.84 (0.078)
94	D	38.0 (3.53)	1.41 (0.131)	3.54 (0.329)	2.50 (0.232)	1.50 (0.139)
			1.56 (0.145) ^A		2.34 (0.217) ^A	1.39 (0.129) ^A
98	B	59.0 (5.48)	1.15 (0.107)	6.13 (0.570)	1.50 (0.140)	3.60 (0.334)
98*	B	33.0 (3.07)	N/A	2.87 (0.267)	1.30 (0.121)	0.78 (0.073)
			2.60 (0.242) ^A		1.36 (0.126) ^A	0.64 (0.060) ^A
99	B	3.09 (0.287)	N/A	0.35 (0.033)	0.25 (0.023)	0.43 (0.040)
					0.23 (0.021) ^A	0.29 (0.027) ^A

Table 3b. Permeability results of aquifer test analyses for wells tested during study.

Well no.	Saturated thickness (ft [m])	Method of analysis for permeability (ft/d[m/d])				
		Agarwal	Theis (pumpage) (log-log)	Theis (recovery) (log-log)	Jacob (semilog)	Theis (recovery) (semilog)
22	22.9 (6.97)	0.546 (0.166)	0.020 (0.0060)	0.028 (0.0085)	0.028 (0.0084)	0.028 (0.0086)
22*	126.9 (38.7)	0.0114 (0.0035)	N/A	0.0064 (0.0020)	N/A	0.0015 (0.0005) 0.0017 (0.0005)
73	192.9 (58.8)	N/A	0.073 (0.0223) 0.047 (0.0142) ^A	0.414 (0.126) ^e 0.127 (0.039) ^l	0.518 (0.158) 0.570 (0.174)	0.487 (0.149) 0.461 (0.141) ^A
91	112.7 (34.4)	2.82 (0.861)	0.089 (0.0272) 0.107 (0.0327) ^A	0.235 (0.072)	0.0072 (0.0022) 0.0076 (0.0023) ^A	0.0058 (0.0018) 0.0082 (0.0025)
94	53.2 (16.2)	0.714 (0.218)	0.027 (0.0081) 0.029 (0.0089) ^A	0.067 (0.020)	0.047 (0.014) 0.044 (0.013) ^A	0.028 (0.0086) 0.026 (0.0080) ^A
98	100. (30.5)	0.59 (0.180)	0.0115 (0.0035)	0.061 (0.019)	0.015 (0.0046)	0.036 (0.011)
98*	100. (30.5)	0.33 (0.101)	0.026 (0.0080) ^A	0.029 (0.0087)	0.013 (0.0040) 0.013 (0.0042) ^A	0.0078 (0.0024) 0.0064 (0.0020) ^A
99	63.0 (19.2)	0.049 (0.015)	N/A	0.0056 (0.0017)	0.004 (0.0012) 0.0037 (0.0011) ^A	0.0068 (0.0021) 0.0046 (0.0014) ^A

Table 3c. Transmissivity and permeability results of aquifer (slug) test analyses for wells tested during study.

Well no.	Aquifer	Method of analysis for transmissivity (ft ² /d [m ² /d])		
		Ferris and Knowles (1954)	Cooper and others (1967)	Bouwer and Rice (1976)
107	B	3.60 (0.334)	12.0 (1.11) 81.4 (7.56) ^A	N/A 33.9 (3.15) ^A
126	B	3.96 ^e (0.367) 11.7 ^l (1.09)	28.4 (2.60) 16.5 (1.53) ^A	N/A 34.4 ^e (3.20) ^A 49.0 ^l (4.55) ^A

Well no.	Saturated thickness (ft [m])	Method of analysis for permeability (ft/d [m/d])		
		Ferris and Knowles (1954)	Cooper and others (1967)	Bouwer and Rice (1976)
107	102.9 (31.4)	0.035 (0.0107)	0.116 (0.035) 0.791 (0.241) ^A	N/A 0.329 (0.100) ^A
126	121.1 (36.9)	0.033 ^e (0.010) 0.097 ^l (0.0295)	0.234 (0.588) 0.136 (0.0415) ^A	N/A 0.284 ^e (0.0866) ^A 0.405 ^l (0.123) ^A

D = Diablo Plateau aquifer

B = Hueco Bolson silt and sand aquifer

N/A = not applicable

* Pumping test results after deepening total depth from 615.0 ft to 719.0 ft.

^e Early phase of recovery

^l Late phase of recovery

⁺ Well no. 98 was retested after extensive well development in attempt to remove drilling mud artifact from aquifer.

^A Solutions for transmissivity and permeability based on computer analysis using ACTESOLV software.

Table 4. Transmissivities assigned to permeability zones in the model.

Permeability zones	Description	Transmissivity (ft²/ d)
Zone 1	Cretaceous strata, Diablo Plateau (west)	1.0
Zone 2	Cretaceous strata, Diablo Plateau (east)	15.0
Zone 3	Cretaceous strata, escarpment (west)	0.1
Zone 4	Cretaceous strata, escarpment (east)	2.5
Zone 5	Cretaceous strata downdip from escarpment	1.0
Zone 6	Cretaceous strata parallel to Campo Grande fault	50.0
	Cretaceous strata perpendicular to Campo Grande fault	10.0
Zone 7	Cretaceous/bolson strata northeast of Campo Grande fault	5.0
Zone 8	Bolson, mud-rich deposits north of Campo Grande fault	0.1
Zone 9	Bolson, sand-rich deposits, north of Campo Grande fault	50.0
Zone 10	Bolson deposits south of Campo Grande fault	5 to 10
Zone 11	Rio Grande alluvium	1000.0
Zone 12	Flow barrier associated with Campo Grande fault	0.5

Table 5. Water wells within 10 mi of principal study area.

ID	Owner/operator	Production equipment	Operational status	Depth to water (ft)	Producing aquifer
22	GLO/BEG	—	Open	592.0	Cret. Ls.
72	GLO/BEG	—	Open	361.5	Bolson
73	GLO/BEG	Subm. pump	Active	377.1	Bolson
91	F. Owens	—	Capped	317.25	Cret. Ls.
94	GLO	Windmill	Inactive	294.0	Cret. Ls.
96	J. Moseley	Subm. pump	Active	400*	Cret. Ls.
97	J. Moseley	Subm. pump	Active	400*	Cret. Ls.
98	GLO/BEG	Subm. pump	Active	200.0	Bolson
99	F. MacGuire	—	Open	140.0	Bolson
106		Thaxton Spring	Active	0	Cret. Ls.
107	Tierra Del Sol	Windmill	Inactive	347.1	Bolson
108	Fort Hancock Water District	Turbine	Active	93.0	Bolson
111	F. MacGuire	Windmill	Active	327.0	Bolson
112	F. MacGuire	Windmill	Active	267.0	Cret. Ls.
113	S. Wilkey Est.	Pump jack	Inactive	600*	Cret. Ls.
114	S. Wilkey Est.	Subm. pump	Active	76*	Cret. Ls.
115	Gunsight Ranch	Windmill	Active	627.0	Cret. Ls.
116	F. Owens	Pump jack	Active	300.0	Cret. Ls.
126	GLO/BEG	Bennett pump	Active	478.9	Bolson

* Depth to water reported by owner

— No production equipment in well

